

Team #2  
E2-229  
Winnipeg, Manitoba, R3T 5V6  
December 7<sup>th</sup>, 2016

Dr. P. Labossiere, P. Eng.  
E1-546 EITC  
75 Chancellor's Circle  
Faculty of Engineering  
University of Manitoba  
Winnipeg, Manitoba, R3T 5V6

Dear Dr. P. Labossiere, P. Eng.

Enclosed is our final design report entitled "Carbon Fibre Curling Broom Handle Analysis and Design," submitted on December 7<sup>th</sup>, 2016.

The purpose of this report is to present a concept for the redesign of the "Xtreme Force" curling broom handle. The design was created on behalf of the customer Gerry Sande, of Sande Curling Innovations, along with Alastair Komus P. Eng., of Composites Innovation Centre. Provided is a recommendation for the final design selected as a solution to the customer's requirements. Additional provided information includes a final recommendation for the material and manufacturing process. Preliminary static finite element analysis results are provided to validate the final design. Supplemental information included in the report includes a detailed analysis of material and manufacturing of the first generation of the handle.

Please contact any of the group members via email for any concerns and comments regarding this report.

Yours truly,

Spencer Cabel

Brandon Dash

Lucas Schulz

Jovanni Tubog

Team #2  
E2-229  
Winnipeg, Manitoba, R3T 5V6  
December 7<sup>th</sup>, 2016

Alastair Komus  
158 Commerce Drive  
Composites Innovation Centre  
Winnipeg, Manitoba, R3P 0Z6

Dear Alastair Komus, P. Eng.

Enclosed is our final design report entitled “Carbon Fibre Curling Broom Handle Analysis and Design,” submitted on December 7<sup>th</sup>, 2016.

The purpose of this report is to present a concept for the redesign of the “Xtreme Force” curling broom handle. The design was created on behalf of the customer Gerry Sande, of Sande Curling Innovations, along with Alastair Komus P. Eng., of Composites Innovation Centre. Provided is a recommendation for the final design selected as a solution to the customer’s requirements. Additional provided information includes a final recommendation for the material and manufacturing process. Preliminary static finite element analysis results are provided to validate the final design. Supplemental information included in the report includes a detailed analysis of material and manufacturing of the first generation of the handle.

Please contact any of the group members via email for any concerns and comments regarding this report.

Yours truly,

Spencer Cabel

Brandon Dash

Lucas Schulz

Jovanni Tubog



UNIVERSITY  
OF MANITOBA

## Carbon Fibre Curling Broom Handle Analysis and Design

Final Report

**MECH 4860**

**Prepared For:**

**Dr. Paul Labossiere, P. Eng**

**Aidan Topping**

**Alastair Komus, P. Eng**

**Gerry Sande**



**Composites  
Innovation Centre**

[1]

**December 7, 2016**

**Proposal prepared by:**

**Team 2**

Spencer Cabel

Brandon Dash

Lucas Schulz

Jovanni Tubog

## EXECUTIVE SUMMARY

The team was tasked with designing the second generation Xtreme Force curling broom handle based on market feedback from the first generation handle. The existing handle features two angled grips built into the straight shaft, with the intention of allowing the user to apply force vertically downward while sweeping. The result is an increase in pressure applied by the broom head onto the ice, especially during the back stroke which is usually lacking in pressure.

The most common complaints about the first generation handle were that the grips are too large, are too restrictive on hand placement, have too large an angle with respect to the shaft, and cause blisters on the user's hands due to rubbing on the lips. The team generated concepts with the primary goals of improving comfort and adaptability to the user while maintaining the sweeping effectiveness of the first generation handle. The selected concept was to have only one grip, and to reduce the grip diameter to equal that of the shaft. Since the ideal grip angle is subjective, the team decided to proceed with three variations on the design: one with a 19° grip, a 38° grip and 51° grip.

To help in selection of materials and manufacturing methods, and because the client did not have information of how the first generation handle was produced, the team performed mechanical testing on a sample Xtreme Force handle. Through analysis of the internal structure and mechanical properties of the handle's components, the team determined that the first generation handle consists of carbon fibre composite with foam cores in the grips. The shaft sections are hollow, and the grips are bonded to the shafts using an adhesive.

After consideration of the benefits of various methods of production, the team decided to produce the part as a single body, eliminating the need for adhesives and improving mechanical properties due the lack of joints. The part is manufactured using oven prepreg. The prepreg is layed up around a core consisting of a permanent foam section for the grip, and two removable aluminum rods for the

hollow shaft sections. The selected materials are NB301 carbon fibre epoxy prepreg and Fibre Glast 2 Lb. Polyurethane Mix and Pour Foam.

The masses of the 19°, 38° and 51° final designs are 394.6g, 369.1g, and 367.2g respectively, and the estimated cost of materials per handle for 19°, 38° and 51° designs are \$22.76, \$21.37 and \$21.2 respectively.

## TABLE OF CONTENTS

LIST OF FIGURES .....	VII
LIST OF TABLES.....	IX
1. INTRODUCTION .....	1
1.1 PROBLEM BACKGROUND .....	1
1.2 PROBLEM STATEMENT .....	3
1.3 PROJECT OBJECTIVES AND SCOPE .....	4
1.4 PROJECT NEEDS, CONSTRAINTS, AND SPECIFICATIONS .....	5
1.4.1 CUSTOMER NEEDS .....	6
1.4.2 TARGET SPECIFICATIONS.....	7
1.4.3 CONSTRAINTS AND LIMITATIONS .....	9
2. MECHANICAL TESTING AND RESEARCH .....	12
2.1 DEVELOPMENT OF TARGET SPECIFICATIONS .....	12
2.1.1 PREPARATION .....	12
2.1.1.1 DIVIDING THE HANDLE .....	13
2.1.1.2 CORE .....	15
2.1.1.3 GRIPS .....	17
2.1.2 TESTING.....	18
2.1.2.1 DENSITY .....	18
2.1.2.1.1 UNIFORM CROSS SECTION .....	19
2.1.2.1.2 NON-UNIFORM CROSS SECTION.....	19
2.1.2.2 TENSION .....	21
2.1.2.3 COMPRESSION .....	24
2.1.2.4 THREE POINT BENDING .....	25
2.1.3 RESULTS .....	27
2.1.3.1 DENSITY .....	27
2.1.3.2 PRELIMINARY TENSILE TEST RESULTS.....	28
2.1.3.3 IMPROVED TENSILE TEST RESULTS .....	31
2.1.3.4 STRENGTH OF BOND.....	33
2.1.3.5 COMPRESSION TEST RESULTS .....	34
2.1.3.6 THREE POINT BENDING TEST RESULTS.....	37
2.1.3.7 RESULTS DISCUSSION .....	38
2.2 MATERIAL AND MANUFACTURING .....	39
2.2.1 FIBRES.....	39
2.2.1.1 CARBON FIBRES.....	40
2.2.1.2 FIBREGLASS .....	42
2.2.1.3 KEVLAR.....	44
2.2.1.4 COMPARISON OF FIBRE PROPERTIES .....	45
2.2.2 MATRIX.....	46
2.2.2.1 IDEAL CHARACTERISTICS OF A MATRIX .....	46
2.2.2.2 MATRIX TYPES.....	46
2.2.2.3 EPOXY.....	47
2.2.2.4 POLYESTER .....	48
2.2.2.5 VINYL ESTER.....	48
2.2.2.6 COMPARISON OF MATRIX PROPERTIES.....	48
2.2.3 BONDING.....	49
2.2.3.1 MECHANICAL FASTENERS.....	50
2.2.3.2 ADHESIVES .....	50
2.2.4 MANUFACTURING.....	51
2.2.4.1 CONTACT MOULDING .....	51
2.2.4.2 AUTOCLAVE MOULDING.....	52
2.2.4.3 FILAMENT WINDING.....	52

2.2.4.4	RESIN TRANSFER MOULDING (RTM).....	53
2.2.4.5	PULTRUSION.....	53
2.2.4.6	COMPARISON OF MANUFACTURING PROCESSES.....	54
3.	CONCEPTUAL DESIGN.....	56
3.1	PRELIMINARY DESIGN.....	56
3.1.1	NUMBER OF GRIPS.....	56
3.1.2	REMOVAL OF GRIP LIPS.....	56
3.1.3	GRIP ANGLE.....	57
3.1.3.1	INITIAL METHODS.....	57
3.1.3.2	STUDY GROUP ANALYSIS.....	58
3.1.4	FINGER INDENTATION.....	60
3.2	STATIC ANALYSIS.....	61
3.3	CONCEPT MODELS.....	65
4.	FEA METHODOLOGY.....	67
4.1	MATERIAL PROPERTIES.....	67
4.2	GEOMETRIC CONSTRAINTS.....	68
4.3	LOADING.....	69
4.4	MESHING.....	70
4.5	INITIAL FEA RESULTS.....	74
4.6	INITIAL DESIGN OPTIMIZATION.....	78
4.6.1	LAYUP DETERMINATION WORKFLOW.....	78
4.6.2	MATERIAL LAYUP.....	81
4.6.3	RESULTS DISCUSSION.....	84
5.	DESIGN OPTIMIZATION.....	91
5.1	MODEL OPTIMIZATION.....	91
5.2	PRELIMINARY FEA RESULTS.....	92
5.2.1	MESH CONVERGENCE.....	94
5.2.2	FINAL COMPOSITE LAYUP.....	97
5.2.3	COMPOSITE FAILURE CRITERIA ANALYSIS.....	99
5.3	SUMMARY OF RESULTS.....	100
6.	MATERIAL AND MANUFACTURING.....	102
6.1	FAILURE MODE EFFECTS ANALYSIS.....	102
6.2	EXISTING HANDLE MATERIAL AND MANUFACTURING.....	104
6.2.1	VISUAL INSPECTION.....	104
6.2.2	ANALYSIS OF TEST RESULTS.....	106
6.2.3	SUMMARY OF EXISTING HANDLE MATERIAL AND MANUFACTURING.....	107
6.3	MATERIAL ANALYSES.....	107
6.3.1	CORE MATERIAL.....	107
6.3.1.1	CORED CROSS SECTION.....	108
6.3.1.2	HOLLOW CROSS SECTION.....	111
6.3.2	SHAFT AND GRIP MATERIAL.....	113
6.4	MANUFACTURING METHODS ANALYSIS.....	115
6.5	RECOMMENDATION FOR FINAL MATERIAL AND MANUFACTURING.....	118
6.5.1	FINAL MATERIAL PROPERTIES.....	118
6.5.2	FINAL MANUFACTURING RECOMMENDATION.....	120
6.6	COST ANALYSIS.....	122
7.	RECOMMENDATIONS.....	124
8.	CONCLUSION.....	126

<b>8. REFERENCES .....</b>	<b>129</b>
<b>APPENDIX A: NEEDS AND METRICS .....</b>	<b>A1</b>
<b>APPENDIX B: PRELIMINARY CONCEPT EVALUATION.....</b>	<b>B1</b>
<b>APPENDIX C: SUPPLEMENTAL DATA.....</b>	<b>C1</b>



## LIST OF FIGURES

Figure 1: Various curling broom uses, including balancing and sweeping.....	1
Figure 2: Example of data obtained through the use of the pressure sensor head.....	2
Figure 3: Xtreme Force handle, with nomenclature used in the report identified .....	3
Figure 4: Experimental handle specification .....	12
Figure 5: The provided experimental handle prior to cutting .....	13
Figure 6: Seam along the middle of the grip.....	13
Figure 7: Cross section of cut grip showing internal core. ....	14
Figure 8: Final cut sections of the handle, with identification labeling.....	14
Figure 9: Hole saw used and pilot hole created to obtain core sample from piece ...	16
Figure 10: Top view (left) and side view (right) of core samples.....	16
Figure 11: Dremel being used to isolate grip composite material.....	17
Figure 12: Inside view of coreless piece C highlighting the seam.....	18
Figure 13: Core sample taken from piece B.....	19
Figure 14: Volume of water .....	20
Figure 15: Volume of water prior to hollow grip piece C submersion.....	20
Figure 16: MTS Insight load frame showing mounted clamps.....	21
Figure 17: Dog bone shape testing samples.....	22
Figure 18: Conventional clamp grips (left) and modified clamp grips (right).....	22
Figure 19: Shaft (left) and grip (right) samples mounted into clamp grips.....	23
Figure 20: Skid marks produced on a sample while it slips through clamp grips.....	23
Figure 21: MTS Insight load frame with mounted compression plates.....	24
Figure 22: Shaft (left) and core (right) samples undergoing compression testing....	25
Figure 23: MTS Insight load frame showing mounted bending supports .....	26
Figure 24: Shaft (left) and grip (right) samples undergoing three point bending....	26
Figure 25: Stress-Strain graph for tensile testing. ....	29
Figure 26: Stress-Strain graph of tensile test on specimen 3. ....	30
Figure 27: Fracture failure in specimens 2, 3, 5, and 6 during tensile test .....	31
Figure 28: Improved tensile test specimens, cut from grip composite .....	32
Figure 29: Stress-Strain graph for improved tensile testing. ....	33
Figure 30: Irregularity in the shapes of specimens 9, 10, and 11 .....	34
Figure 31: Stress-strain curves from the compression test. ....	35
Figure 32: Sequence of events showing the behavior of specimen 4.....	36
Figure 33: Roll of carbon fibre fabric .....	41
Figure 34: Rolls of carbon fibre tape.....	41
Figure 35: Carbon fibre sleeve .....	42
Figure 36: Carbon fibre pre-preg.....	42
Figure 37: Comparison of common manufacturing methods. Based on. ....	54
Figure 38: Side view of conceptual design BCFP.....	56
Figure 39: Grip lips which are to be removed .....	57
Figure 40: Mockup handle created .....	58
Figure 41: Example of broom handle angle measurement in ImageJ software.....	59
Figure 42: Free body diagram setup used in analytical calculations of the stresses.	61
Figure 43: Decomposition of the applied load into two vectors .....	62

Figure 44: Free body diagram of the statics system with resolved components. ....	62
Figure 45: Decomposition of the relative axial and normal forces .....	63
Figure 46: 19° BCFP (XtremeForce Pro).....	65
Figure 47: 38° BCFP (XtremeForce Original).....	65
Figure 48: 51° BCFP (XtremeForce 51).....	65
Figure 49: Fixed geometries applied to the 19° angle model. ....	69
Figure 50: Application of the distributed 300 lb .....	70
Figure 51: 3D mesh elements .....	70
Figure 52: Coarse mesh of 19° handle using default settings in ANSYS Workbench	71
Figure 53: Contour plot showing max principal stress in the 19° .....	72
Figure 54: Mesh of entire handle after controls applied. ....	73
Figure 55: Mesh at the location of rear hand. ....	73
Figure 56: Close up view of the refined mesh at the location of rear hand.....	73
Figure 57: Mesh at the location of grip.....	73
Figure 58: Close up view of the refined mesh at the location grip. ....	73
Figure 59: Mesh at the location of the head. ....	73
Figure 60: Close up view of the refined mesh at the location of the head.....	73
Figure 61: Introduction of supplementary coordinate systems.....	75
Figure 62: Introduction of supplementary coordinate systems of the 38° .....	75
Figure 63: Introduction of supplementary coordinate systems of the 51° .....	76
Figure 64: Predicted failure modes on the critical region shown as text .....	80
Figure 65: Divided sections of 19°. 81	
Figure 66: Overall view of the vector plot.....	82
Figure 67: Close up of vector plot of principle stresses in a bend region. ....	82
Figure 68: Overview of the plot of the maximum principle stresses.....	83
Figure 69: Close up of section 5 of the plot of the principle stresses .....	83
Figure 70: Probed surfaces of the handle where monitored stresses are .....	85
Figure 71: Variation in the monitored Max principal stresses .....	85
Figure 72: Max IRF of each ply in the stackups for sections A, B, and C.....	89
Figure 73: Max IRF of each ply in the stackups for sections A, B, and C .....	89
Figure 74: Max IRF of each ply in the stackups for sections A, B, and C .....	90
Figure 75: 3D render of the 19° variation of the second generation handle.....	92
Figure 76: 3D render of the 38° variation of the second generation handle.....	92
Figure 77: 3D render of the 51° variation of the second generation handle.....	92
Figure 78: Isometric view of the von Mises stress distribution about the .....	93
Figure 79: Close up view of the stress distribution about the end.....	93
Figure 80: Alternate front view of the stress distribution about the end.....	94
Figure 81: Locations of the von Mises stress probes used in the calculation .....	94
Figure 82: Stress convergence graph for isotropic behavior of 19° model.....	95
Figure 83: Seam along the middle of the grip.....	105
Figure 84: Cross section of cut grip showing internal core.....	105
Figure 85: Inside view of coreless piece C highlighting the seam.....	106
Figure 86: FDM process schematic. ....	112

## LIST OF TABLES

TABLE I: CUSTOMER NEEDS ORGANIZED BY CATEGORY .....	6
TABLE II: RELATIVE IMPORTANCE OF CUSTOMER NEEDS.....	7
TABLE III: DEVELOPED METRICS AND TARGET SPECIFICATIONS .....	8
TABLE IV: INTENDED PURPOSE OF CUTS.....	15
TABLE V: EXPERIMENTALLY DETERMINED DENSITY VALUES .....	27
TABLE VI: TENSILE TEST RESULTS .....	28
TABLE VII: SUMARY OF IMPROVED TENSIL TEST RESULTS.....	32
TABLE VIII: STRENGTH OF BOND BETWEEN GRIP AND SHAFT .....	33
TABLE IX: COMPRESSION TEST RESULTS.....	37
TABLE X: RESULTS FROM THREE-POINT BENDING TEST .....	37
TABLE XI: EXAMPLES OF COMMON CARBON FIBRE PRODUCTS .....	41
TABLE XII: DIFFERENT TYPES OF FIBREGLASS .....	44
TABLE XIII: COMPARISON OF PROPERTIES .....	45
TABLE XIV: COMPARISON OF MATRIX PROPERTIES .....	49
TABLE XV: AVERAGE RECORDED BROOM HANDLE ANGLES IN DEGREES.....	59
TABLE XVI: ANALYTICAL STRESS CALCLUATIONS FOR HANDLE AT 19° .....	64
TABLE XVII: ANALYTICAL STRES CALCULATIONS FOR HANDLE AT 38° .....	64
TABLE XVIII: ANALYTICAL STRESS CALCULATIONS FOR HANDLE AT 51° .....	65
TABLE XIX: ASSUMED ISOTROPIC PROPERTIES .....	68
TABLE XX: COMPARISON OF RESULTS BETWEEN COARSE AND REFINED MESH..	74
TABLE XXI: FEA RESULTS FOR 19° HANDLE .....	74
TABLE XXII: FIVE SECTIONS OF THE HANDLE.....	75
TABLE XXIII: FEA AND STATICS RESULTS FOR 19° HANDLE .....	76
TABLE XXIV: FEA AND STATICS RESULTS FOR 38° HANDLE.....	76
TABLE XXV: FEA AND STATICS RESULTS FOR 51° HANDLE .....	77
TABLE XXVI: RECOMMENDED FAILURE CRITERIA .....	79
TABLE XXVII: MAXIMUM, MIDDLE AND MINIMUM PRINCIPAL STRESSES.....	84
TABLE XXVIII: INITIAL CONCEPT REQUIRED LAYUP.....	87
TABLE XXIX: OPTIMIZED STACKUPS FOR THE 38° AND 51° HANDLES.....	88
TABLE XXX: DATA FROM MESH CONVERGENCE PLOT PART 1 .....	96
TABLE XXXI: DATA FROM MESH CONVERGENCE PLOT PART 2 .....	96
TABLE XXXII: FINAL LAY-UP FOR 19° GRIP .....	97
TABLE XXXIII: FINAL LAY-UP FOR 38° AND 51° GRIP.....	98
TABLE XXXIV: FINAL LAY-UP FOR 51° GRIP .....	98
TABLE XXXV: FAILURE CITERIA ANALYSIS FOR 19° HANDLE .....	99
TABLE XXXVI: FAILURE CITERIA ANALYSIS FOR 38° HANDLE.....	100
TABLE XXXVII: FAILURE CITERIA ANALYSIS FOR 51° HANDLE .....	100
TABLE XXXVIII: FINAL MODEL VOLUME AND MASS .....	101
TABLE XXXIX: COMPARISON OF ORIGINAL MODEL TO FINAL MODEL MASS .....	101
TABLE XL: FMEA.....	104
TABLE XLI: SUMMARY OF IMPROVED TENSILE TEST RESULTS .....	106
TABLE XLII: TYPES OF CORE MATERIALS.....	109
TABLE XLIII: CCOMMON THERMOPLASTICS USED IN FDM .....	112

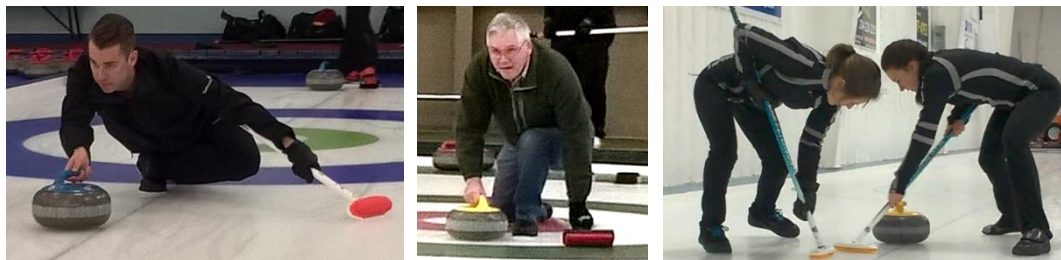
TABLE XLIV: MATERIAL CRITERIA WEIGHTING MATRIX.....	114
TABLE XLV: MATERIAL SCORING MATRIX.....	115
TABLE XLVI: PROPERTIES OF SELECTED UNIDIRECTIONAL .....	119
TABLE XLVII: BILL OF MATERIALS FOR SECOND GENERATION.....	122
TABLE XLVIII: COST OF MATERIAL PER UNIT FOR EACH HANDLE VARIATION....	123
TABLE XLIX: RECOMMENDATIONS BASED ON OUT OF SCOPE TASKS.....	124
TABLE L: RECOMMENDATIONS INDEPENDENT OF AFOREMENTIONED .....	125

# 1. INTRODUCTION

This report outlines the detailed final design of the second generation Xtreme Force curling broom handle. Introductory material presented in the leading section includes background, problem statement, objectives, scope, needs, constraints and target specifications. Based on the developed needs and constraints, the selected conceptual design was then evaluated. This evaluation involved the use of computer aided design (CAD) and finite element analysis (FEA), with verification via statics calculations. Using the validated results of the conceptual design analysis, a recommendation for the material and manufacturing processes of the final design is determined. Applying the selected composite material to the final design, the concept was evaluated again using FEA, and a final design recommendation is presented at the conclusion of the report.

## 1.1 PROBLEM BACKGROUND

Over the past 100 years, the sport of curling has significantly evolved through technological advancements. The broom has benefitted from these advancements, as it is one of the most integral pieces of equipment used in the sport. It is used for both sweeping the ice and as a balance while throwing a curling rock. Figure 1 shows some examples of the various ways a curling broom is used.

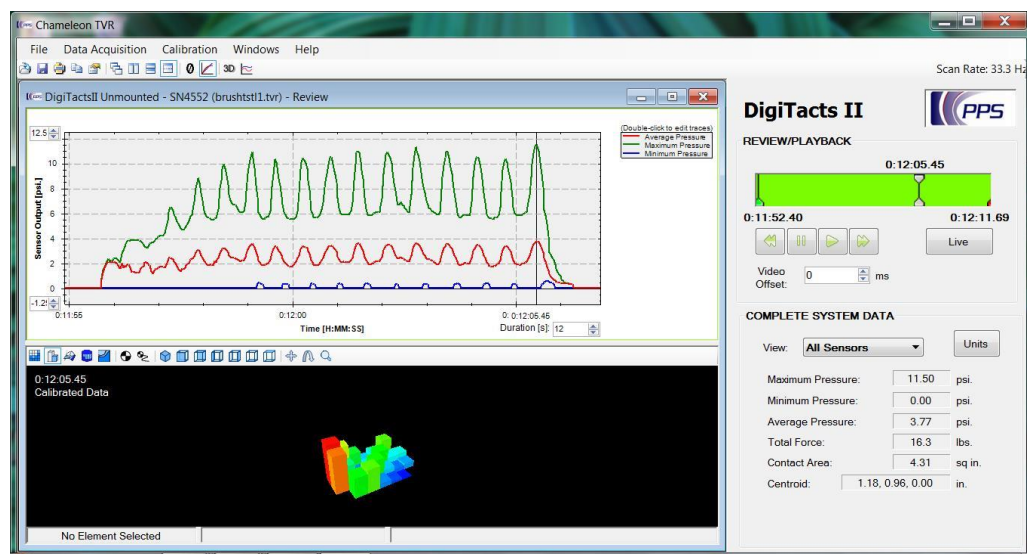


**Figure 1: Various curling broom uses, including balancing and sweeping [2].**

From the early wood and corn straw brooms to the modern carbon fibre shafts and specially-engineered fabric brush heads, there is always an interest in new ways to increase sweeping effectiveness [3]. Gerry Sande, CEO of Sande Curling Innovations,

has partnered with the Composites Innovation Centre to develop a new broom handle that helps increase sweeping effectiveness by permitting sweepers to apply pressure more uniformly onto the ice throughout the sweeping motion.

Gerry Sande saw an opportunity to improve this aspect of sweeping from the data acquired by a specially designed broom head which records the pressure applied during sweeping. This data showed that the applied pressure during the push stroke is significantly higher than the pressure applied during the pull stroke. Figure 2 shows an example of the pressure readout from one of these specially equipped broom heads.



**Figure 2: Example of data obtained through the use of the pressure sensor head created by Sande Curling Innovations. The data shown is merely an example of the readout provided by the pressure sensor head, and is intended for illustration purposes only [4].**

With this data, Sande Curling Innovations developed the "Xtreme Force" broom handle in an attempt to help improve the uniformity of a sweeper's applied pressure. The handle features unique angled grips built into the traditionally straight shaft. The angled grips are designed to be more parallel with the ice (in contrast to a traditional shaft) as the user sweeps. The working theory behind the geometry is that the alteration in the sweeper's wrist orientation will allow them

to maintain a greater uniformity in the applied pressure while sweeping. Figure 3 shows the Xtreme Force broom handle, labelled with the nomenclature of the broom sections as they are referred to in this report.



**Figure 3: Xtreme Force handle, with nomenclature used in the report identified [5]**

The Xtreme Force handle is a bold new concept for a curling broom handle, as current research is typically focused on the broom's head, rather than the handle [3]. After testing this handle using the pressure-recording broom head, the data has revealed significant improvements to sweeping efficiency in contrast to traditional straight broom handles. In spite of these favorable performance metrics, feedback from users has indicated that the design requires some revision.

The Composites Innovation Centre and Sande Curling Innovations employed us to design the second generation model for the Xtreme Force handle based on customer feedback.

## **1.2 PROBLEM STATEMENT**

The Xtreme Force broom handle has not produced the market reaction which Sande Curling Innovations had anticipated. A common complaint among curlers using standard curling brooms is that the pull stroke needs to be improved [6]. This complaint inspired the design of the original Xtreme Force broom handle, which was designed to increase sweeping efficiency by improving the pull stroke [7]. This is an area where the first generation handle has been largely successful. Despite its

successes, the first generation broom handle has experienced some qualitative shortcomings, which have been compiled from market feedback, and are as follows:

- The grips wear too quickly
- Overall handle geometry is not comfortable or adaptable
- Current geometry does not allow for (or heavily limits) throwing use, and feels unnatural to the user

Each of these three shortcomings were addressed in the design of the second generation product.

### 1.3 PROJECT OBJECTIVES AND SCOPE

The main goal of the project was to redesign the Xtreme Force curling broom handle based on market feedback. Throughout the redesigning process, the group was responsible for the completion of the following objectives:

- Identify the target specifications by evaluating the performance of the first generation broom handle with respect to the needs of the project.
- Produce a new (second generation) handle design that adheres to the identified target specifications.
- If time permits, make the new handle adaptable to different users' handling styles

These objectives were then used to develop the project scope, which specified the general tasks that were included in the final design project. The scope of the project consists of the following tasks:

- Determine the material and manufacturing method used to produce the first generation handle, as well as the grip's material properties. The lack of communication between the client and the manufacturers of the first generation handle facilitated the need for this task.



- Select an appropriate material and manufacturing method for the second generation handle.
- Produce a CAD model of the second generation handle.
- Perform preliminary FEA on the final design under static loading conditions to determine the nature of the stress distribution across the handle and the location(s) of the high stress areas.
- Estimate the cost of producing the final design.
- Submit a report to the client that makes a recommendation for material choice and manufacturing process for the second generation handle.

The following tasks were not undertaken, as they are beyond the project scope:

- Production of a physical prototype of the second generation broom handle
- Production of CAD models other than the redesigned broom handle (such as the broom head)
- Preliminary FEA on both the first and second generation broom handles under dynamic loading
- Recommendation of maintenance procedure(s) and proper disposal of the first and second generation broom handles

Although the goal of redesigning the handle is to improve its comfort (without compromising sweeping efficiency) by adjusting the size, angle and shape of the grips, the ergonomics are not measurable until a prototype has been produced. As such, after a prototype has been produced, focus groups and product testing shall need to take place to determine the grip's ergonomic suitability.

#### **1.4 PROJECT NEEDS, CONSTRAINTS, AND SPECIFICATIONS**

Customer needs and metrics were developed to help ensure that the final product delivered to the customer matches what was originally desired by the customer. Based on the needs, associated metrics were developed to measure the degree to which the needs will be met.

### 1.4.1 CUSTOMER NEEDS

Based on the information gathered from the initial client meeting, the developed customer needs were organized into four different categories: ergonomics, performance, safety, and manufacturing and materials. TABLE I outlines the customer needs organized by category. In order to isolate which customer needs are of highest priority, the team assigned each need an importance rating based on a scale of 1 – 5 (with 5 being the most important, and 1 being the least important). A total of 14 discrete customer needs were developed and approved by the client.

**TABLE I: CUSTOMER NEEDS ORGANIZED BY CATEGORY**

#	Need		Importance
1. Ergonomics			
N1.1	The handle	is comfortable to hold	5
N1.2	The handle	has a thinner grip	4
N1.3	The handle	has a new hand angle	5
N1.4	The handle	grips have a new shape	3
N1.5	The handle	is adaptable to the user	1
2. Performance			
N2.1	The handle	is stiff	5
N2.2	The handle	is light	4
N2.3	The handle	maintains sweeping efficiency	5
3. Safety			
N3.1	The handle	does not harm user's hands	5
N3.2	The handle	is strong	5
N3.3	The handle	reduces operator fatigue	4
4. Manufacturing and Materials			
N4.1	The handle	is inexpensive	2
N4.2	Material selection compatibility		5
N4.3	Manufacturing process compatibility		5

After establishing this defined list of needs, they were given a relative importance through the use of a scoring matrix. The results of this scoring matrix are given in TABLE II, and discussed in APPENDIX A.

**TABLE II: RELATIVE IMPORTANCE OF CUSTOMER NEEDS**

Ranking	Need ID	Customer Need	Weight %
1	N4.2	Material Selection Compatibility	14.61
2	N4.3	Manufacturing Process Compatibility	13.48
3	N3.2	Strong	12.36
4	N3.1	Does not harm users hands	10.11
5	N2.3	Maintains sweeping efficiency	8.99
6	N3.3	Reduces operator fatigue	8.99
7	N1.1	Comfortable to hold	7.87
8	N1.3	New hand angle	6.74
9	N1.2	Thinner handle	5.62
10	N1.4	Grips have a new shape	4.49
11	N2.1	Stiff	3.37
12	N2.2	Light	2.25
13	N1.5	Adaptable to the user	1.12
14	N4.1	Inexpensive	0.00

#### 1.4.2 TARGET SPECIFICATIONS

Before developing the target specifications of the design, which are inherently quantifiable, it was necessary to first determine the appropriate metrics which govern these specifications. TABLE III outlines the various metrics alongside their target values which were considered in the design of the second generation broom handle.

TABLE III: DEVELOPED METRICS AND TARGET SPECIFICATIONS

Metric #	Metric	Units	Marginal Value	Ideal Value
M1	Ergonomic	Subj	-	Subj
M2	Grip width	mm	33.5	< 33.5
M3	Grip length	mm	50.8	50.8
M4	Grip angle	deg	38	>38
M5	Grip locations	cm	18/70	18
M6	Handle rotation	deg	0	Subj
M7	Number of handles	Count	2	1
M8	Broom deflection	mm	-	-
M9	Applied load	N	667	>667
M10	Composite modulus	GPa	9.45	9.45
M11	Total mass	g	618	< 618
M12	Broom head pressure	Pa	-	-
M13	Lip size	mm	7	< 7
M14	Lip shape	Subj	-	-
M15	Internal stress	MPa	127	127
M16	Unit manufacturing cost	\$ CAD	225	< 225

The methods used to determine the limits and the priorities of each of these metrics are detailed in APPENDIX A. In summary, these exact target specifications were developed in accordance with the material properties of the first generation handle. The material properties had to be determined through a series of tests since the manufacturing process had not been transparent in the production of the first generation handle [7]. The details of these tests also discussed in APPENDIX A.

### 1.4.3 CONSTRAINTS AND LIMITATIONS

The constraints and limitations which affected the design process include time, allowable materials, ergonomics, cost, and the performance metrics (relative to the first generation broom). Each of these constraints and their implications will be detailed in this section.

The amount of time available to complete the project was one of the biggest constraints. Although the main objectives of the project included CAD modeling, material selection, finite element analysis results and manufacturing process selection, Sande Curling Innovations would have also liked the incorporation of an adaptability mechanism into the final design if time permitted. However, given the limited time frame of two months, there was not enough time available to properly implement an adaptability feature.

The quantitative performance of the first generation broom handle applies constraints on the design of the second generation handle. If the second generation handle does not exceed the performance of the first generation handle (or anything else currently available on the market), the redesigned handle is unlikely to experience improved market success. Even if the second generation handle ends up being lighter, stronger and stiffer than its predecessor, but it fails to deliver an improved performance, the second generation handle will experience an average market reaction, as the first generation handle did. This constraint does not apply to the project in a direct manner, as the production of a physical prototype is not within the scope of the project. However, it may affect future iterations and refinements of the design once working prototypes of the handle are manufactured and tested.

Ergonomics was another constraint on the design. If the product is not comfortable to hold or it harms the user's hands, the improved performance metrics will become irrelevant once the product is on the market. Therefore, certain limitations existed on both the material selection (particularly relating to surface finish) and the grip

geometry in order to ensure user comfort. These limitations may only be applied in theory, as it will be difficult to predict the ergonomics of the second generation broom handle until a prototype is manufactured and tested.

Although one of the main objectives of the redesign was to ensure that the performance of the second generation broom handle exceeds that of the first, the redesigned broom handle must above all be safe to use. It follows that limitations were imposed on the upper limits of the handle's various technical specifications relating to weight, strength and rigidity in order to ensure a safe product. Failure to do so puts the user's health at risk. The limits of these metrics have been determined by a series of tests performed on the first generation handle, and are discussed in section 1.4.2. Only static loading analyses were performed throughout the design process to ensure a safe final design. Although dynamic loading analyses would have shown a more realistic representation of the stresses acting throughout the handle, this type of analysis was outside of the project scope. Therefore, the analyses given in section 4 should be considered as preliminary.

The only constrained metric that was not developed through any sort of testing was cost. Although cost is generally a significant constraint in most engineering projects, the client did not voluntarily provide the team with a definitive cost limit, only a range of \$5 - \$10 for the grip component [7]. In an effort to save on production costs, the distributor of the first generation handle had outsourced some of the manufacturing and assembly labour to Asia. This outsourcing ultimately compromised the quality of the final product. As such, the client stated a willingness to spend more (if necessary) in order to ensure both manufacturing transparency and a higher quality final product. The willingness to spend more by the client is reflected in the results of TABLE II, where need N4.1 (inexpensive) is ranked last in importance relative to every other discrete need.

In conclusion, the amount of time available to complete each of the available objectives limited the potential of this design. Above all, the redesigned handle must be a safe product to use. Moreover, curlers will not be willing to replace their

current broom handles with the second generation Xtreme Force handle if it does not outperform their current handle, the first generation handle or have comfortable grips. Consequently, the client values the quality of the final product, so the cost of production is of relatively low importance.

## 2. MECHANICAL TESTING AND RESEARCH

The following section outlines the mechanical testing and research which was considered in the concept generation and development process. Researched topics include test results (on the first generation handle), development of target specifications, sweeping mechanics, materials and manufacturing options and an analysis of existing products.

### 2.1 DEVELOPMENT OF TARGET SPECIFICATIONS

Through mechanical testing, the target specifications of the first generation handle were developed. The results of these tests place physical limitations on the design of the second generation handle. The following topics are included in the proceeding sections: how the provided handle was prepared for testing, an explanation of the performed tests, and the results of the tests.

#### 2.1.1 PREPARATION

To identify the materials and their properties used in the first generation handle, the handle needed to be prepared in such a way that each material was isolated to test independently. Prior to initiating this preparation process, each readily measurable metric of the experimental handle was recorded, as outlined in Figure 4.

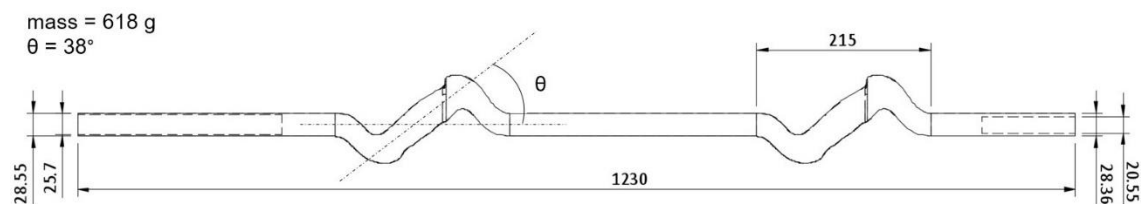


Figure 4: Experimental handle specification, unless specified all dimensions are in mm.

With measurements of the complete handle determined, the handle was then cut into sub sections to be used for mechanical testing.



### 2.1.1.1 DIVIDING THE HANDLE

Figure 5 shows an image of the provided experimental handle prior to preparing it for testing.



Figure 5: The provided experimental handle prior to cutting [2].

The first step in the preparation process was to isolate each of the materials by cutting the broom into desirable sample sizes. The initial cuts involved sawing the broom at the points of interest using a hack saw. One of the significant unknowns prior to cutting the broom was how the grips were assembled. Through physical and visual inspection of the handle, it was difficult to distinguish whether the grips were hollow or solid. The only distinguishable characteristic was the appearance of a seam down the middle of the grip, highlighted in Figure 6.

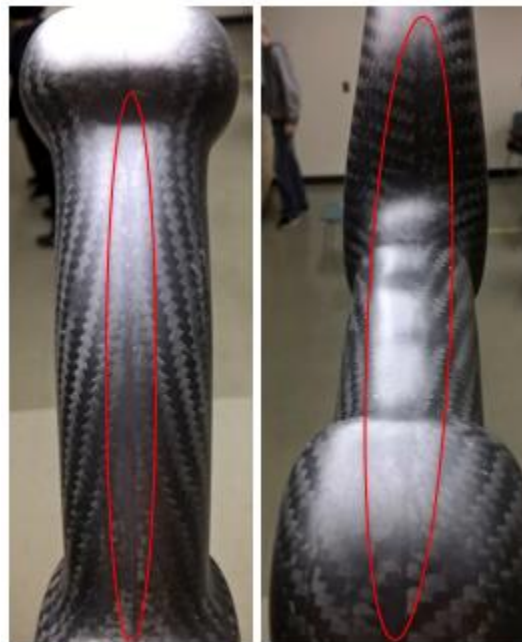


Figure 6: Seam along the middle of the grip [2].

Upon cutting apart the grip, it was determined to feature a solid core composed of only one material, shown in Figure 7.



Figure 7: Cross section of cut grip showing internal core [2].

An overview of the final cut sections of the broom handle are shown in contrast to the handle prior to the cuts in Figure 8.



Figure 8: Final cut sections of the handle, with identification labeling [2].

TABLE IV shows the purpose of each of the labeled cuts corresponding to those in TABLE IV.

TABLE IV: INTENDED PURPOSE OF CUTS

Sample	Intent	Type(s) of Tests Performed		
		Tension	Compression	3 Point Bend
A	Determine tensile, compressive and flexural strength of reinforced lower shaft	•	•	•
B	Determine density and compressive strength of grip core. Investigate seam along the middle of the grip		•	
C	Determine density of grip core. Determine density, tensile and flexural strength of isolated grip composite. Investigate seam along the middle of the grip	•		•
D	Determine bond shear strength. Uncover any additional bond properties obtained within this shaft. Determine tensile, compressive and flexural strength of middle shaft	•	•	•
E	Determine flexural strength of cored grip composite			•
F	Determine tensile and compressive strengths of the top shaft.	•	•	

The pieces **A** through **F** labeled in TABLE IV, were then cut down into smaller, coupon size pieces to accommodate the size limitations imposed by the testing machines, which is discussed in further detail in section 2.1.2.

#### 2.1.1.2 CORE

In addition to cutting the provided handle into smaller testable lengths, core samples from the grips were removed to isolate the exterior grip composite. Prior to removing this core, measurable samples of the core were taken from pieces **B** and **C** using a hole saw in order to determine the properties of the core. Figure 9 shows the hole saw used along with the pilot hole created in the core of **C**.



Figure 9: Hole saw used and pilot hole created to obtain core sample from piece C [2].

Once the pilot hole and groove were created, the direction for the hole saw to cut into the core was established. As the main goal of obtaining the core sample is to keep it intact (in the form of a measurable cylinder), the pilot drill bit was not used to continue the cut. Although using the pilot bit would have likely resulted in a more uniform diameter of the resulting core sample, the concentric hole that would have been created as a result of this type of cut would have compromised the structural integrity of the already porous and brittle core. The size of the obtainable core samples was limited to the depth of the hole saw. Figure 10 shows two views of the two core samples removed from C.



Figure 10: Top view (left) and side view (right) of core samples taken from piece C [2].

A core sample was also taken from piece B, without the use of a pilot hole. A pilot hole was not needed in this case as the geometry of piece B was more favorable in regards to the dimensional limitations of the hole saw blade. The core sample

properties obtained from piece **B** and piece **C** include density and compressive strength, which will help identify the material.

#### 2.1.1.3 GRIPS

After desirable core samples were obtained, the portions of the grips from cuts **B**, **C** and **D** were isolated from the core material using a dremel. Figure 11 shows the dremel being used on piece **C** to isolate the grip composite from the core.



Figure 11: Dremel being used to isolate grip composite material [2].

The suspected seam along the grip previously mentioned became more apparent once the core was removed from the grip. An inside view of piece **C** with one of the seams highlighted is shown in Figure 12.





Figure 12: Inside view of coreless piece C highlighting the seam [2].

Using a saw bit, strips of the grip were cut from the flat faces of piece C using a dremel, similar to the one pictured in Figure 11. This provided flat samples that were testable using the available equipment, as outlined in section 2.1.2.

### 2.1.2 TESTING

With the handle cut into favorable sample sizes, testing was then performed on the samples to determine the properties of the three materials of the core, grip and shaft. The following section outlines the equipment and processes used to determine these properties. The test results are given and discussed following the description of the testing methods.

#### 2.1.2.1 DENSITY

The processes used to determine the density of each of the three materials in the handle are outlined in the proceeding sections. In curling, a desired trait for the curling broom is for the handle to have the least amount of mass possible. This low mass permits the sweepers to operate the brooms at a higher frequency before fatigue sets in. To determine the mass, it is helpful to first determine the density.

#### 2.1.2.1.1 UNIFORM CROSS SECTION

The shaft is assumed to be uniformly circular, so conventional measurements of inner diameter, outer diameter, length and mass will yield the densities of both the bottom reinforced shaft, and the top and middle thinner shafts.

The only other sample which featured a uniform cross section was the core sample taken from piece **B**. As such, the density of the core sample from piece **B** was determined in a similar fashion as the shafts. However, this core sample features a solid cross section, whereas the shaft cross section was hollow. Therefore, the only required dimensions are height, diameter and mass. Figure 13 shows a side view of the cylindrical core sample taken from piece **B**.



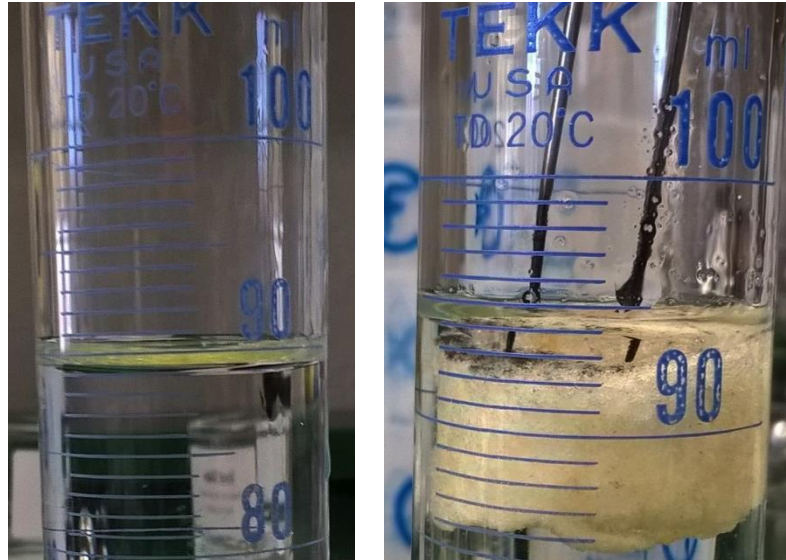
Figure 13: Core sample taken from piece B [2].

Results from these computations are summarized and tabulated in section 2.1.3.

#### 2.1.2.1.2 NON-UNIFORM CROSS SECTION

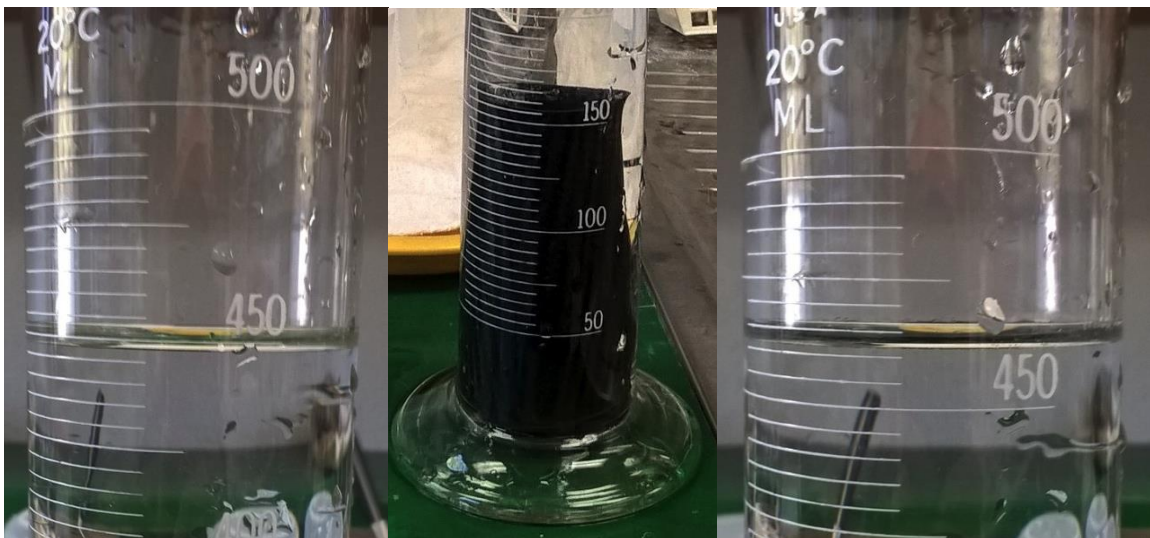
In contrast to the core sample taken from piece **B** (Figure 13), neither of the two samples taken from piece **C** (Figure 10) featured a uniform cylindrical geometry. Therefore, caliper measurements of the height and diameter of piece **C** would not yield accurate results for the density.

As an alternative, fluid displacement was used to determine the volume of the core samples. The masses of the samples were taken prior to recording the volume to account for the fact that the samples may absorb water once submerged. Figure 14 shows the change in volume of distilled water inside of a graduated cylinder, before and after one of the piece **C** core samples was submerged.



**Figure 14: Volume of water prior to piece C core submersion (left) and after submersion (right) [2].**

Similar to the irregular geometry core samples, the cross section of the grip is irregular due to the contours of its geometry. Therefore, fluid displacement was also used to determine the volume of the hollow grip piece C. The change in volume of distilled water inside of a graduated cylinder once the hollow grip sample was submerged is shown in Figure 15.



**Figure 15: Volume of water prior to hollow grip piece C submersion (left) and after submersion (right) [2].**

Fluid displacement offers higher accuracy when used to determine the volume of an object, in contrast to measuring an irregular shape, however this volumetric reading



is only as accurate as the scale on the graduated cylinder(s). Results from these computations is summarized and tabulated in section 2.1.3.

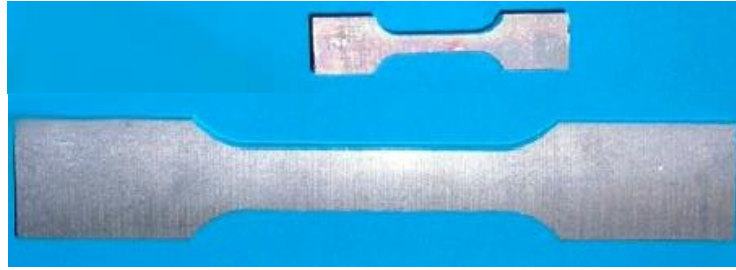
#### 2.1.2.2 TENSION

An MTS Insight 30 kN load frame was used to perform the tension tests on the coupon size samples. The frame equipped with the clamps used to perform the tension tests is shown in Figure 16.



Figure 16: MTS Insight load frame showing mounted clamps [2].

Ideally, the coupon size specimens used in the load frames have a flat rectangular cross section that are dog bone shaped. The ends of the samples feature a larger cross section which are held in the clamps during testing, while the break occurs at the thinner cross section. However, due to a limitation of available equipment, the samples taken from the handle were not fabricated into this dog bone shape. Examples of the dog bone specimen geometry are shown in Figure 17.



**Figure 17: Dog bone shape testing samples [8].**

The tested samples were taken from the shaft, which is a round rigid object. As a result, conventional clamp grips were not suitable to the sample geometries. Therefore, the clamp grips were modified prior to testing. Figure 18 shows the difference between conventional clamp grips used on dog bone specimens, and the modified clamp grips used to test the round samples.



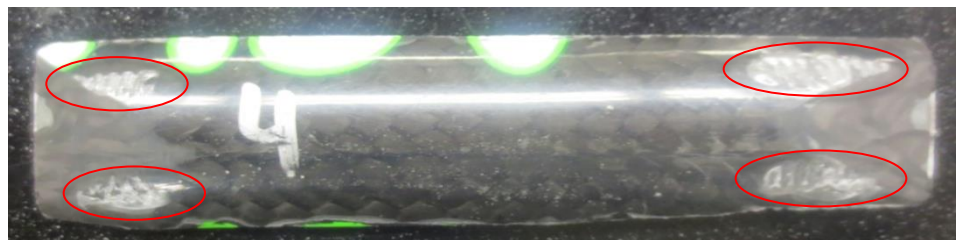
**Figure 18: Conventional clamp grips (left) and modified clamp grips (right) [2].**

The modification to the grips allows for more surface area contact between the curved specimen and the clamp grips, thus decreasing the probability of the sample(s) slipping through the clamp grips during testing. The tensile tests performed on samples from the shaft used the modified clamp grips, while the samples of the grip used the conventional clamp grips. This was made possible because certain portions of the contoured grip geometry were flat enough to produce flat samples which fit into the conventional clamp grips. Figure 19 shows examples of both shaft and grip samples mounted into the clamps.



**Figure 19: Shaft (left) and grip (right) samples mounted into clamp grips [2].**

To prevent slippage, both edges of the arced samples needed to be sanded down in order to better fit into the modified grips. Measures were taken to minimize the potential for slip, as certain samples had experienced some slip through the clamp grips. Evidence of slip was noted by the appearance of skid markings along the surface finish of the sample, as shown in Figure 20.



**Figure 20: Skid marks produced on a sample while it slips through clamp grips [2].**

Results from the tensile tests are summarized and tabulated in section 2.1.3.

### 2.1.2.3 COMPRESSION

The MTS Insight load frame was also used to perform the compression tests on the samples. Figure 21 shows the frame equipped with the mounted plates used to perform the compression tests.



Figure 21: MTS Insight load frame with mounted compression plates [2].

Samples from the shaft, grip, and core underwent compression testing to determine the core compressive strength, and shaft and grip critical buckling load. The compression tests performed on the shaft and grip samples provided knowledge of the material and/or mold underneath the surface composite. Through compressive testing, allowed the observation of material characteristics such as the direction of crack propagation and elastic restoration capabilities. Figure 22 shows examples of the shaft and core samples undergoing compression testing in the load frame.



Figure 22: Shaft (left) and core (right) samples undergoing compression testing [2].

Figure 22 shows the contrast between compressive failure due to buckling (shaft) and compressive failure due to plastic deformation (core). The larger slenderness ratio of the shaft sample is one of the factors which explains this difference in response to the applied load. Another factor which contributes to this buckling behavior is the large eccentricity in the load applied to the shaft sample, in contrast to a more unidirectional deformation seen in the core sample test.

Results from the compressive tests are summarized and tabulated in section 2.1.3.

#### 2.1.2.4 THREE POINT BENDING

The MTS Insight load frame was also used to perform three point bending tests on the samples. Figure 23 shows the frame equipped with the supports used to perform the bending tests.



**Figure 23: MTS Insight load frame showing mounted bending supports [2].**

Three-point bending tests were performed on samples from both the shaft and grip. The tests allow for a determination of flexural strength of each composite, which aid in the material identification process. Figure 24 shows examples of the shaft and grip samples undergoing three point bending in the load frame.



**Figure 24: Shaft (left) and grip (right) samples undergoing three point bending [2].**

Results from the three point bending tests will be summarized and tabulated in section 2.1.3.



### 2.1.3 RESULTS

The resulting material properties obtained from the experiments outlined in section 2.1.2 are presented in this section. Discussed are the experimental results for the density, tensile and compressive testing, three point tests and bond strength tests.

#### 2.1.3.1 DENSITY

The following section presents sample calculations for determining the densities of both uniform and non-uniform cross section samples. The data required to perform these calculations follows the methods discussed in section 2.1.2.1. Equation 1 is the formula for calculating the density of a uniform cross-section sample, and equation 2 is the method for calculating the density using fluid displacement.

$$\rho = \frac{m}{V} = \frac{m}{AL} = \frac{m}{\pi(r_o^2 - r_i^2)L} \quad 1$$

$$\rho = \frac{m}{V} = \frac{m}{V_f - V_i} \quad 2$$

Using equation 1 and 2, TABLE V shows the results of the density measurements of all three materials found across the handle.

TABLE V: EXPERIMENTALLY DETERMINED DENSITY VALUES

Material	Density [kg m <sup>-3</sup> ]	
	Non-uniform Cross Section	Uniform Cross Section
Top shaft	-	1903.5
Bottom shaft	-	1548.8
Grip	1241.3	-
Core C <sub>1</sub>	245	-
Core C <sub>2</sub>	265	-
Core B	-	256.5

Of the values listed in TABLE V, the bottom shaft density is the least accurate. As the bottom shaft is thicker than the top shaft, its density should be the greatest between the two. This discrepancy may be attributed to the variation between assumed and actual values of cross sectional area. Both the amount of material lost off the shaft due to sanding, and the presence of holes along the shaft which were not accounted

for during measurement affected both the uniformity of the cross sectional area and the sample mass. The discrepancies resulted in less accurate calculations of the density of these members.

### 2.1.3.2 PRELIMINARY TENSILE TEST RESULTS

Using the coupon shaped test pieces, preliminary tensile tests were performed. TABLE VI lists the key results from the preliminary tensile test performed on specimens 2, 3, 5, and 6.

TABLE VI: TENSILE TEST RESULTS

Specimen	Piece	Length (mm)	Cross-section Area (mm <sup>2</sup> )	Peak Load (N)	Ultimate Tensile Stress (MPa)	Modulus of Elasticity (MPa)
2	A	72	79	15,877	201	2,071
3	A	81	68	10,303	151	1,829
5	D	58	28	10,237	372	5,539
6	D	60	38	15,445	406	2,952

The values of peak stress were estimated using the equation 3 for engineering stress. The equation assumes that the cross-sectional area of the specimen remains constant during the application of the load.

$$\sigma_p = \frac{L_p}{A} \quad 3$$

Where,

$L_p$  = Peak load measured during testing

$A$  = Cross-sectional are of the specimen

The results for the peak load and stress show that specimens 5 and 6, which were parts of Piece D (bottom shaft) have higher values for ultimate stress than specimens 2 and 3 from Piece A (bottom shaft). This is counter-intuitive since as shown in the TABLE VI, specimens 2 and 3 have lower lengths and cross-sectional areas than specimens 5 and 6. Thus, based on length and cross-sectional area, the capabilities of specimens 5 and 6 to sustain a given load before failure occurs was



expected to be lower than those of specimens 2 and 3. This result suggests that the combination of materials used to make the bottom shaft, which based on visual inspection is thought to be a combination of carbon fibre and fibreglass composites, is weaker in tension than the bottom shaft. The bottom shaft appears to be mostly carbon fibre composite with a relatively thin layer (about 0.4 mm) of fibreglass on the underside compared to the thick layer (around 3 mm) of the fibreglass on underside of the top shaft.

The values of modulus of elasticity reported on the previous table were estimated from the stress-strain curve. Figure 25 shows a combined stress-strain plots containing data from all tensile specimens.

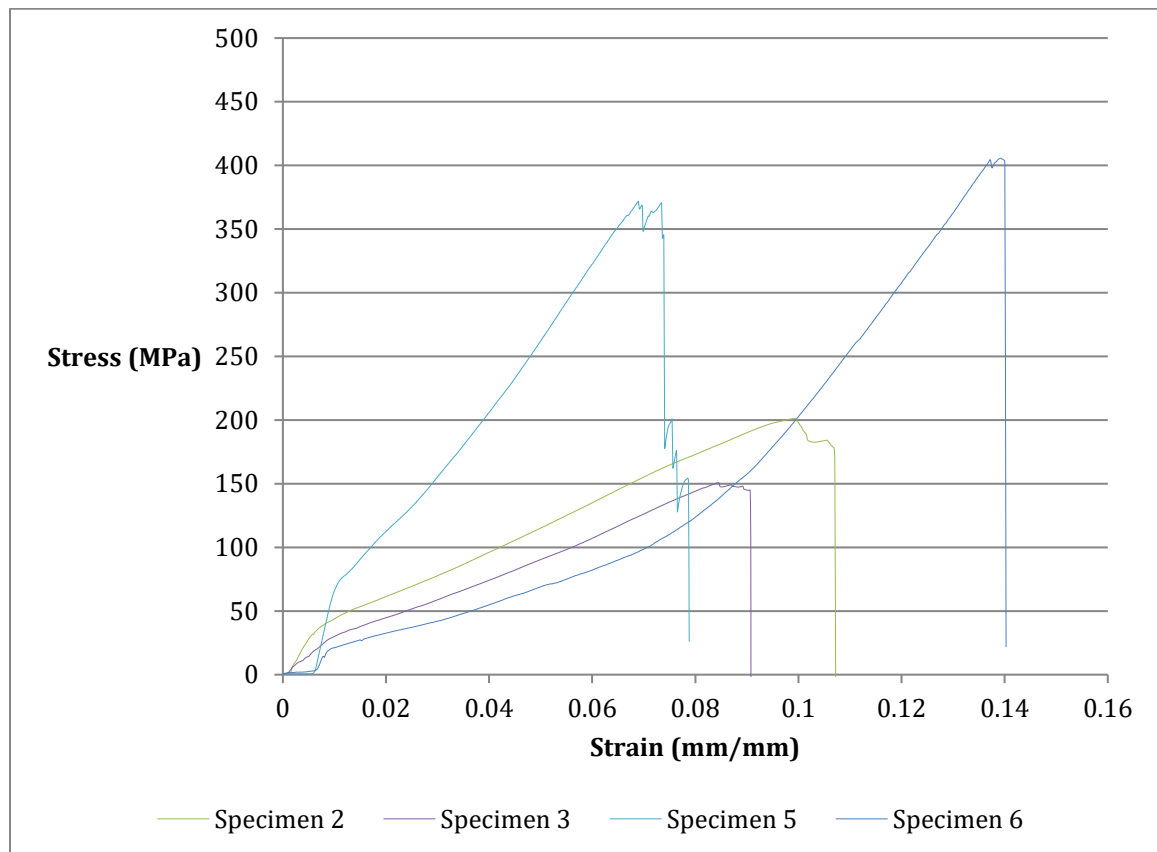
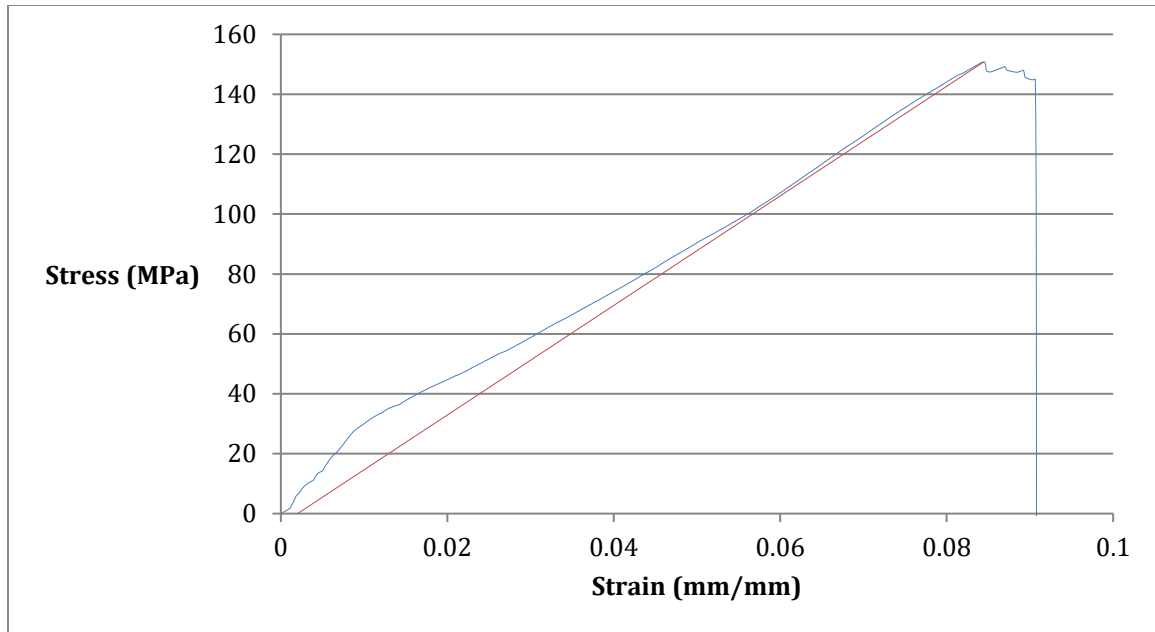


Figure 25: Stress-Strain graph for tensile testing.

To help explain the methodology used to estimate the values for the modulus of elasticity, the stress-strain graph for Specimen 3, from Figure 25, is integrated into Figure 26.



**Figure 26: Stress-Strain graph of tensile test on specimen 3.**

In Figure 26, the blue line represents the relationship between stress and strain in the material during tension. The modulus of elasticity of the specimens were estimated using the 'Offset Method' [9]. A line, shown in red, starts at a point where the value of strain is 0.002 mm/mm and ends at a point where the stress reach its maximum, which in Figure 26 is around 151 MPa. Taking the slope of this line gives the estimated value for the modulus of elasticity for the given specimen.

As the data measured through the preliminary tensile testing was inconsistent between trials, and the samples were not of uniform shape, the values determined for the elastic modulus cannot be relied upon. Additional tests will be required to produce data that is accurate enough to be used.

The main failure mode exhibited by most specimens during the tensile testing is similar to that of a brittle material. Fracture failure in the specimens occurred suddenly, with little to no sign of yielding. The sudden failure can be seen in Figure 25, with the sudden drop in the value of stress after reaching its peak indicates this phenomenon. Photos of specimens 2, 3, 5, and 6 after the tensile tests showing the location of fracture are shown in the Figure 27.

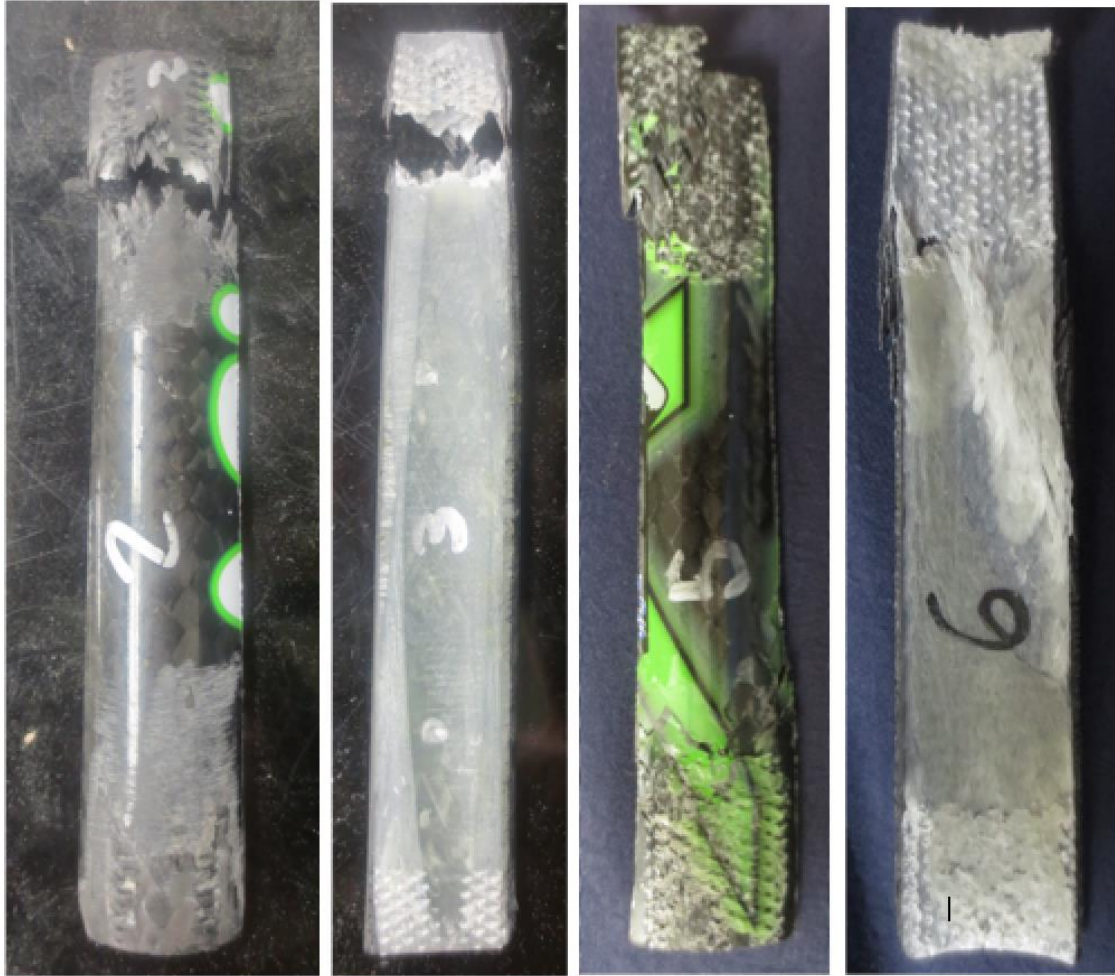


Figure 27: Fracture failure in specimens 2, 3, 5, and 6 during tensile test [2].

Shown in Figure 27, the particular regions where the fractures occurred in all specimens have distinct marks going towards the edge, indicating the areas where the specimens were clamped to the mounts. Also visible on specimen 3, and hidden on specimen 2 is a thick layer of white material, this white material is thought to be fibreglass, beneath the handles outer shell of carbon fibre.

### 2.1.3.3 IMPROVED TENSILE TEST RESULTS

After gaining access to better tools for cutting and shaping specimens, additional tensile tests were performed using samples of the grip composite with a shape more suited to tensile testing. The specimens were flatter, which reduced applied stresses caused by tightening the clamps. The samples also featured a smaller width in the

centre, allowing control over the fracture location. The improved test specimens produced for tensile testing are shown in Figure 28.



Figure 28: Improved tensile test specimens, cut from grip composite [2].

The results of the improved tensile sample tests are shown in the TABLE VII.

TABLE VII: SUMMARY OF IMPROVED TENSIL TEST RESULTS

Specimen	Length (mm)	Cross-Sectional Area (mm <sup>2</sup> )	Peak Load (N)	Ultimate Tensile Stress (MPa)	Modulus of Elasticity (MPa)
1	50.8	10.4	1326	127	9611
2	50.8	8.2	1016	124	9353

The data in TABLE VII was obtained using similar methods to those outlined for the preliminary tensile tests. Figure 29 shows the data the plot of the stress vs strain of the for the improved tensile tests. Of note in Figure 29 is the similar nature of the curves of the two specimens. The similarity indicates improved specimen quality, resulting in accurate, repeatable data.

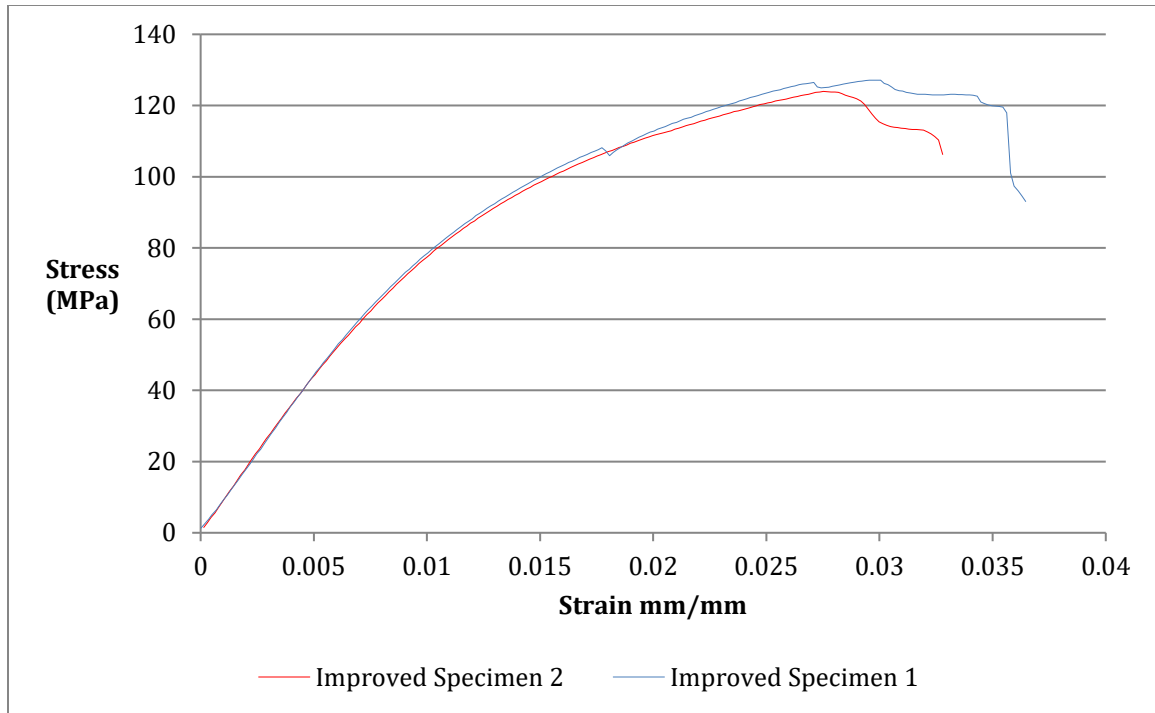


Figure 29: Stress-Strain graph for improved tensile testing.

The ultimate tensile stress is the most important data from these tests. This value, calculated using the ultimate load and cross-sectional area, indicates the maximum permissible tensile stress for the composite. It was calculated to be 127 and 124 MPa, respectively.

#### 2.1.3.4 STRENGTH OF BOND

Using cut samples of the handle, which contained portions of the grip and the shaft, tensile tests were performed to determine the bond strength. TABLE VIII lists the values of the peak load at around the same time that cracks began to form around the joint connecting the grip and the shaft, indicating the strength of the bond. The tests were done for specimens 9, 10, and 11 under tensile loading.

TABLE VIII: STRENGTH OF BOND BETWEEN GRIP AND SHAFT

Specimen	Piece	Peak Load (N)
9	A	1,820
10	A	956
11	A	1,420

The specimens used were irregular in shape (shown in Figure 30). Therefore, deciding on the appropriate cross section to be used to estimate the stress that corresponds to the peak load proved to be difficult. Thus, the values for the aforementioned peak stress were excluded from the table.



Figure 30: Irregularity in the shapes of specimens 9, 10, and 11 [2].

Based on the tests performed to determine the strength of the bond between the grip and the shaft, the group concluded that the bond is capable of withstanding an average load of around 1400 N or 1.4 kN before failure. Above this value, cracks will form and propagate causing the joint regions to fracture, separating the handle and the shaft from each other.

#### 2.1.3.5 COMPRESSION TEST RESULTS

Similar to the ultimate tensile stress, the ultimate compressive stress is the maximum stress experienced by the specimen under compression. The ultimate compressive stress corresponds to the peak load at which point the specimens begin to plastically deform. Based on the values of the stress measured, it is apparent that specimens cut out from the top shaft can withstand more stress than specimens cut out from the bottom shaft. The stress-strain graph for specimen 4 and 7 shows the

behavior of the specimens under compressive loading is shown in the Figure 31 below.

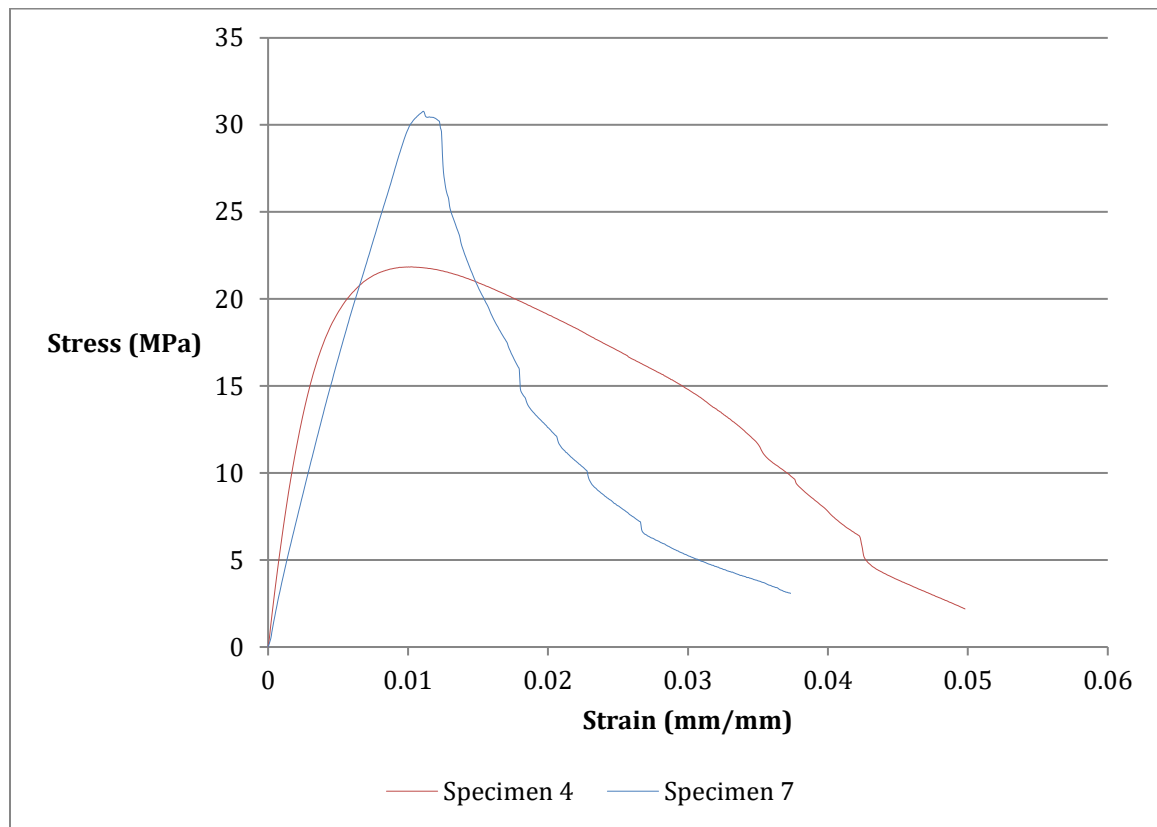


Figure 31: Stress-strain curves from the compression test.

During the test, it was determined that failure at the bottom shaft would likely occur due to buckling, as restorative elastic properties were observed in Specimen 4. Under compression, specimen 4 buckled before the testing machine stopped compressing the specimen. After unloading the specimen and removing it from the machine, the group watched as specimen 4 returned to its approximate original shape. Figure 32 shows the buckling of specimen 4.



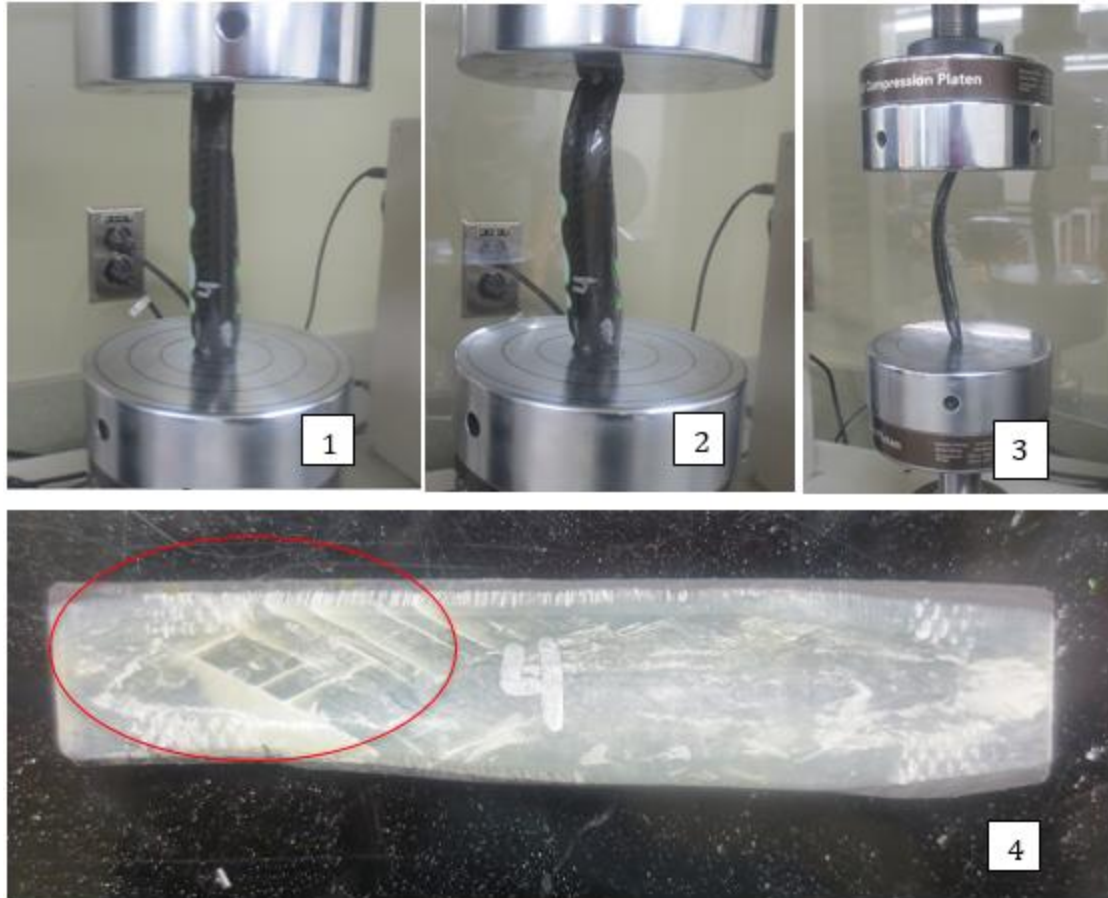


Figure 32: Sequence of events showing the behavior of specimen 4 during compression test [2].

Figure 32, step 1, shows the loaded coupon sample in the test saddles. After an applied compressive load was applied, steps 2 – 3, the coupon buckled. This deformation, caused by the compressive load, was partially elastic and partially plastic type of deformation. However, it can be seen in step 4 that some permanent deformation indeed occurred in the specimen, based on the fracture marks (circled in the photo) around the deformed region.

Specimen 7, however, deformed rather differently under compression, most likely due to its thin cross-section (around 1.7 mm) compared to the thicker cross-section of Specimen 4 (around 4 mm). The load was absorbed uniformly by the specimen, causing the middle of the specimen to fracture.

TABLE IX lists the key results from the compression tests performed on Specimens 4 and 7.



TABLE IX: COMPRESSION TEST RESULTS

Specimen	Piece	Length (mm)	Cross-section Area (mm <sup>2</sup> )	Peak Load (N)	Ultimate Compressive Stress (MPa)
4	A	64	76	1,650	22
7	D	69	37	1,128	31

Based on the data listed in TABLE IX, the ultimate compressive stress experienced by the coupon samples ranged from 22 – 31 MPa.

#### 2.1.3.6 THREE POINT BENDING TEST RESULTS

To obtain the values for the flexural stress at the peak load we assumed that the original curve-shaped specimen has a rectangular cross-section. With this assumption, the equation below for flexural stress for a rectangular cross-section can be applied.

$$\sigma_f = \frac{3FL}{2wt^2} \quad 4$$

Where,

$F$  = Peak load

$L$  = Specimen length

$w$  = Specimen width

$t$  = Specimen thickness

The results are summarized in the TABLE X below.

TABLE X: RESULTS FROM THREE-POINT BENDING TEST

Specimen	Piece	Peak Load (N)	Compressive Stress (MPa)
1	A	2,564	N/A*
8	D	764	1,242
* Specimen span is too short to apply classical beam theory			

#### 2.1.3.7 RESULTS DISCUSSION

The data obtained from the preliminary tests are a result of the group's best judgment. Using the assumptions made while performing each test, estimated values were obtained from preliminary test data. The accuracy of these values are limited by the accuracy of both the preparation methods and available equipment.

For example, the values of strain were obtained by assuming that the crosshead extension equals to the change in the length in the specimen. The problem with this assumption is that it does not take the slippage of the sample into consideration, as discussed in section 2.1.2.2. To accommodate the curved cross sections of the samples, the only way by which the group was able to mitigate these issues was to sand the ends of the specimens as flat as possible and modifying the clamp grips. Another considered solution to help decrease slip was to tighten the clamp grips on the sample more than usual. After a brief attempt, this method was deemed unsuitable, as it introduced unfavorable residual stresses in the material before the application of the test load which would have significantly altered the results.

It also should be noted that the abnormality of the sample shapes may have influenced the types of failure observed during testing. For example, fractures that occurred on the curved tensile specimens may have been influenced by stress concentrations induced by the clamp grips. As a result, fractures may have been more likely to occur near the sample and clamp grip contact points.

The second round of tensile tests were improved by using better tools to make the test specimens more suitable for the test machine. The two tests using the improved geometries (grip samples) yielded very similar results. Therefore, these results are much more reliable than the preliminary tests. It is possible that they could still be affected by systematic error, such as the previously stated strain assumptions. But the group is confident that these improved test results are an accurate representation of the actual mechanical properties of the material used in the first generation handle.

## 2.2 MATERIAL AND MANUFACTURING

Several material types and manufacturing processes commonly used in the advanced composite materials industry were considered for the final design. The suitability of various materials and manufacturing processes to the curling broom design will be compared. The first section gives a brief discussion of the different types of fibre reinforcements and resin systems that are commonly used in fibre-reinforce composites (FRP). Fibre types include synthetic or man-made fibre reinforcements carbon, fibreglass, and Kevlar, and synthetic resin systems epoxy, polyester, and vinyl ester. A brief description of the basic steps in fibre manufacturing, and examples of the types of products that are made from each fibre is included. Lastly, bonding methods of composite materials, manufacturing processes used to form composite materials are all discussed at the conclusion of the section.

### 2.2.1 FIBRES

Composite reinforcements come in many forms, such as particulates, whiskers, and fibres. Particulates are small, irregularly shaped reinforcements that are typically used as fillers to reduced material cost. Whiskers, or short fibres, have a rod-like shape and are smaller in both length and diameter than fibres. Whiskers are extremely strong but hard to disperse in the resin uniformly [10]. Fibres, which are the focus of this section, are long, thin cylindrically shaped reinforcements with properties highest along the fibre axis.

Fibre reinforcement fall under two types: natural fibres and synthetic fibres. Natural fibres include plant-based (as well as animal-based) fibres such as flax, hemp, wheat, and barley. Many of these fibres are abundant in nature, renewable, and inexpensive, which leads to their growing use in many industries such as automotive, aerospace, and sporting goods. However, natural fibre composites are still under development, and the majority of their implementations are still in the research and development stages. The second type of fibre is synthetic fibres, which

include the three fibres discussed in the following sections: carbon fibre, fibreglass, and Kevlar. Although they are more expensive than natural fibres, synthetic fibres are used more in advanced composites, due to their superior mechanical properties, lower moisture and thermal sensitivity properties than natural fibres [11].

#### 2.2.1.1 CARBON FIBRES

Carbon fibre is an organic or synthetic polymer material, which is characterized by a long chain of carbon atoms that are tightly linked together in microscopic crystals. A single strand of carbon fibre is extremely fine with a diameter somewhere between 5 - 10 microns [12], about 10 times smaller than a human hair (40 - 120 microns) [13]. The raw material used to make carbon fibre is called the precursor. There are two kinds of precursor materials:

- Polyacrylonitrile (PAN), which makes up about 90% of all carbon fibre produced
- Rayon or petroleum pitch, which constitutes the remaining 10%

The typical process for making carbon fibre consists of the following steps:

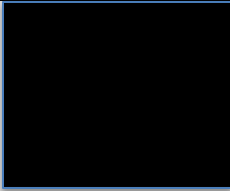

1. Spinning
2. Stabilizing
3. Carbonizing
4. Surface treatment, and
5. Sizing

The process starts by drawing the precursor material into the fibres, followed by heating the fibres in an oxygen-free gas mixture. Heating in these condition removes other non-carbon atoms in each fibre, leaving a fibre composed of mostly carbon atoms. The surface of each fiber is then treated to enhance chemical and mechanical bonding with resins, and other materials used in making composites. In the last step, sizing, the fibers are coated with materials such as epoxy, polyester, nylon or urethane. These coating materials protect the fibers from damage that may occur during the winding and weaving processes [12].

After the sizing step, multiple fibres are then twisted together to form a yarn. The yarn can be used 'as is', or woven into a fabric to suit many other applications. Several common varieties of carbon fibre products, including different fabric types, are listed and described in TABLE XI.

TABLE XI: EXAMPLES OF COMMON CARBON FIBRE PRODUCTS [14] [15] [16] [17]

Name		Features
Carbon Fabric	<p>Figure 33: Roll of carbon fibre fabric [14].</p>	<ul style="list-style-type: none"> <li>- Used with epoxy, polyester, and vinyl ester resins</li> </ul> <p><u>Uni-directional fabrics</u></p> <ul style="list-style-type: none"> <li>- Non-woven fabrics consisting of all fibres running in a single direction, where properties are highest in the direction of the fibre</li> <li>- Ideal for applications where optimum properties in a single direction is desired</li> </ul> <p><u>Bi-directional Fabrics</u></p> <ul style="list-style-type: none"> <li>- Consist of fibres running in two directions resulting in uniform strength in the specified directions</li> <li>- Is relatively weaker than UD fabric due to crimping of fibres</li> <li>- Comes in two varieties, plain weave and 2x2 twill weave, and distinct weave patterns</li> </ul>
Carbon Fibre Tape	<p>Figure 34: Rolls of carbon fibre tape [15].</p>	<ul style="list-style-type: none"> <li>- Used with epoxy, polyester, and vinyl ester resins</li> <li>- Non adhesive woven fibreglass tape that are ideal for winding applications and selective reinforcement of fibreglass laminates</li> <li>- Uniform strength in both horizontal and vertical directions</li> </ul>

Name	Figure	Features
Carbon Sleeve	 <p>Figure 35: Carbon fibre sleeve [16].</p>	<ul style="list-style-type: none"> <li>- Used with epoxy, polyester, and vinyl ester resins</li> <li>- Braided sleeve that has a cylindrical shape capable of conforming to the exact shape of products with changing geometry</li> <li>- Ideal for making precise composite products</li> <li>- Can be stretched and compressed, respectively, by up to 30% and down to 70% of its based diameter</li> </ul>
Carbon Prepreg	 <p>Figure 36: Carbon fibre pre-preg [17].</p>	<ul style="list-style-type: none"> <li>- Resin pre-impregnated fabrics</li> <li>- Uniform resin content, and curing agent is already included</li> <li>- Reduces cure time and minimizes wasted material</li> </ul>

The properties of carbon fibre make it a great choice as reinforcement for composite parts. Several of the desirable properties for carbon fibre include:

- high stiffness
- high tensile strength
- high fatigue resistance
- lightweight
- high chemical and corrosion resistance
- high temperature tolerance
- low coefficient of thermal expansion

The main disadvantage of carbon fibre is that it is a brittle material. As such, mode of failure could be catastrophic (i.e., parts will fracture or splinter) once the material is pushed beyond its capabilities [18] [19] [20].

#### 2.2.1.2 FIBREGLASS

Fibreglass is another synthetic polymer material made from a mixture of silica sand and other raw materials such as limestone, soda ash, and recycled or waste glass [21]. Silica is the basic element found in a naturally occurring rock called quartz.

Quartz is produced by heating pure silica just above 1200°C, which is immediately followed by rapid quenching. This results in crystallization of the heated material, forming quartz in the process. However, when pure silica is put through the same process of heating and rapid cooling but using temperature above its melting point of around 1720°C, the process of crystallization is prevented. This results in the production of an amorphous material known as glass [22].

Glass fibres are manufactured through the following sequence of steps:

1. Batching
2. Melting
3. Fibreization
4. Coating, and
5. Drying/Packaging.

Batching involves careful and accurate weighing of the raw materials, mixing the silica sand and the other raw materials together to form a batch. This batch is then fed into a high temperature furnace for melting before being transformed into fine strands through mechanical extrusion. Each strand of fibreglass typically has a diameter between 4 - 34 microns [22].

The types of fibreglass products available in the market today come in similar varieties to carbon fibre products. Among the products are unidirectional and bi-directional fabrics, mats, tapes, and sleeves. Fibres can take the form of long continuous fibres, or short chopped fibres. Fibreglass, when sold, is designated with a special name to indicate the unique characteristics. TABLE XII provides a list of common types of glass fibre along with their specific properties.

**TABLE XII: DIFFERENT TYPES OF FIBREGLASS AND THEIR SPECIFIC PROPERTIES [23]**

<b>Fibreglass Type</b>	<b>Property</b>
E-Glass (E = Electrical)	High electrical resistance
S-Glass (S = Strength)	High tensile strength
C-Glass (C = Chemical)	High chemical resistance
M-Glass (M = Modulus)	High modulus of elasticity
A-Glass (A = Alkali)	High alkali content
D-Glass (D = Dielectric)	Low dielectric constants
ECR-Glass (ECR = Electrical & Corrosion)	High electrical and corrosion resistance

Glass fibres are organized into two categories. The first category is called the general-purpose fibres, which constitutes over 90% of all glass fibres. The types of glass fibres in this category are the E-Glass variants: boron-containing E-Glass and boron-free E-Glass. The second category includes all the remaining types of glass fibres and is referred to as special-purpose glass fibres [23].

Fibreglass is an all-purpose type of composite reinforcement and is the most widely used fibre in the composite industry. The cost of fibreglass is relatively low compared to its counterparts, carbon fibre and Kevlar. It is often used for projects where lower cost is more important than achieving minimum weight for the composite part. Although the density of fibreglass is relatively higher than carbon fibre or Kevlar, its density is significantly lower than conventional materials such as wood and steel [20].

#### **2.2.1.3 KEVLAR**

Kevlar belongs in the aromatic polyamide or aramid family. It is characterized by a long chain of repeated chemical compounds made from low-temperature polycondensation reaction of 1,4-phenyl-diamine or para-phenylene diamine (PPD) and terephthaloyl chloride (TCl). A liquid mixture of PPD, TCl, and other solvents forms the precursor material, which is heated to a suitable temperature in 100% sulphuric acid, and drawn into fine strands of Kevlar by an extrusion method such as dry-jet wet spinning process [24].



There are three types or grades of Kevlar: Kevlar 29, Kevlar 149, and Kevlar 49. Kevlar 49 is made specifically for composite reinforcement [25]. As an alternative to carbon fibre and fibreglass, Kevlar is an excellent choice for high abrasion, and impact resistance applications. The main disadvantages of Kevlar are that the material can be difficult to cut, sand, and machine, and is not suitable for applications where the composite part is subjected to mainly compressive loading [26].

Products that can be made from carbon and fiberglass are typically also available for Kevlar. These products include woven fabrics, tapes, sleeves, and prepregs.

#### 2.2.1.4 COMPARISON OF FIBRE PROPERTIES

TABLE XIII provides a relative comparison of the physical properties of fibreglass, carbon, and Kevlar, with each fibre assigned a rating of either: P for poor, F for fair, G for good, or E for excellent.

TABLE XIII: COMPARISON OF PROPERTIES FOR CARBON FIBRE, FIBREGLASS, AND KEVLAR [27]

Specifications	Fibreglass	Carbon	Kevlar
Density	P	E	E
Tensile Strength	F	E	G
Compressive Strength	G	E	P
Stiffness	F	E	G
Fatigue Resistance	G-E	G	E
Abrasion Resistance	F	F	E
Sanding/Machining	E	E	P
Conductivity	P	E	P
Heat Resistance	E	E	F
Moisture Resistance	G	G	F
Resin Compatibility	E	E	F
Cost	E	P	F

TABLE XIII shows that carbon fibre is excellent in the majority of the above specifications. It performs better than fibreglass and Kevlar in terms of mechanical properties, but is inferior to both in cost. Fibreglass is the most economical option, followed by Kevlar. Kevlar performs better than carbon fibre in fatigue and abrasion resistance categories. However, since the group had identified that the customer

needs of strength and durability for the new design were weighted more than the cost, carbon fibre is the best choice for reinforcement.

### **2.2.2 MATRIX**

Matrices are polymers that are used in combination with fibre reinforcements to create composite materials. The resin forms the matrix of the composite, which allows for the efficient transfer of the applied load to the fibres. Their main role is to protect the fibres from harmful substances in the environment and bind the fibres together in an array of different arrangements to suit numerous applications [28].

#### **2.2.2.1 IDEAL CHARACTERISTICS OF A MATRIX**

An article on composite materials in states, the four desirable characteristics of a matrix for making composites are as follows [29] :

1. Mechanical properties
  - The matrix must possess excellent mechanical properties such as high ultimate strength, high elastic modulus, high strain to failure, etc.
  - The resin must be able to deform, at least up to the same extent of deformation as the fibres during loading
2. Adhesive properties
  - The strength of the bond between the resin and fibres must be high in order to ensure efficient transfer of load from resin to fibre
3. Toughness properties
  - The resin must have high resistance to crack propagation
4. Environmental degradation
  - The matrix must exhibit high resistance to harmful substances in the environment

#### **2.2.2.2 MATRIX TYPES**

Matrices are classified under two types. The first type is called thermoplastic, which includes polymers such as nylon, polypropylene, and acrylonitrile butadiene styrene (ABS). Thermoplastics are unique because their polymers do not form cross-linkages during the heating process. In other words, no bonding occurs between the

polymers contained in the resin. This unique characteristic allows thermoplastic resin to be remolded and recycled, as it can be reheated from a solid state to a liquid state and back many times without significant degradation of the material properties in either state [30]. However, the resin will start to deteriorate in the molten state. Therefore, there is a limit to how often thermoplastics can be reused [31].

The second type of matrix is called thermosets. When mixed with a curing agent, and in the presence of an initiator during the curing process, this type of resin undergoes an irreversible chemical reaction causing the formation of cross-linkages between polymers in the resin. This chemical reaction is called polymerization. Unlike a thermoplastic resin, thermosets cannot be reheated and remolded once the resin 'sets' or hardens after the initial curing process. Prolonged exposure to heat will cause the material to degrade rather than melt [31]. Thermosets include the three most commonly used matrices in the composite industry, namely epoxy, polyester, and vinyl ester.

#### **2.2.2.3 EPOXY**

In terms of performance, epoxy typically performs better than all the other types of matrices in the market today. They are popular due to their outstanding mechanical properties and resistance to environmental degradation. Epoxy resins are widely used for low and moderate temperatures of up to 135 °C or 275 °F and provides better high-temperature performance compared to polyester and vinyl ester [28]. Depending on the choice for the curing or cross-linking agent, the resin is also relatively easy to handle during the curing process. They can cure at temperatures between 5°C to 150°C. They exhibit less shrinkage during curing when compared to polyester resins, resulting in lower internal stresses. Furthermore, epoxy's high electrical insulation and good chemical resistance enhance the resin's high adhesive strength and high mechanical properties [30].

#### 2.2.2.4 POLYESTER

Polyesters are the most widely used type of matrix in the composite industry and commercial applications (e.g., clothing, home furnishing, and insulation). They are popular in the industry because they cost less than either epoxy or vinyl ester, and offer easier handling. Polyesters consist of the polyester resin itself, a curing agent, and an initiator or catalyst (unlike epoxy, which uses a hardener). Styrene is usually used as the curing agent, which not only allows for the cross-linking of the polymers in the resin, but also helps in lowering the viscosity of the resin for ease of processing. A catalyst like methyl ethyl ketone peroxide or benzoyl peroxide helps initiate and speed up the polymerization reaction between the resin and the curing agent. [28] Polyesters can be used for both continuous and chopped fibres and are referred to as 'contact' or 'low pressure' resins because they can be molded without the need to apply high pressure [30].

#### 2.2.2.5 VINYL ESTER

Vinyl ester is sometimes referred to as 'epoxy' vinyl esters because they share the same molecular backbone as epoxy [32]. However, its full molecular structure closely resembles that of polyester. Although vinyl esters and polyesters share some structural similarities, the two resins differ in their molecular structures, particularly in the locations of their respective reactive groups. The difference gives vinyl esters an edge over polyesters in terms of toughness and resilience. Furthermore, vinyl esters are also more resistant to water degradation and other harmful substances than polyesters and epoxy resins [28] [30].

#### 2.2.2.6 COMPARISON OF MATRIX PROPERTIES

TABLE XIV shows a relative comparison of specific properties for the three resin matrices discussed in the previous sections. Each matrix has been assigned a rating of either: P for poor, F for fair, G for good, or E for excellent.

TABLE XIV: COMPARISON OF MATRIX PROPERTIES [28] [30] [32] [33] [34]

Specifications	Epoxy	Polyester	Vinyl Ester
Mechanical Properties	E	P	F-G
Adhesion Capability	E	F	G
Toughness	G	P	E
Chemical & Environmental Resistance	G	P	E
High Temperature Capability	E	P	F
Ease of Handling	F	E	G
Cure Shrinkage Resistance	E	P	F
Fibre* Compatibility	G	F	F
Cost	P	E	G
Shelf Life	F-G	F	P
* Carbon Fibre, Fibreglass, and Kevlar			

Overall, the superior matrix among the three selections is epoxy. It is followed by vinyl ester and then polyester. Epoxy is superior in terms of mechanical properties, adhesion capability, high temperature capability, and resistance to shrinkage during curing. It is highly compatible with all three types of fibres, carbon fibre, fibreglass, and Kevlar (except with fibreglass mats) [33]. Polyester and vinyl ester tend to bond well with only fibreglass. Similar to carbon fiber, the greatest drawback of epoxy is its cost, as it is the most expensive matrix of the three. However, as mentioned earlier, strength and durability should not be sacrifice to achieve a cheaper product in the end. Thus, with its mechanical properties, epoxy would be the best option for the matrix. The combination of carbon fiber and epoxy would make for a super lightweight, strong, and durable new design of the handle.

### 2.2.3 BONDING

It is often impractical to manufacture products whole. When it is impractical to manufacture a product whole, post-manufacturing bonding is required. For the Xtreme Force curling broom handle, the shaft and the grips were manufactured separately, and then they were bonded together. There are two methods to bond composite parts together: mechanical fasteners and adhesives.

### 2.2.3.1 MECHANICAL FASTENERS

Some examples of mechanical fasteners include rivets, pins and bolts. Mechanical fasteners provide a high strength, single point reinforcement, are easy to install and disassemble when necessary, and function with any part thickness or surface area. However, there are several factors that should be considered when using fasteners in a composite [35].

Drilling through a composite can compromise the structural integrity compared to metals. Composites also have relatively poor bearing properties compared to metals, meaning the fastener must be larger to prevent it tearing through the composite. As composites on their own are very light, fasteners can add a considerable amount of weight. As well, exposed fibres can absorb moisture causing localized weakness.

### 2.2.3.2 ADHESIVES

Adhesives avoid the problems associated with mechanical fasteners by eliminating the need to drill through the composite. However, there are also associated disadvantages to adhesives. The process is more complicated as adhesives require careful preparation of the surfaces to be bonded, and defects are much more difficult to detect. The cost of tools and materials for adhesive bonding are much higher than those for mechanical fastening. Also, the adhesive material could have associated environmental concerns.

The most common adhesives used to bond composites are epoxies, acrylics and urethanes [35]. Epoxies consist of a resin and a hardener, and are very versatile as there are many different epoxy resins and hardeners available to join most materials [36]. Epoxies have good strength, however they are a brittle adhesive. Epoxies are commonly used with epoxy-based composites because they have similar flow characteristics.

Acrylics are fast curing and offer high toughness in addition to strength. They are available in one-part or two-part systems and bond well to a wide range of materials. Urethanes provide strong impact resistant joints and have better low temperature strength than any other adhesive, and are often used for bonding glass fibre composites.

Since the curling broom is already a very light product, the weight would be greatly affected by metal fasteners. The smooth surface offered by adhesive bonding makes the broom more comfortable to hold. Additionally, as the current design's surface to be bonded is a cylinder that fits into another, it can be extended as far as necessary to provide enough bonding area for the required strength. Therefore, adhesives will be preferable over mechanical fasteners for the final design. However, the type of adhesive used in the final design will depend on the materials used in the final design.

#### **2.2.4 MANUFACTURING**

Composite manufacturing methods are the processes used to shape the part, wet the fibres with the resin, and cure the part. Desirable qualities of manufacturing processes are high productivity, minimum material cost, maximum geometrical flexibility (compatibility with shape complexity and size), maximum property flexibility (such as fibre volume fraction and fibre direction), and reliable, high quality manufacture [37]. Some of the most common composite manufacturing methods are described in this section. They include the following: contact moulding, autoclave moulding, filament winding, resin transfer moulding, and pultrusion.

##### **2.2.4.1 CONTACT MOULDING**

The simplest method of composite manufacturing is contact moulding. Contact moulding involves manually placing the dry fibre reinforcement onto a tool surface and applying the resin. The resin allows the reinforcement to stick to the tool and maintain the desired shape during the process. The tool and part are then enclosed in a vacuum bag, and the air is removed to cure the part under pressure. Once the

part is fully cured, it is removed from the tool, which is then ready to begin a new part.

The advantage of contact moulding is that it is highly flexible in terms of part shape, and requires minimal infrastructure making it very inexpensive [37]. However, the quality of the finished part is highly dependent on the skill of the worker, and therefore, it is difficult to guarantee high quality parts. Also, because the applied pressure is relatively low, the natural packing density limits the volume fraction of fibre.

#### **2.2.4.2 AUTOCLAVE MOULDING**

This method commonly uses fibre fabrics that are pre-impregnated with uncured resin, called pre-pregs. These pre-pregs can be unidirectional or woven, and can be cut and moulded into various shapes. These pre-pregs are layered onto the tool to the desired thickness, then placed in a vacuum bag. The entire assembly is placed into an autoclave, a pressure tank with elevated temperatures, to cure the part.

Autoclave moulding results in more reliable quality compared to contact moulding. The higher pressure and temperatures used allow for much more control over the physical properties of the final part. However, the initial costs of the autoclave are very high, and the ongoing costs of the pre-preg material are higher than that of the basic materials used for other processes. Still, autoclave moulding is one of the most dominant methods of composite manufacturing [37].

#### **2.2.4.3 FILAMENT WINDING**

Commonly used for cylindrical structures, this method involves winding the fibres under tension around a rotating mandrel. The fibres are continuously drawn through a resin bath to wet them immediately prior to being placed on the part. Once the mandrel is covered to the desired thickness, heat is then applied to the part to cure the resin. Small parts can be heated in an oven, while very large parts are



surrounded by heaters. After curing, the mandrel can be removed or it can remain as a part of the finished product.

Filament winding method is capable of producing parts very quickly. It is also highly automated which reduces labour costs, and increases reliability and quality. However, the geometry is limited to open or closed end cylinders [37].

#### **2.2.4.4 RESIN TRANSFER MOULDING (RTM)**

Resin transfer moulding describes processes wherein dry fibre is formed into the desired shape in a closed mould, prior to the introduction of resin. Directly before the curing process begins, resin is injected using a differential pressure, and is allowed to permeate the fibre. After the resin has fully wetted (complete resin flow over the fibre) the entirety of the reinforcement, the part is cured using normal pressure and temperature methods.

The advantages of resin transfer moulding are the high geometrical and property flexibility. Any fibre weaves can be used in this method, and formed into complex shapes. The resin injection can be varied to control the fibre volume fraction of the part. However, the resin injection must also be controlled to ensure complete wetting of the fibres. As a result, advanced fluid dynamic solutions, and extensive testing are required to create a mould shape that allows even resin flow across the entire part [37].

#### **2.2.4.5 PULTRUSION**

Similar to filament winding, fibres are continuously drawn through a resin bath immediately prior to being shaped, but instead of being wound around a mandrel, bundles of wet fibres are pulled through a die to create a long part of constant cross-section. An initial pre-die is used to remove excess resin and pre-form the approximate final shape. A curing die is used to finalize the cross-sectional shape and apply heat to the part to cure it.

This method has a very high rate of production, but is restricted to constant cross-section components with unidirectional fibres, meaning geometrical and property flexibility are low [37].

#### 2.2.4.6 COMPARISON OF MANUFACTURING PROCESSES

To help determine appropriate manufacturing methods to be used in the design, the following Figure 37 summarizes the relative strengths of the five manufacturing methods discussed.

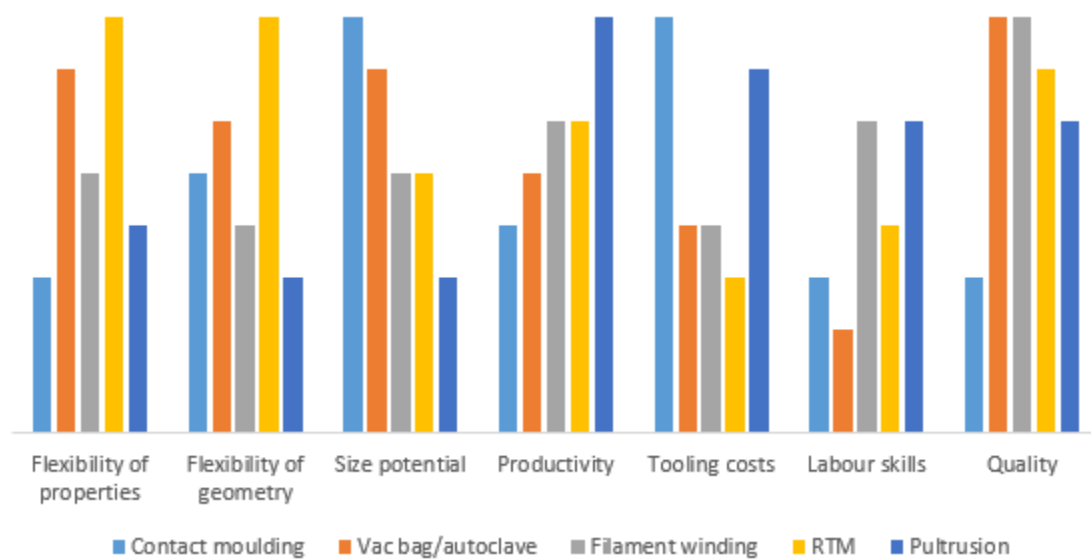


Figure 37: Comparison of common manufacturing methods. Based on [37].

There are two main components of the curling broom design: the shaft and the grip. The handle is a long constant cross section cylinder, and the grip is a shorter complex shape. Due to its present shape, the grip cannot be manufactured using filament winding or pultrusion. If the final grip design has complex geometry similar to the current design, and requires the use of a foam core, the higher geometrical flexibility of autoclave moulding or resin transfer moulding will be preferred, and so they will be the most likely candidates for manufacturing the grip.

Unlike the grip, the shaft has a constant cross section, and so all the manufacturing methods described above are possible. To maximize productivity, filament winding or pultrusion could be used to create very long shafts that can then be cut to length.

Out of these two processes, filament winding allows for control over fibre direction, and therefore more control over properties, and also requires less tooling expenses. If the shaft is to be produced in smaller sections, autoclave moulding may be a good choice as it could share a manufacturing method and pre-preg material with the grip, reducing costs.

In summary, based on the current curling broom handle design, the most likely candidates for manufacturing the grip are autoclave moulding or resin transfer moulding, due to their high geometrical flexibility. The plausible candidates for manufacturing the shaft are filament winding for productivity and fiber direction control, or autoclave moulding for the opportunity to use the same manufacturing method as the grips.

### 3. CONCEPTUAL DESIGN

The selected conceptual design was chosen through the use of screening and scoring 30 preliminary concepts, the details of which may be found in APPENDIX B. Before discussing the details used to develop the physical and technical specifications of the final design, the basic characteristics of the selected conceptual design will first be outlined.

#### 3.1 PRELIMINARY DESIGN

The design that was selected through the concept screening and scoring process was called design BCFP. This design contained a number of features that met the customer needs which were previously discussed in section 1.4.1. Figure 38 shows a conceptual image of this design which was pursued.



Figure 38: Side view of conceptual design BCFP.

##### 3.1.1 NUMBER OF GRIPS

A common complaint in the market feedback on the first generation curling broom handle was that the hand grip locations were too restrictive on the user. One of the common suggestions provided in the feedback was to remove the top grip to help alleviate this restrictiveness [6] [38] [39]. Since most of a sweepers weight is transferred via their lower hand to the ice, users felt that having only one grip at the bottom of the handle would result in a more comfortable and versatile handle, while retaining its effectiveness. By removing the upper grip, the user comfort would be improved, while still maintaining the sweeping efficiency that the original handle had.

##### 3.1.2 REMOVAL OF GRIP LIPS

The next feature incorporated into the concept was the removal of the grip lips. Market feedback indicated that the lips caused blisters on the user's hands [38]. As

the purpose of the product is to increase sweeping effectiveness without compromising comfort, the potential for user harm presented by the lips is of considerable concern. Moreover, a person is generally less likely to use a product, such as this broom handle, if prolonged use can potentially cause harm. Figure 39 shows an image of the location lips on the first generation handle.



Figure 39: Grip lips which are to be removed with the redesign of the curling broom handle. The area of the lips is circled.

### 3.1.3 GRIP ANGLE

The next incorporated aspect of concept BCFP is the adjusted grip angle. As with the removal of the second grip, user feedback indicated that the grip angle felt uncomfortable and unnatural [6] [39]. To determine the new hand angle relative to the shaft, three different methods were used.

#### 3.1.3.1 INITIAL METHODS

The first generation of the Xtreme force curling broom handle featured an angle of 38°. The first adjusted angle, which was suggested by the customer, was half that of the first generation handle resulting in a new angle of 19°. This change in the angle was suggested based on customer feedback, and the realization that the adjusted angle would more closely resemble a standard handle. While the angle approaches a standard handle, it would still provide the user with the improved sweeping effectiveness

The next method of grip angle determination was through the creation of a mockup handle, Figure 40. Using the mockup, the team adjusted the model and determined an angle which felt most natural to use, while simulating a sweeping motion. From the mockup, the team decided that the most natural feeling angle was approximately that of the original grip. Therefore, the group decided to proceed with a variation containing the original 38° angle.



Figure 40: Mockup handle created to determine the handle angle which felt most natural [2].

### 3.1.3.2 STUDY GROUP ANALYSIS

The third method used to determine a new grip angle was through analysis of curlers using standard handles. The angle at which a curling broom is held with respect to the ice was analyzed by watching a large sample size of curlers sweeping using standard handles. In order to have this data represent a wide variety of curlers, the broom handle angles of 15 different sweepers were recorded. These 15 sweepers belonged to three different categories of curlers to help represent a wide variety of users. The analyzed sweepers included elite male curlers (five sweepers - early 20s), elite female curlers (three sweepers - early 20s) and recreational senior male curlers (seven sweepers - 60-80 years old).

The broom handle angles were measured using still photos of sweepers at the outer and inner positions of their pull strokes and push strokes respectively. These still photos were acquired by filtering through footage of each sweeper frame by frame using SMPlayer video playback software. The broom handle angles were collected from each of these still photos using the “angle tool” feature in ImageJ image analysis software. Figure 41 shows an example of a still photo angle measurement using the software.

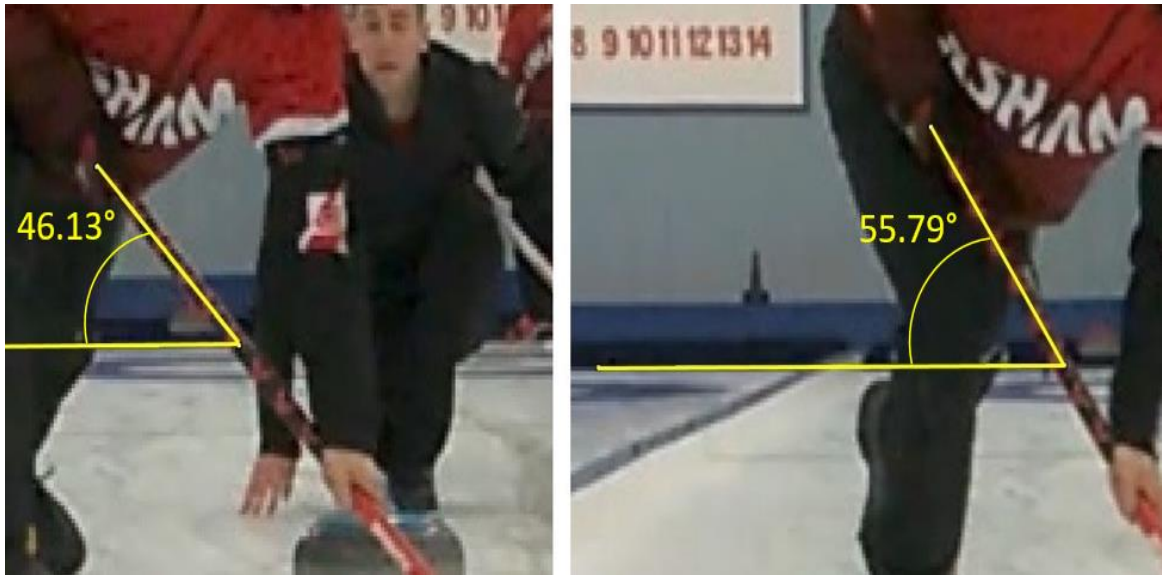


Figure 41: Example of broom handle angle measurement in ImageJ software. Left photo shows apex of push stroke, right photo shows apex of pull stroke. Line used to measure the broom angle is shown in yellow along the broom handle, and the recorded angle is highlighted in the orange box [2].

Available filming equipment did not allow for an ideal filming angle, which would have been perfectly parallel with the sheet, as close to the ice as possible. Therefore, the angle of the broom handle was taken with respect to a “horizontal” reference behind the sweeper, which adequately represents the angles true projection. It should also be noted that the accuracy of the ImageJ angle tool is limited to human error, as the angle is constructed by freehand without the use of concrete reference points in the photo. To help mitigate the element of human error and validate each recorded broom angle, the majority of the sweepers had their broom angles recorded using multiple trials. An average of each recorded angle was then taken to be that particular sweeper’s push or pull stroke angle. TABLE XV shows the average push and pull stroke angles organized by sweeper type.

TABLE XV: AVERAGE RECORDED BROOM HANDLE ANGLES IN DEGREES

Stroke	Males	Females	Seniors	Average
Pull Stroke	55.7	56.8	56.6	56.4
Push Stroke	45.8	44.4	50.8	47.0
Change in angle	9.9	12.4	5.7	9.4

Although each type of curler represented in TABLE XV ends the pull stroke at very similar angles, a greater variation exists between their push stroke angles. This is somewhat expected due to the different strengths and weaknesses possessed by each of these three sweeper types. The data reflects the potential benefits to be gained by incorporating an adaptability mechanism into a future iteration of the design. The greatest measured pull stroke angle was  $68^{\circ}$  while the smallest measured push stroke angle was  $36^{\circ}$ , which is a significant variation.

The sweeping analysis confirm that there is simply no perfect grip angle that will suit every curler, as the handle angle variations between each sweeper is too great to ignore. The rounded-down average angle of the push and pull stroke of all three sweeper types was selected as the third variation to be proceeded with. This corresponded to a grip angle of  $51^{\circ}$ .

#### **3.1.4 FINGER INDENDATION**

The last potential feature which was considered for the pursued final design was the inclusion of more pronounced finger indentations. The goal of this potential feature was to improve the user's capability of holding the grip. However, after consulting with the customer on this matter, it was determined that this feature would be omitted from the final design. Since market feedback had already characterized the handle as being too restrictive, increasing the pronunciation of the finger indentations would further increase the restrictiveness of the handle and diminish the user's experience.

After concept BCFP was selected by the team, all concepts, including those which were not pursued (APPENDIX B), were presented to the client. Once the clients became familiarized with all of these concepts, they agreed that concept BCFP would best match their needs in contrast to the other concepts.



### 3.2 STATIC ANALYSIS

After having selected a concept, the next step in the design process was to determine the required properties of the materials which would withstand the load applied by a sweeper onto the handle. To determine these material properties, the team elected to use Finite Element Analysis (FEA), a numerical method used to determine solutions to complex problems.

However, in order validate the results obtained from FEA, the problem must first be evaluated using analytical methods to confirm the accuracy of the numerical results. To verify the results, simplified 2D static loading analyses were performed on the handle, treating it as a beam. Figure 42 shows the setup used to analytically compute the static reactions on the broom.



Figure 42: Free body diagram setup used in analytical calculations of the stresses.

Referring to Figure 42, the right hand side of broom handle is treated as if it is being held with a fixed support. This type of support restricts all movements of the broom in the X and Y coordinates at this location, simulating the connection between the broom handle and the broom head. Towards the left hand side of the broom handle, a roller support is applied, which restricts the movement of the broom in only the Y direction. This support simulates the upper hand holding the broom, free to move with the handle in the X direction. The assumption of a roller support on left hand side of the broom allowed the analysis to be statically determinate. In contrast, treating the left hand support as if it were fixed would have resulted in the problem becoming statically indeterminate. The computations required to solve a statically indeterminate system are significantly more complex, and would not significantly have affected the accuracy of the results. Furthermore, there are no loads or

reactions to the left of the roller support (i.e. above the sweepers top hand), so analysis of this section is omitted from future analyses and discussion.

The load  $P$  applied to the beam in Figure 42 is located at the center of the grip and acting perpendicular to the surface. Since the grip is on an angle with respect to the global coordinate system, the applied load must be resolved into both X and Y components matching this coordinate system. Figure 43 shows a diagram of the decomposition of the applied load into its components, and equations 5 and 6 represent the equations used to resolve the applied force into the global coordinate components.

$$P_x = P \sin \theta \quad 5$$

$$P_y = P \cos \theta \quad 6$$

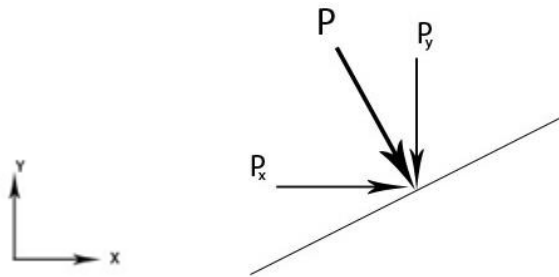


Figure 43: Decomposition of the applied load into two vectors corresponding to global coordinate system.

Using the resolved components of the applied load, the overall reaction forces of the system were then determined. Figure 44 shows the global reactionary forces.

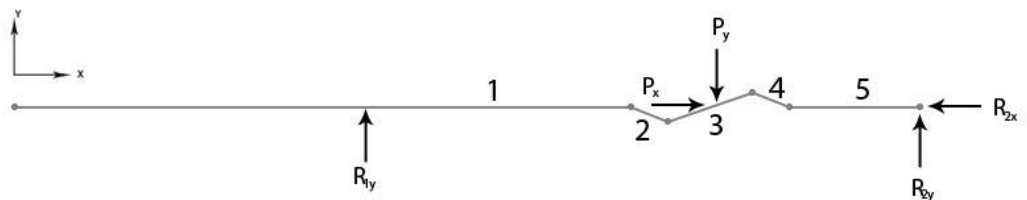


Figure 44: Free body diagram of the statics system with resolved components.

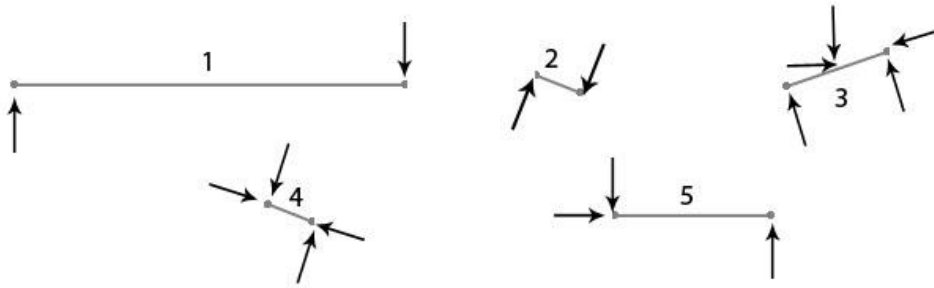
Based on Figure 44, three unknown values exist in the system,  $R_{1Y}$ ,  $R_{2X}$ ,  $R_{2Y}$ . The values of these reactions were determined by balancing the forces and moments acting on the system, as shown in equations (7 - 9).

$$\sum F_X = 0 = P_X - R_{2X} \quad 7$$

$$\sum F_Y = 0 = R_{1Y} + R_{2Y} - P_Y \quad 8$$

$$\sum M_2 = 0 = x_2 P_Y - x_1 R_{1Y} \quad 9$$

With the overall global reactions were determined, the relative local reactions were next determined. By separating the handle into five different sections Figure 45, the handle was treated as being entirely composed of two-force members.



**Figure 45: Decomposition of the relative axial and normal forces in each member. The axial forces are treated as acting in the x direction and the normal forces are treated as acting in the y direction.**

Starting with the section 5 and applying equations 5 and 6, the local reaction forces for each of the five members were decomposed from the global reference frame. This separation process allowed for the isolation of both the axial and normal forces applied at each section. From the axial forces, the tensile and compressive stresses were calculated using equation 10, with  $A$  being the cross-sectional area of the handle.

$$\sigma_a = \frac{F_a}{A} \quad 10$$

From the normal forces, the moment experienced by each member was then calculated, using equation 11, where  $d$  represents the distance between the two normal forces.

$$M = F_N * d \quad 11$$

Using the calculated moments, the bending stress of each section can be calculated using equation 12.

$$\sigma_{bending} = \frac{My}{I_x} \quad 12$$

Where  $y$  is the distance from the outer edge of the handle to the neutral axis, and  $I_x$  is the area moment of inertia, which can be calculated using equation 13.

$$I_x = \frac{\pi}{4} (r_2^4 - r_1^4) \quad 13$$

Using equations 5 – 13, TABLE XVI through TABLE XVIII contains the calculated axial and bending stress for each of the three selected grip angles. Calculations used to produce these results are provided in APPENDIX C. Using a factor of safety of 2, this resulted in a load of 300 lb (1334.5 N) being applied along  $P$ .

**TABLE XVI: ANALYTICAL STRESS CALCULATIONS FOR HANDLE AT 19° AT 300 LB APPLIED**

Member	Axial Stress [MPa]	Bending [MPa]
1	0.00	216.55
2	1.37	29.38
3	- 1.21	100.74
4	- 5.48	29.29
5	- 3.43	173.98

*(-) denotes compressive*

**TABLE XVII: ANALYTICAL STRESS CALCULATIONS FOR HANDLE AT 38° AT 300 LB APPLIED**

Member	Axial Stress [MPa]	Bending [MPa]
1	0.00	180.50
2	1.65	22.30
3	- 1.91	77.36
4	- 8.26	6.17
5	- 6.49	145.00

*(-) denotes compressive*

TABLE XVIII: ANALYTICAL STRESS CALCULATIONS FOR HANDLE AT 51° AT 300 LB APPLIED

Member	Axial Stress [MPa]	Bending [MPa]
1	0.00	144.15
2	1.39	17.39
3	- 1.93	85.83
4	- 9.11	7.53
5	- 8.19	115.80

*(-) denotes compressive*

Comparing the axial stress values for each member in TABLE XVI through TABLE XVIII, it can be seen that increasing the grip angle results in increased compressive stresses and decreased tensile stresses along the handle. A comparison of the bending stresses shows that for sections 1,2 and 5 the bending stress decreased, and increased for sections 3 and 4.

The analytical results listed in TABLE XVI through TABLE XVIII were used as a reference to verify that the results obtained through FEA are valid.

### 3.3 CONCEPT MODELS

Initial models of the three analyzed variations of concept BCFP, are provided in Figure 46 through Figure 48. The difference in the hand angle variation between the 3 grip angles is visible.



Figure 46: 19° BCFP (XtremeForce Pro).



Figure 47: 38° BCFP (XtremeForce Original).



Figure 48: 51° BCFP (XtremeForce 51).

Many of the geometrical features such as the overall length of the handle, diameter of the shaft, and the shaft thickness are the same for all three variations. The difference between each variation is the angle that the grip makes with the longitudinal axis of the handle.

## 4. FEA METHODOLOGY

FEA is a numerical method which is used to determine solutions to complex problems. Initially, the user must define a geometry using CAD, and specify the loading conditions acting on this geometry within the FEA software. The program, otherwise known as the finite element code, then subdivides the inputted geometry into smaller elements. This array of elements, which is governed by the user defined geometry, is referred to as a mesh. Each element within the mesh consists of a multitude of nodes, or end points, which results in a multiple sided element.

For this analysis, the geometries of the concepts outlined in section 3.3 were produced using two different CAD softwares, Fusion 360 and SolidWorks. These geometries were then imported into the FEA program ANSYS Workbench for numerical evaluation.

### 4.1 MATERIAL PROPERTIES

Composite materials exhibit orthotropic properties, a subset of anisotropic properties. Orthotropic materials exhibit different material properties with respect to the material's three orthogonal axes. When selecting a composite for a desired application, its orthotropic properties need to be determined, and specifically tailored, to the design for which they are to be used. Therefore, determination of the material properties and the layup was the first aspect involved in the design.

Initially, the three designs were analyzed assuming isotropic properties in order to determine the magnitudes and directions of the principal stresses greater ease in contrast to initially assuming anisotropic properties. Once the principal stresses were determined, the required strength in each orthogonal direction was determined. Using the computed principal stress values, both the layup and the required fibre – resin combination for each variation of the design were then selected. Details of the layup and material selection will be further discussed in section 4.6.

The assumed isotropic properties used in this initial portion of the analysis are representative of actual standard carbon fibre properties. These assumed values are given in TABLE XIX.

**TABLE XIX: ASSUMED ISOTROPIC PROPERTIES REPRESENTATIVE OF STANDARD CARBON FIBRE**

Property	Value	Units
Young's Modulus	70	GPa
Poisson's Ratio	0.1	-

## 4.2 GEOMETRIC CONSTRAINTS

Once the initial material properties were defined, the application of geometric constraints to the model were considered. The application of constraints to a geometry restricts specified locations in the way that they react to the applied loads. The application of these constraints is necessary to allow for the applied, and transmitted forces, to be simulated and computed using FEA. Ultimately, these constraints are directly applied to the defined region of elements within the mesh.

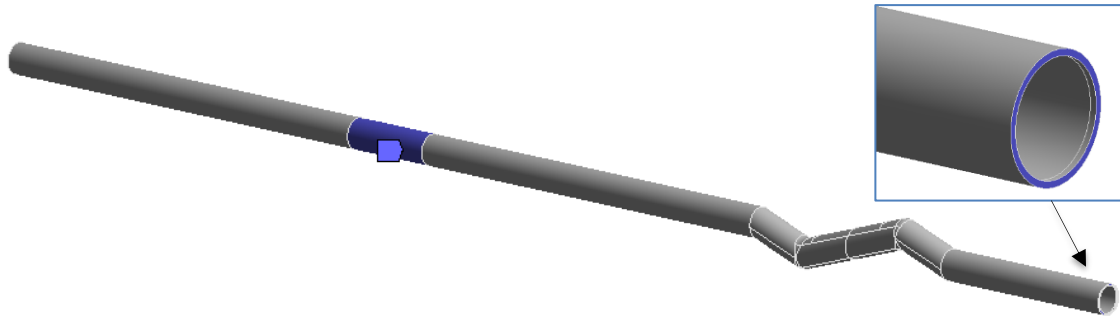
Geometric constraints may be applied in a variety of ways within FEA. The most common type of constraint is to fix the location of an element, where its freedom of displacement is restricted in respect to any combination of the globally defined X, Y or Z axes (UX, UY, UZ). Another commonly used geometric constraint is to restrict the rotation of an element, or an array of elements, about the globally defined X, Y or Z axes (ROTX, ROTY, ROTZ).

In order to set up an FEA in ANSYS, the user must apply geometric constraints to model faces, edges or lines, along with the mesh nodes and elements. The geometric constraint applied to the analysis of this design consisted of two fixed supports.

The first fixed support was applied at the bottom cross sectional face of the handle (closest to the ice). This fixed support restricts the shaft face in respect to all six of the aforementioned displacement constraints. The application of this constraint is intended to simulate the transmission of the forces through the handle, to the broom head, and finally to the ice. The second fixed support is applied at the



longitudinal location the top grip from the first generation handle (farthest from the ice). The application of this constraint is intended to simulate an approximation of the sweeper's upper hand location. Figure 49 shows the application of these geometric constraints to the 19° model.



**Figure 49: Fixed geometries applied to the 19° angle model. Close up of the end of the handle constraint is included.**

The geometric constraint applied to the upper portion of the shaft in Figure 49 spans 84 mm, which represents the average male hand width [40]. This value was also used in determining the area on which the load is applied on the upper side of the grip.

### 4.3 LOADING

The World Curling Federation tests broom handles using an applied load of 150 lbf (667.2 N) [7]. However, this value does not take into account a factor of safety. In order to ensure a safe final design, the group elected to pursue the analysis considering a safety factor of 2. The factor of safety is typically applied in one of two ways: decreasing the allowable stress, or increasing the applied load. For simplicity, the team elected to apply the safety factor the applied load. In doing so, the applied load considered throughout the analyses increased to 300 lbf (1334.5 N). This load is applied onto the geometrically constrained model as a distributed load along the grip face, normal to the grip angle. The direction and location of the applied load is intended to simulate a sweeper operating at maximum force. The red highlighted region in Figure 50 shows both the direction and location of the applied load.

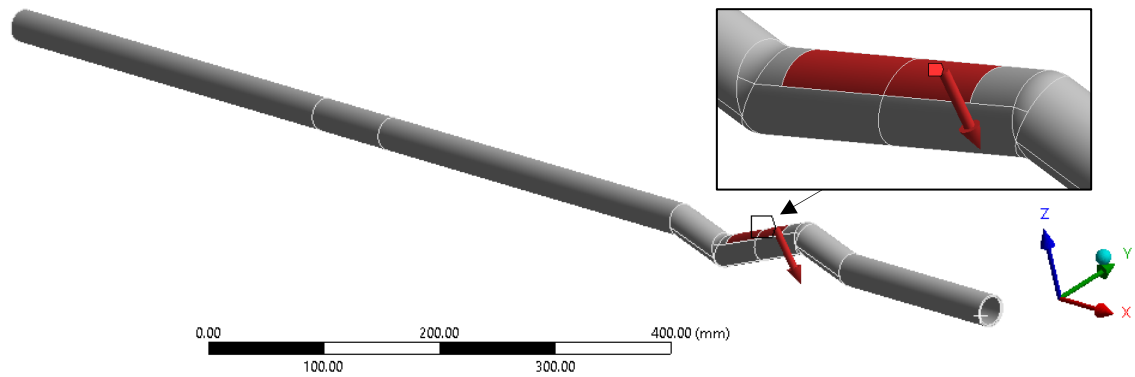


Figure 50: Application of the distributed 300 lb load along the top edge of the grip.

#### 4.4 MESHING

With the material properties of the handle selected and the boundary conditions set, the next phase in the FEA process is to select an appropriate meshing for the model. By default, when meshing is performed in ANSYS workbench, the mesh that was produced consisted of mostly tetrahedral (tet) elements. These elements are used as the default type since they are adaptable to different shapes and can efficiently populate curved sections of a model, even if the mesh is relatively coarse.

In addition to the tet element type, the three other element types used to mesh objects in ANSYS Workbench include hexahedrals (hex), prisms, and pyramids. All of these element types that are shown in Figure 51.

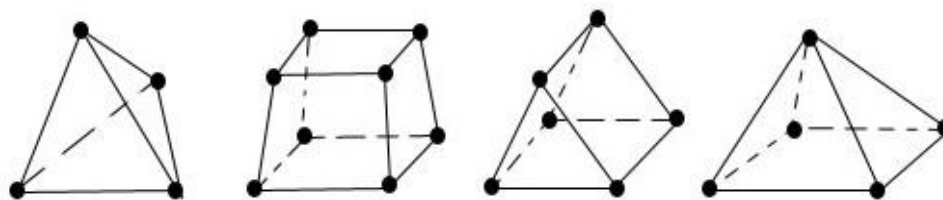
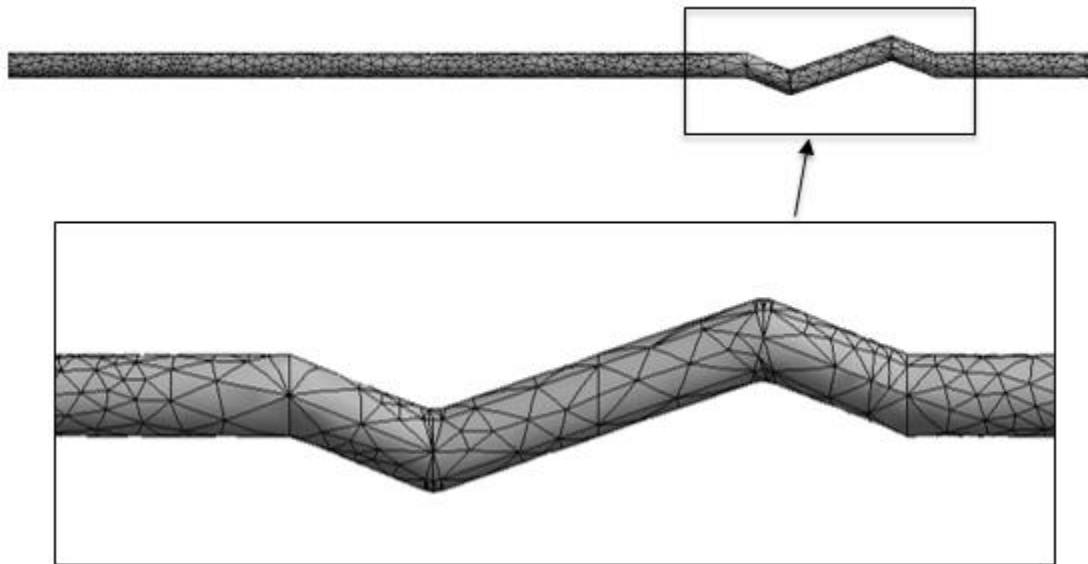


Figure 51: 3D mesh elements from left to right: tetrahedral, hexahedral, prism, and pyramid. Based on [41].

The round objects located at every vertex of an element are referred to as nodes. Material properties, as well as all solution variables, are stored at these nodes. In ANSYS Workbench, the user has an option to turn on the mid-side nodes of an element, giving the elements extra nodes for storage. Generally, a higher element

count (i.e. more nodes in the mesh) will yield more accurate results. However, this is not always the case, as solution accuracy often depends on an explicit analysis of the mesh to ensure that it is representative of the geometry's response to the defined loading condition. This mesh analysis typically includes, but is not limited to, localized mesh refinement in high stress concentration areas, as well as performing a mesh convergence to verify its validity. It should be noted that the preliminary FEA only considered the mesh refinement aspect of the mesh analysis. A detailed description of a mesh convergence analysis is given following the finalization of the optimized design in section 5.1.

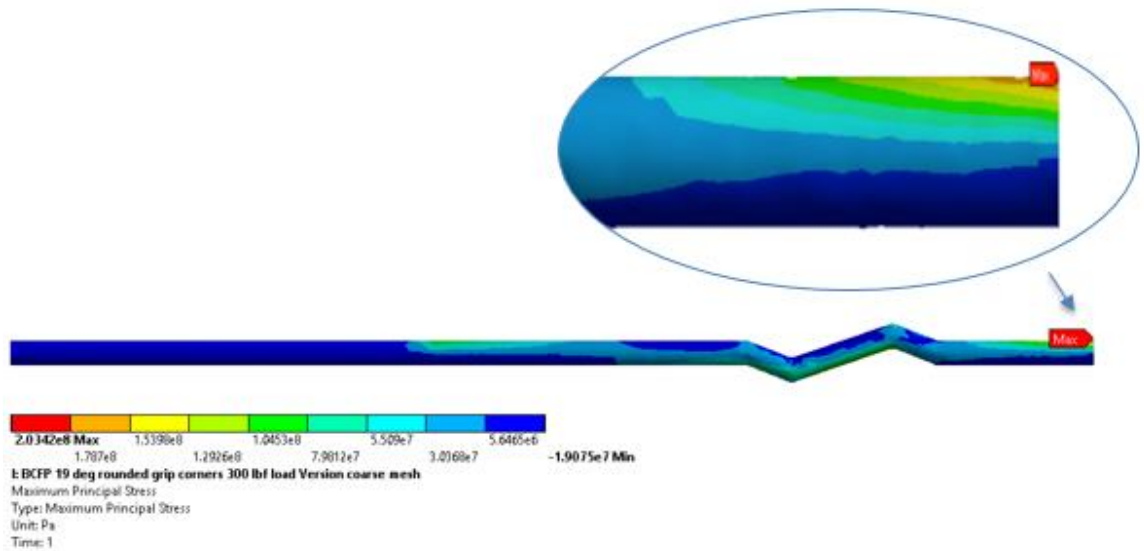
The mesh refinement controls in ANSYS can be used in various combinations to refine specific areas of the geometry. As an example, Figure 52 shows a coarse mesh for the 19° BCFP model generated using the default settings in ANSYS Workbench.



**Figure 52: Coarse mesh of 19° handle using default settings in ANSYS Workbench, showing a close up of the mesh elements generated around the grip.**

Figure 52 shows how the elements are resolved around the handle and the relative size of the elements. Initial FEA performed on the mesh yielded the peak stress location at the fixed end of the handle, and significant variability of stresses at the two fixed regions and along the entire grip. A contour plot of the maximum principal

stress showing the location of the peak stress and the stress variation in the handle is shown in Figure 53.



**Figure 53: Contour plot showing max principal stress in the 19° handle using a coarse mesh.**

Since stresses are expected to vary considerably in these critical areas of the handle, the element size was reduced in these areas. A preliminary reduced element size of 3.8 mm was applied to the ANSYS geometry to obtain a finer mesh. This element size was arbitrarily chosen as a means of illustrating the effects that a reduced element size has on the analysis results. The finer mesh generated using this element size featured approximately twice as many elements as the previous coarse mesh. Figure 54 through Figure 60 show close ups of the regions in the geometry where this mesh refinement was applied.



Figure 54: Mesh of entire handle after controls applied.



Figure 55: Mesh at the location of rear hand.



Figure 56: Close up view of the refined mesh at the location of rear hand.



Figure 57: Mesh at the location of grip.

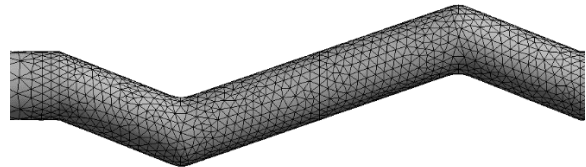


Figure 58: Close up view of the refined mesh at the location grip.

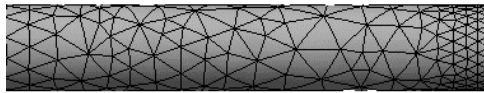


Figure 59: Mesh at the location of the head.

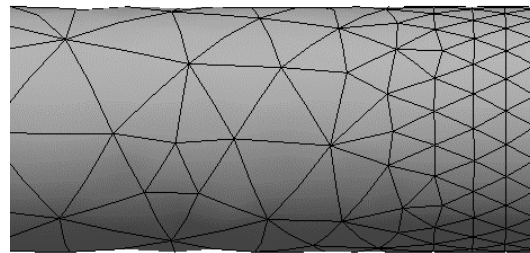


Figure 60: Close up view of the refined mesh at the location of the head.

In contrast to the initial coarse mesh previously shown in Figure 52, the refined model features a denser mesh in the critical regions. Using the same material properties, geometric constraints and loading conditions outlined in sections 4.1 to 4.3, a second analysis was then repeated on this finer mesh.

TABLE XX lists the maximum values of several monitored values for each of the two discussed meshes. These values include maximum total deflection, maximum Von Mises stress, maximum normal stress in three directions, x, y, and z of the default global coordinate system, and the maximum principal stress.

TABLE XX: COMPARISON OF RESULTS BETWEEN COARSE AND REFINED MESH.

Mesh		Coarse	Refined	% Difference
Total Deflection (mm)		3.6883	4.1735	12.3
Von Mises Stress (Mpa)		192	248.66	25.7
Max Principal Stress (MPa)		203.42	225.16	10.1
Normal Stress (MPa)	Global x-direction	202.67	224.66	10.3
	Global y-direction	70.706	149.5	71.8
	Global z-direction	83.517	186.27	76.2

The percent differences of the values given in TABLE XX vary significantly, between 10.1% and 76.2%. The considerable differences between these results signify the need for further analysis of the effect of changing the mesh density on the validity of the results. This additional analysis is done through a mesh convergence, which is discussed in greater detail in section 5.2.1.

#### 4.5 INITIAL FEA RESULTS

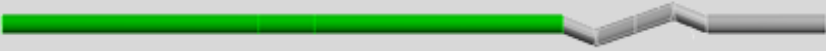
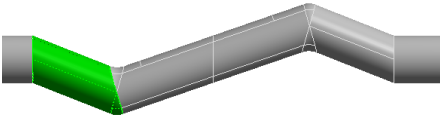
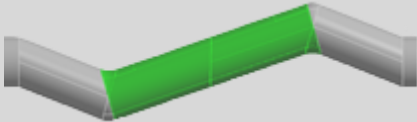
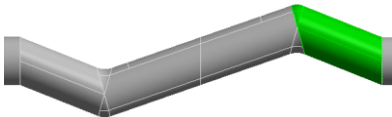

This section provides a brief discussion of the FEA results, along with a comparison between the FEA and statics results for the three grip variations. The FEA results for the three boundary conditions are tabulated for the three handle variations in TABLE XXI.

TABLE XXI: FEA RESULTS FOR 19° HANDLE

Grip Angle	Max Von Mises (MPa)	Global Coordinate System Normal Stress (MPa)			Coordinate System 2 Normal Stress (MPa)			Coordinate System 1 Normal Stress (MPa)			Max Principal stress (MPa)
		x	y	z	x	y	z	x	y	z	
19	248.66	197.66	149.5	182.56	208.13	149.9	168.3	224.66	149.94	186.27	<b>225.16</b>
38	211.96	140.82	112.31	166.8	143.26	112.31	148.13	194.05	112.31	195.59	<b>205.27</b>
51	147.23	109.72	92.925	112.78	103.35	92.925	104.57	147.61	92.925	145.75	<b>151.08</b>

Similar to the statics analysis, the FEA model of the handle was analyzed in five sections representing the five members of the statics model so as to facilitate an analogous comparison of results. TABLE XXII shows the location of these sections on the model.

TABLE XXII: FIVE SECTIONS OF THE HANDLE REPRESENTING THE FIVE LINES OF THE STATICS MODEL

CAD Model Section	Statics Analysis Section	Section (highlighted region)
1	1	
2	2	
3	3	
4	4	
5	5	

Since the stresses calculated in the statics analysis are along the axis of each isolated member, two coordinate systems, in addition to the default global coordinate system are introduced. Due to the differences in the grip angles between the three designs, the two supplementary coordinate systems are oriented differently for each handle variation. The contrast between the orientations of these supplementary coordinate systems are given in Figure 61 to Figure 63.



Figure 61: Introduction of supplementary coordinate systems of the 19° handle variation.



Figure 62: Introduction of supplementary coordinate systems of the 38° handle variation.



Figure 63: Introduction of supplementary coordinate systems of the 51° handle variation.

For simplicity, the two additional coordinate systems are given the names: Coordinate System T (for top portion of grip) and Coordinate System B (for bottom portion of grip). Starting from the left in Figure 61 to Figure 63, the coordinate systems are as follows: Global Coordinate System (default), Coordinate System T, and Coordinate System B. TABLE XXIII through TABLE XXV contain comparisons between the numerical and analytical results.

TABLE XXIII: FEA AND STATICS RESULTS FOR 19° HANDLE

Section	Coordinate System	FEA		Statics	
		Max Normal Stress in +x-axis (MPa)	Min Normal Stress in +x-axis (MPa)	Combined Tensile Stress (MPa)	Combined Compressive Stress (MPa)
1	Global	198.8	(-) 113.8	216.55	(-) 216.55
2	1	197.66	(-) 137.11	30.75	(-) 28.01
3	2	178.11	(-) 203.64	99.53	(-) 101.95
4	1	95.041	(-) 100.43	23.81	(-) 34.77
5	Global	224.66	(-) 219.46	170.55	(-) 177.41

(-) denotes compressive

TABLE XXIV: FEA AND STATICS RESULTS FOR 38° HANDLE

Section	Coordinate System	FEA		Statics	
		Max Normal Stress in +x-axis (MPa)	Min Normal Stress in +x-axis (MPa)	Combined Tensile Stress (MPa)	Combined Compressive Stress (MPa)
1	Global	137.38	(-) 104.44	180.50	(-) 180.50
2	1	117.93	(-) 114.3	20.65	(-) 23.95
3	2	143.26	(-) 125.15	75.45	(-) 79.27
4	1	95.507	(-) 107.43	-2.09	(-) 14.43
5	Global	194.05	(-) 193.61	138.51	(-) 151.49

(-) denotes compressive



TABLE XXV: FEA AND STATICS RESULTS FOR 51° HANDLE

Section	Coordinate System	FEA		Statics	
		Max Normal Stress in +x-axis (MPa)	Min Normal Stress in +x-axis (MPa)	Combined Tensile Stress (MPa)	Combined Compressive Stress (MPa)
1	Global	108.99	(-) 81.33	144.15	(-) 144.15
2	1	94.69	(-) 76.65	16	(-) 18.78
3	2	103.35	(-) 92.44	83.90	(-) 87.76
4	1	67.97	(-) 73.03	-1.58	(-) 16.64
5	Global	147.61	(-) 153.68	107.61	(-) 123.99

*(-) denotes compressive*

At this point, a methodology had developed to determine the significant stresses in each of the three grip variations. The next steps required the application of orthotropic properties into the numerical model where the layup was then iteratively determined while maintaining a suitable mesh (which satisfies convergence).

## 4.6 INITIAL DESIGN OPTIMIZATION

With the material and lay-up of the final design selected, the next step is to validate and optimize the design. This includes applying the composite lamina lay-up into the designed models using a function within ANSYS called ACP (ANSYS Composite Prep/Post). ACP is a powerful tool incorporated into ANSYS which permits the user to divide up a part and apply different material orientations to each division. These divisions act as the lamina, and the orientation is the way in which the lamina is aligned. Typical values for the orientation are  $0^\circ$ ,  $\pm 45^\circ$  and,  $\pm 90^\circ$ . The buildup of the lamina of varying orientations, effectively models an orthotropic composite material such as carbon fibre for static FEA. The following sub-sections provides an overview of the basic steps in the layup determination process using the aid of ANSYS ACP and a discussion of the end results, which identifies the appropriate laminates for the three handles.

### 4.6.1 LAYUP DETERMINATION WORKFLOW

The basic workflow starts by importing a shell-based model of the handle into ACP (Pre). A shell-based model is A 2-D mesh consisting of thin elements called shell elements. Fiber orientation and ply material are all defined within ACP (pre), where a number of these plies can be stack together in sequence called stackups (laminate). With the ability to control both fiber orientation and the number of plies in a stackup, an infinite number of stackups can be evaluated to obtain the optimum ply orientation and sequence that satisfies the design criteria.

In addition to being able to create and apply different stackups to the model, the user at the end also has an option to generate a 3-D model of the composite part based on the settings chosen in ACP (Pre). The generated solid model would contain either layered solid elements or solid shell elements depending on the settings chosen. Either the shell mesh data or solid mesh data can be imported into ANSYS Static Structural to perform the FEA.

If the layers of the composite are thick, a solid mesh model has advantages over a shell-based model in terms of accurate representation of the interlaminar stresses and strains in the composite part. However, the main disadvantage of using the solid mesh data is that it is resource intensive. Generating a solid mesh of the composite from the original shell-based model increases the number of nodes and elements of the original shell-based model. The factor by which the number of nodes increased depends on the number of layers of the composite. For this analysis, the shell data were imported into ACP (Pre) instead of the solid data in order to reduce computing time, as well as to ensure that the number of nodes in the model itself does not go above the node limit. After the FEA simulation is completed, the FEA results are imported into ACP (Post), where the results are post-process.

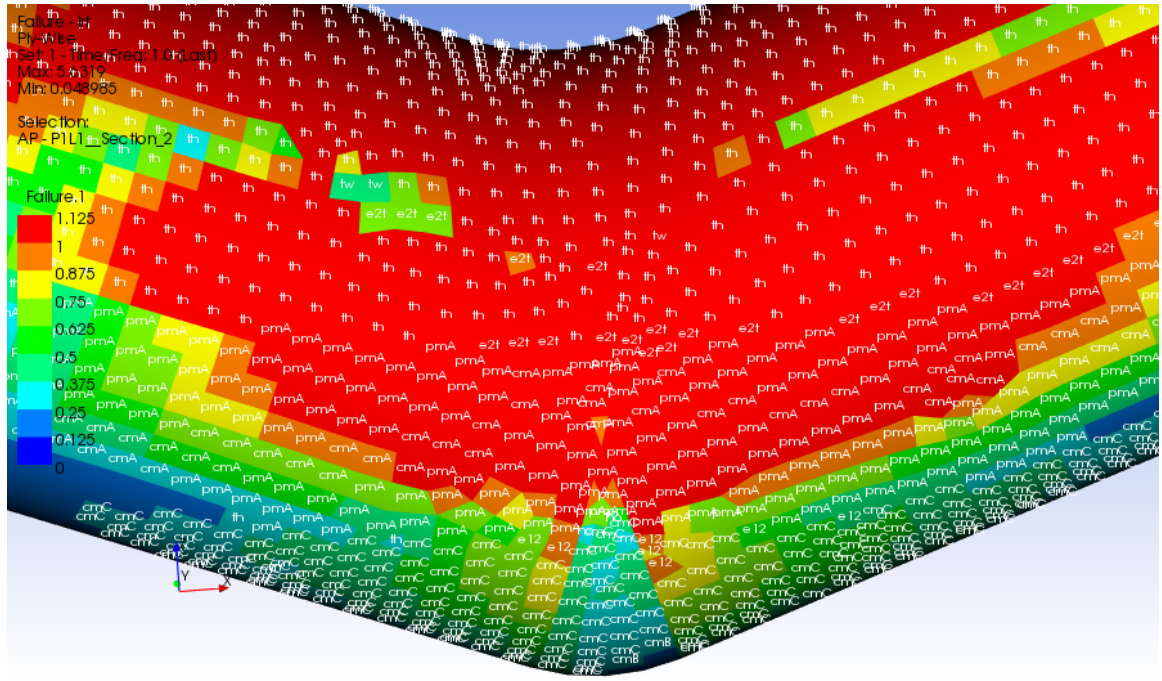
ACP (Post) offers a variety of failure criteria for evaluating the failure mode of the composite part. The table below provides a list of all the recommended failure criteria for a ply consisting of unidirectional fabric based on the ANSYS ACP Guide. The table below provides a list of all the recommended failure criteria for a ply consisting of unidirectional fabric based on the ANSYS ACP Guide.

**TABLE XXVI: RECOMMENDED FAILURE CRITERIA FOR UNIDIRECTIONAL FABRIC**

Failure Criterion	Name	Abbreviation in ACP (Post)
1	Max Strain	e
2	Max Stress	s
3	Tsai-Wu	tw
4	Tsai-Hill	th
5	Hashin	h
6	Hofmann	ho
7	Puck	p
8	Cuntze	c
9	LaRC	N/A

For this analysis, all recommended failure criteria were used to evaluate failure for each ply except for LaRC. This criterion was omitted since the properties of the UD carbon fiber prepreg used in the analysis does not contain the appropriate data needed for the calculation.

In the post-processing stage, if the load calculated on a ply satisfies a given failure criterion, the failure mode of the satisfied criterion is shown as text labels above each element of the critical region (failed region), as can be seen the figure below.



**Figure 64: Predicted failure modes on the critical region shown as text above each element.**

Many of the failure criteria such as Max Stress, Max Strain, and Hashin can distinguished between a number of failure modes. However, other failure criteria such as Tsai-Wu, Tsai-Hill, and Hoffman do not. In the previous figure, the failure modes identified on the critical regions of the grip are Tsai-Hill (th), tensile strain (e2t), Cuntze matrix wedge shape failure (cmC), Puck matrix tension failure (pmA), and Cuntze matrix tension failure (cmA).

The Inverse Reserve Factor or IRF is one of the three safety factors that can be used to evaluate material failure in ACP (Post). It is equal to the ratio of the actual load to the failure load, calculated using the stress limits of the material and predicted values in the FEA. A value of  $IRF < 1$  indicates a safe load and anything above  $IRF=1$  is considered a failure. Since the loading condition already incorporates a safety factor of 2, an IRF value equal to 1 is taken as the margin to failure.

In order to simplify the layup determination process, the handle was divided into three sections. These three sections are the top shaft (Section 1), the grip (Section 2), and the bottom shaft (Section 3). The division of sections of the handle is shown for the 19° handle in the following figure.

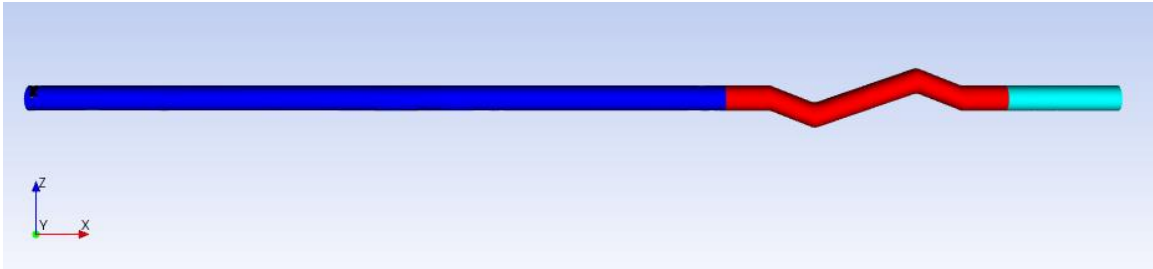


Figure 65: Divided sections of 19°. Section A (Blue), Section B (Red), & Section C (Turquoise).

For all three handles, the grip comprising of sections 2, 3, and 4 were group together since the major directions of the principal stresses identified for each section are in closed agreement with each other. The group also made the decision to extend the layup for the grip section on either ends in order to account for any potential stress concentrations that can lead to failure at the two corners of the grip leading to the top and bottom shafts. For this analysis, due to the limited time available to carry out an analysis to determine an appropriate value for the length of the extension, the group instead decided to use an arbitrary value of 51 mm (2 in) for the length of extension.

The optimum layup for each section is determined by trial and error following the basic workflow outlined above and careful examinations of failure mode plots of each ply. The full results are discussed in the following section.

#### 4.6.2 MATERIAL LAYUP

With the final material and properties selected, the next requirement is to determine the lay-up of the lamina of the composite material. Using the results obtained from ANSYS workbench when evaluating all three grip angles, the principal stresses were determined in the 5 critical areas of the design. The principal stresses represent the values of stress in an element when no shear

stresses are present. ANSYS workbench permits two types of plots in regards to the principal stresses. The first plot type is a vector plot of the stresses on an element which only identifies the direction with which the minimum, middle, and maximum principal stresses “flow” through the object. The second form of principal stress plot identifies the magnitude of these principal stresses. Figure 66 through Figure 69 show images of the two forms of plots of the principal stresses presented by ANSYS workbench, including close ups of regions.

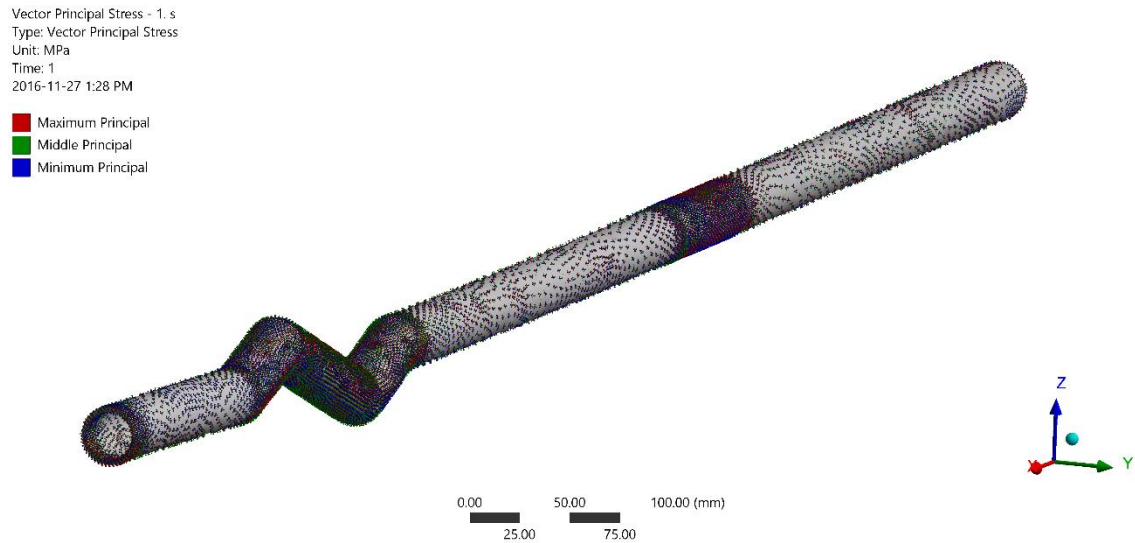


Figure 66: Overall view of the vector plot of the principal stresses along the entire handle.

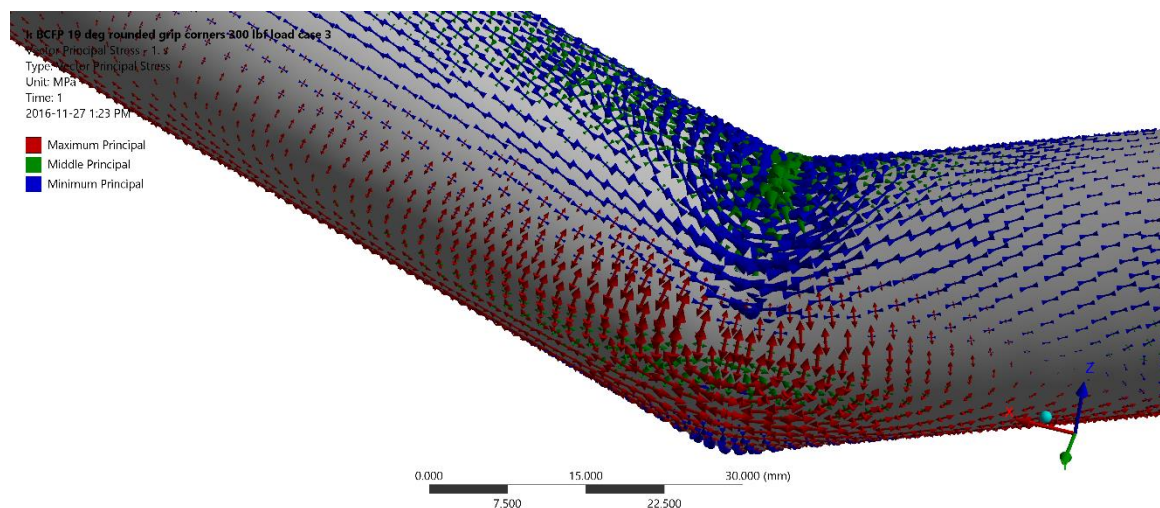
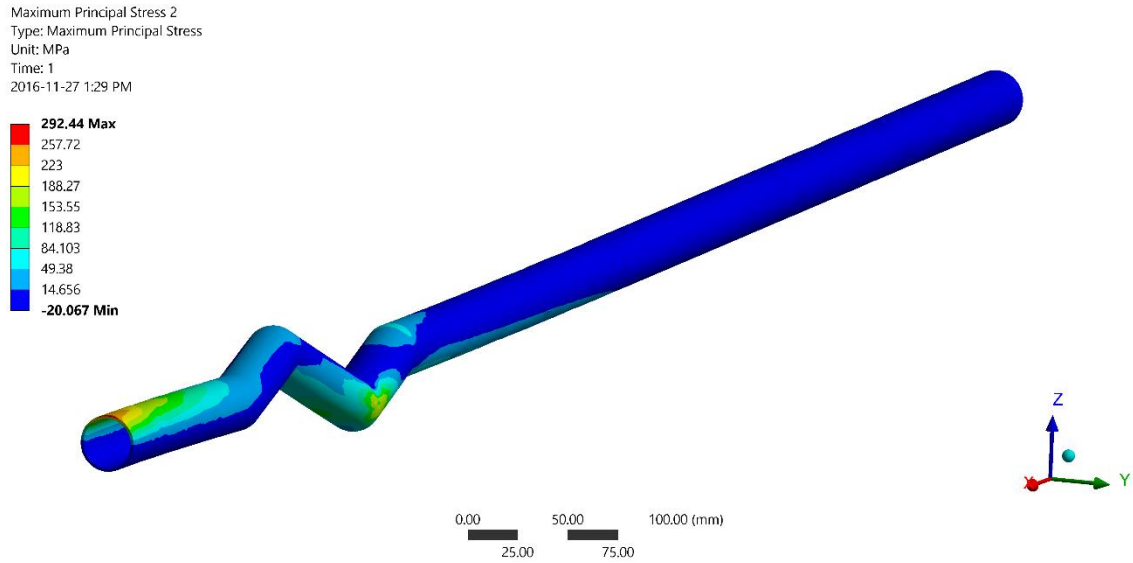
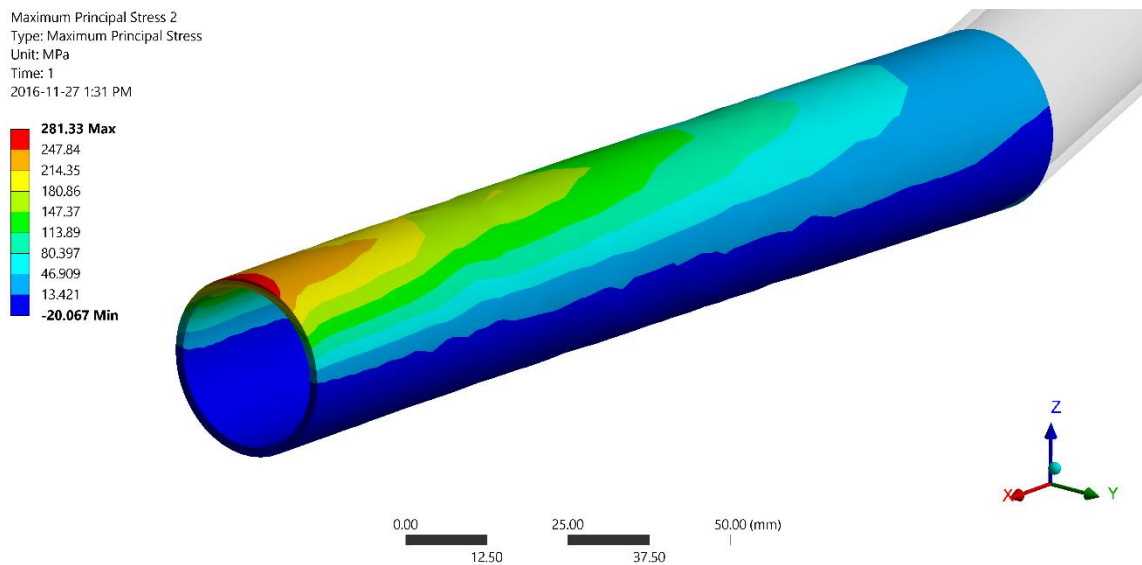


Figure 67: Close up of vector plot of principle stresses in a bend region. The image shows how the vectors orient along the shaft, for the blue (minimum), green (middle), and red (maximum) principal stresses.



**Figure 68: Overview of the plot of the maximum principle stresses along the entire body of the handle.**



**Figure 69: Close up of section 5 of the plot of the principle stresses highlighting the variation of the maximum principle stress in the region.**

Using the plots for the principal stresses, TABLE XXVII presents the compiled data for the maximum, middle, and minimum principal stresses. Also presented is the variation between the maximum and minimum without the principal stress, along with the orientation. An orientation of X represents along the length of the shaft, Y represents out of centre of the shaft, and Z represents along the cross-sectional direction.



**TABLE XXVII: MAXIMUM, MIDDLE AND MINIMUM PRINCIPAL STRESSES IN THE 3 GRIPS**

Section	Principal Stresses	19°				38°				51°			
		Max (MPa)	Orientation	Min (Pa)	Orientation	Max (MPa)	Orientation	Min (MPa)	Orientation	Max (MPa)	Orientation	Min (MPa)	Orientation
1	Min	6.5188	Y	-113.98	X	4.3982	Z	-143.79	Y	3.9105	Z	-128.2	Y
	Middle	155.8	Z	-65.621	Y	170.89	Y	-92.54	X	143.67	Y	-87.913	X
	Max	292.44	X	-4.382	Z	219.38	X	-4.4913	Z	181.81	X	-5.6832	Z
2	Min	6.4829	Y	-382.08	Y	3.4906	Z	-412.37	Y	3.3769	Z	-389.93	Z
	Middle	156.82	Z	-155.94	X	162.45	Y	-126.36	X	120.19	X	-130.6	Y
	Max	292.44	X	-7.3154	Z	218.01	X	-7.2867	Z	201.76	Y	-5.3095	X
3	Min	47.831	Y	-445.37	X	6.3823	Z	-422.46	X	10.669	Z	-399.48	Z
	Middle	202.13	X	-296.3	Y	162.13	Y	-179.44	Y	152.85	X	-152.04	Y
	Max	251.03	Z	-61.188	Z	218.01	X	-42.062	Z	201.76	Y	-23.415	X
4	Min	2.1921	Y	-78.614	Y	1.4799	Z	-52.347	X	0.7093	Z	-74.91	X
	Middle	45.171	X	-40.138	X	38.076	X	-28.972	Y	24.383	X	-25.433	Y
	Max	120.05	Z	-2.1852	Z	71.123	Y	-1.0987	Z	55.075	Y	-1.1482	Z
5	Min	30.555	Y	-303.88	X	18.305	Z	-261.43	Y	13.227	Z	-207.61	Y
	Middle	32.491	Z	-33.309	Y	46.164	Y	-29.661	X	34.245	Y	-27.711	X
	Max	295.65	X	-31.119	Z	249.66	X	-18.988	Z	188.77	X	-14.544	Z

Using the principle stresses listed in TABLE XXVII, estimates of the required layup strengths for the composite. Detailed descriptions of the lay-up determined are provided in proceeding section.

#### 4.6.3 RESULTS DISCUSSION

A mesh convergence study was performed on the 19° shell-based model to obtain the appropriate mesh size to use for the FEA. After each successive refinement, the predicted values of the maximum of the Max principal stresses on 6 probed surfaces on the handle were monitored. The 6 probed locations are shown in the figure below.



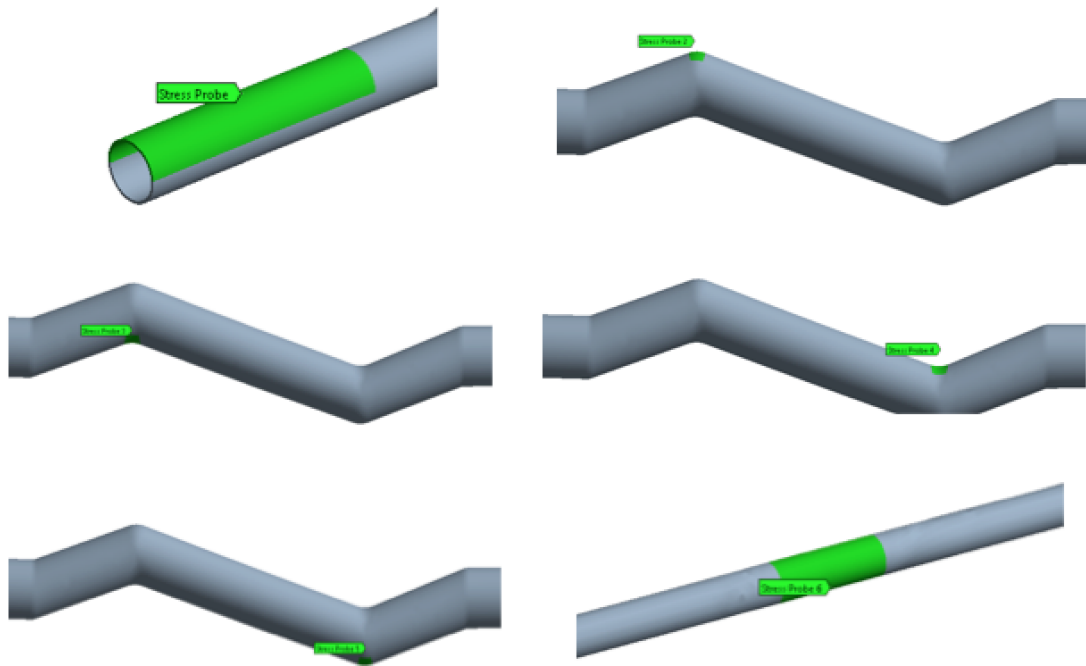


Figure 70: Probed surfaces of the handle where monitored stresses are evaluated for the mesh convergence study.

A plot showing the variation in the stresses on the probe surfaces of the 19° handle is shown in the Figure 71.

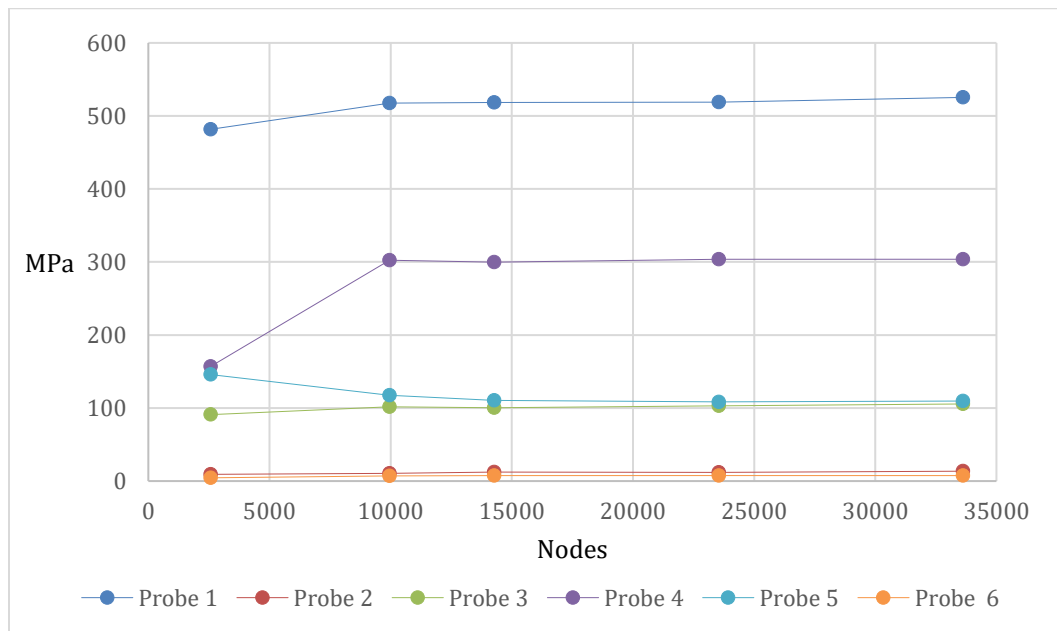


Figure 71: Variation in the monitored Max principal stresses per refinement for the 19° handle.

Based on the above figure, it can be seen that convergence was established at the fourth refinement when the number of nodes is just above 20,000 nodes. Using the mesh size at the fourth refinement, a number of trials were conducted to determine the optimum combination of stackups for the 19° handle. Overall, a total of 39 stackups were developed and at the end of the 22<sup>nd</sup> trial, an optimum combination of stackups was developed for Sections A, B, and C of the handle. A complete list of stack ups is included in APPENDIX C. The plies in each stackup are ordered such that the first ply represents the outer most ply in the stackup, located on the outer surface of the shaft and the last layer represents the bottom ply located on the inner surface of the shaft. Each ply has a thickness of 0.2921 mm [42], which is the thickness of the standard epoxy-carbon prepreg after the material cures.

Overall, the combination of stackups that gave the optimum performance while minimizing the number of plies for the 19° handle are stackups 28 (5 layers), 38 (21 layers), and 34 (12 layers), outlined in XAKSNK.

TABLE XXVIII: INITIAL CONCEPT REQUIRED LAYUP

Ply	Stackup		
	28	38	34
1	0	0	0
2	0	0	0
3	0	0	0
4	90	0	0
5	90	0	0
6		90	0
7		90	0
8		90	0
9		90	0
10		90	90
11		90	90
12		90	90
13		90	
14		90	
15		90	
16		90	
17		90	
18		90	
19		90	
20		90	
21		90	

These stackups were applied to sections A, B, and C, respectively. Since the majority of the orientations of the major principal stresses across all three handles are in closed agreement with each other, the same three stackups were applied to all three sections of both the 38 and 51 degree handles. Further optimizations were then performed to the three stackups in order to minimized the weight of the remaining two handles. The table below gives the optimized stackups of the three sections provided for 38° and 51° handles.

TABLE XXIX: OPTIMIZED STACKUPS FOR THE 38° AND 51° HANDLES

Ply	38 Section Stackup			51 Section Stackup		
	A	B	C	A	B	C
1	0	0	0	0	0	0
2	0	0	0	0	0	0
3	90	0	0	90	0	0
4	90	0	0	90	0	0
5		0	0		0	0
6		90	0		90	0
7		90	0		90	0
8		90	0		90	90
9		90	90		90	90
10		90	90		90	
11		90	90		90	
12		90			90	
13		90			90	
14		90			90	
15		90			90	
16		90			90	
17		90			90	
18		90			90	

The following figures, Figure 72, Figure 74, and Figure 74, shows the variation in the maximum IRF measured for each ply of a stackup for all three handles.

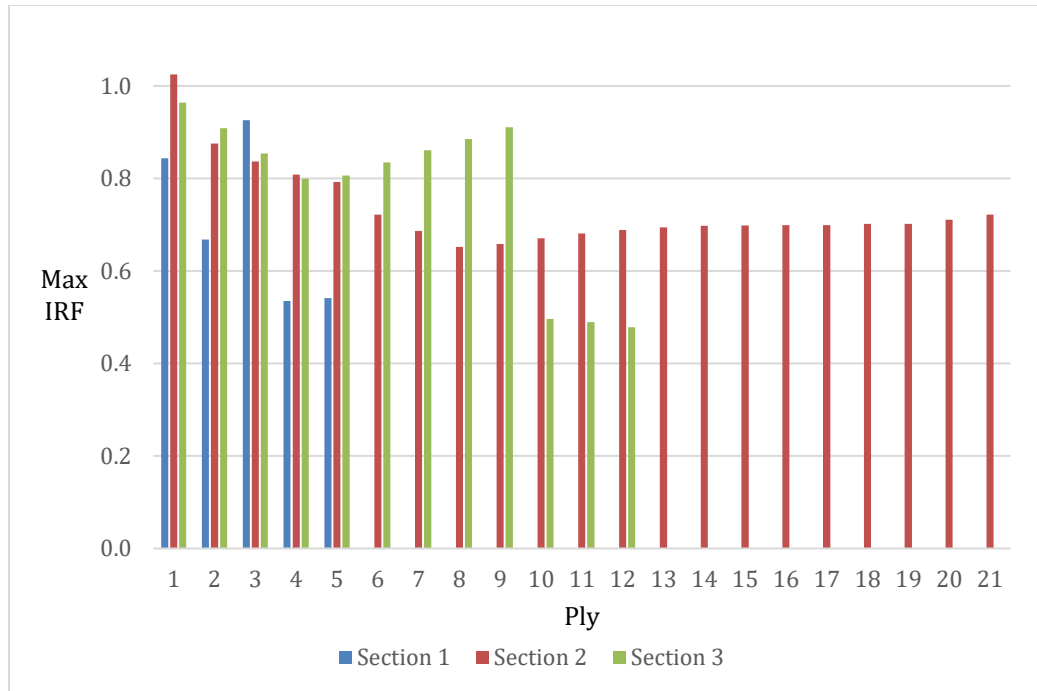


Figure 72: Max IRF of each ply in the stackups for sections A, B, and C of the 19° handle.

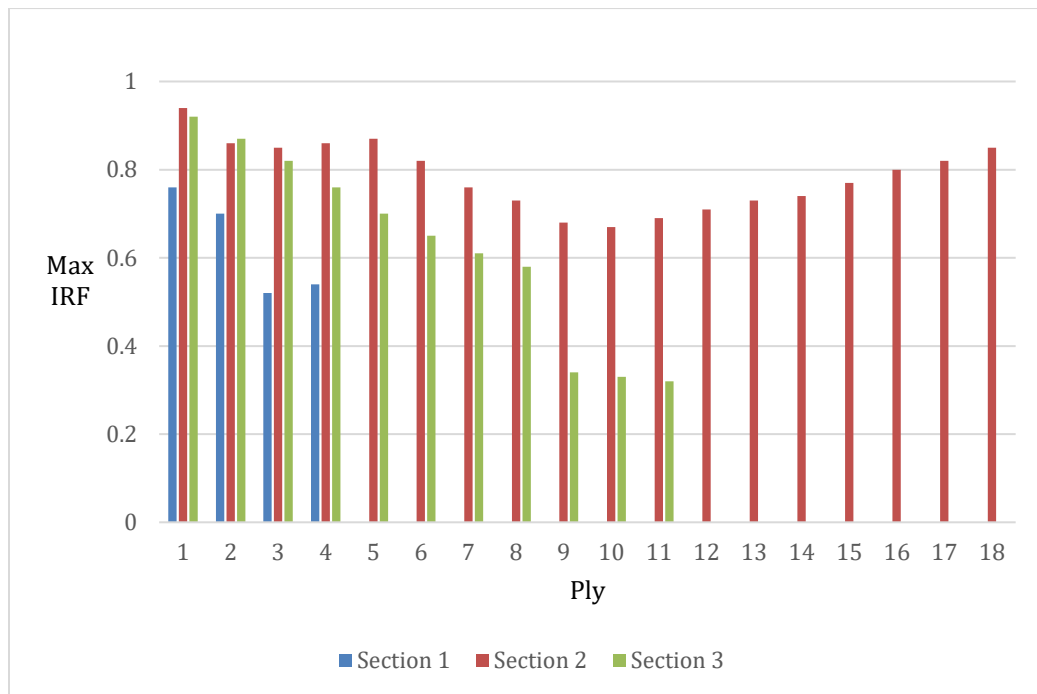


Figure 73: Max IRF of each ply in the stackups for sections A, B, and C for the 38° handle.

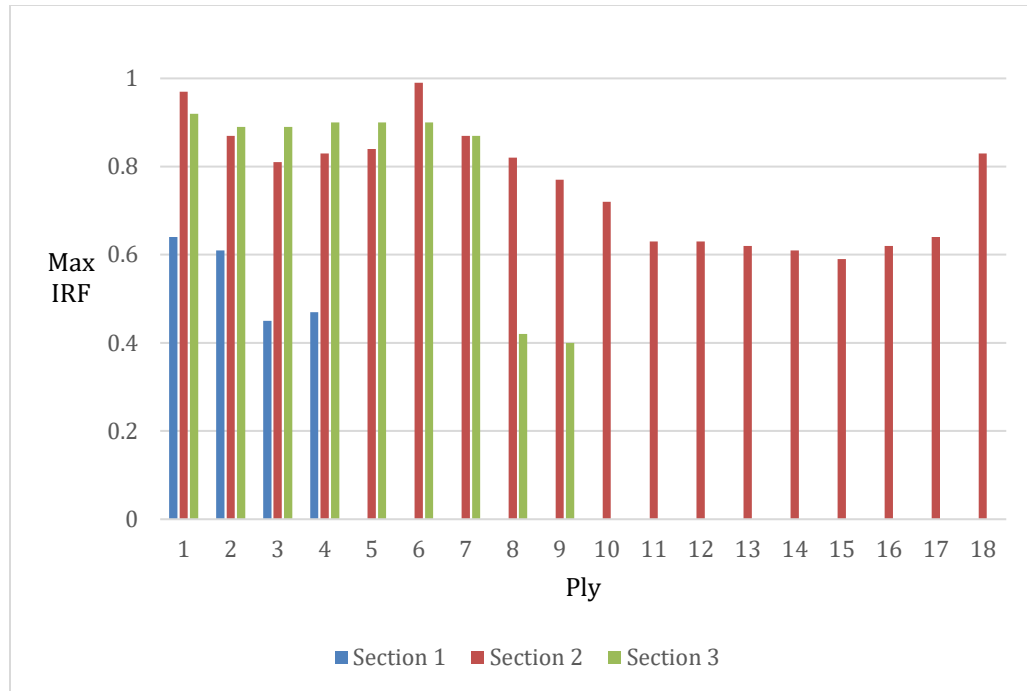


Figure 74: Max IRF of each ply in the stackups for sections A, B, and C for the 51° handle.

As is visible in Figure 72, the IRF for the 19° grip exceeds 1 in section 2. This indicates that the design of this handle is not a success. However, on the other hand, the designs of the 38° and 51° grips do not exceed the limit of 1 and are therefore viable options to be proceeded with. Using the volume calculator in ANSYS, and applying the density of the carbon fibre, the total mass of the 19°, 38°, and 51° handles with the optimized layups are approximately 400 g, 370 g and 390 g, respectively.

## 5. DESIGN OPTIMIZATION

Upon completion of the final design, the team elected to pursue further optimization. Even though the three designs currently has a mass of 370-400 g, masses of composite broom handles currently available on the market are in the range of 200g-300g [43]. As such, the team felt that it would be beneficial to the second generation design's market success if its mass could be modified to fall within this range. Details on how the design was modified to achieve this goal are given in this section.

### 5.1 MODEL OPTIMIZATION

Upon analysis of the stresses within the original evaluated handle, the group determined that issues were arising within the model. Due to the geometry of the models consisting entirely of straight line segments, with filleted edges, this resulted in the model having stress concentrations in the locations of the fillets. After analysis of the issue, and discussion with the groups advisor, Dr. Paul Labossiere, it was suggested that changing the geometry of the handle to a continuous curve could possibly improve upon the results which the group was obtaining [44]. The reasoning behind the change is that FEA programs do not work well with filleted regions, often resulting in stress concentrations in the regions. These stress concentrations are a result of the meshing, in the area of fillets, bunching up and creating discontinuities. As this was an issue that the original model was having, the group opted to take the experienced advice of our advisor and to remodel the design using a continuous contour. Figure 75 through Figure 77 show renders of the 3 new variations of the final design.



Figure 75: 3D render of the 19° variation of the second generation handle.



Figure 76: 3D render of the 38° variation of the second generation handle.



Figure 77: 3D render of the 51° variation of the second generation handle.

## 5.2 PRELIMINARY FEA RESULTS

Using the same geometric constraints and loading scenario as discussed in section 4 of the report, the three new variations of the handle geometry were again analyzed using isotropic properties. Figure 78 through Figure 80 show the plot of the von Mises stresses which occur during the constraint and loading scenario described in section 4.2. In this section of the report on the visual results for the 19° grip angle will be included, for visual representation of the 38° and 51° grips, refer to APPENDIX C.



C: 19 deg - good

Equivalent Stress

Type: Equivalent (von-Mises) Stress - Top/Bottom

Unit: Pa

Time: 1

2016-12-07 6:49 AM

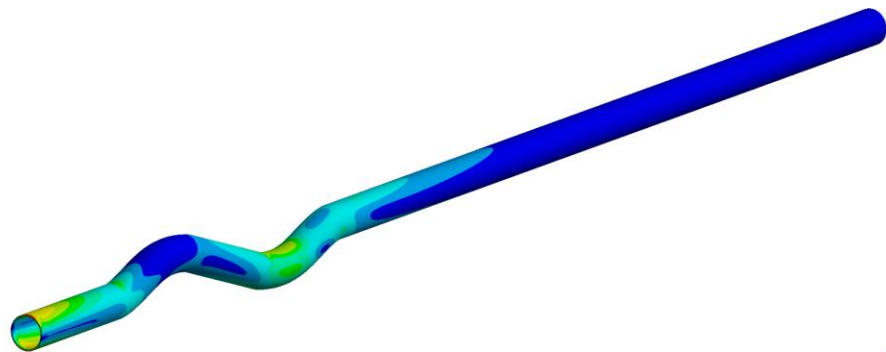
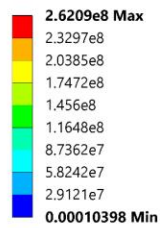


Figure 78: Isometric view of the von Mises stress distribution about the handle with isotropic properties applied.

C: 19 deg - good

Equivalent Stress

Type: Equivalent (von-Mises) Stress - Top/Bottom

Unit: Pa

Time: 1

2016-12-07 6:49 AM

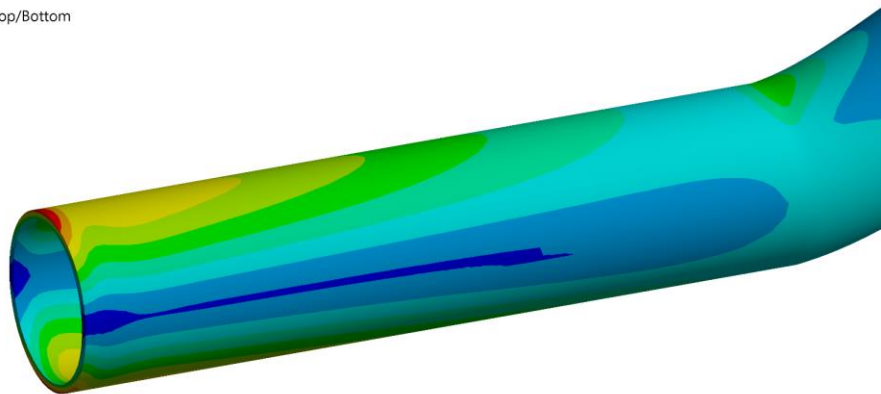
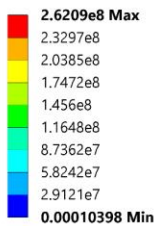


Figure 79: Close up view of the stress distribution about the end of the curling broom section 5.

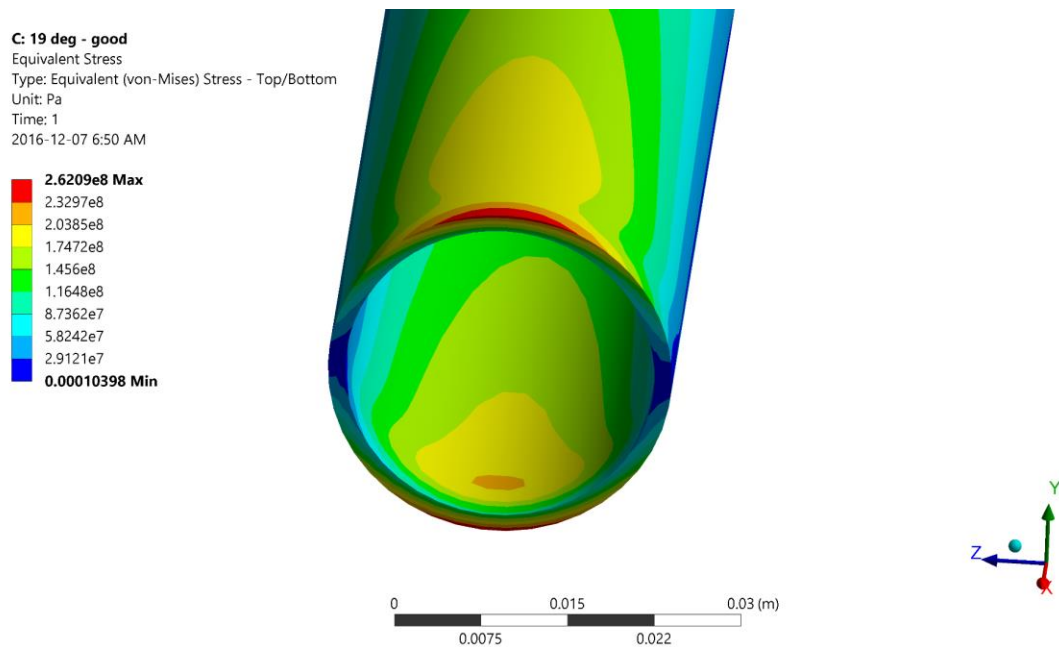


Figure 80: Alternate front view of the stress distribution about the end of the curling broom section 5.

### 5.2.1 MESH CONVERGENCE

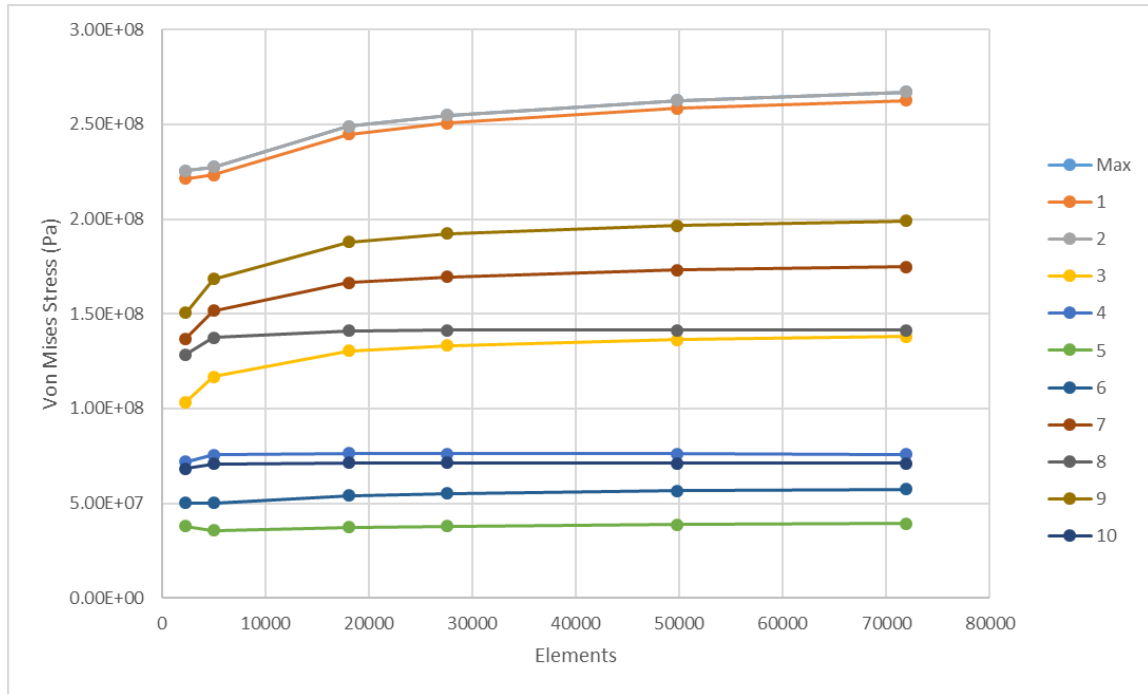
As the model of the handle and the meshing of the design had changed, a convergence analysis of the concept was necessary to be performed to validate that the design obtained stress convergence. Using 10 stress probes located at critical nodes, the Von Mises stresses of the design were evaluated to determine if the stresses converged. Figure 81 shows the location of the placed probes used to evaluate it the stresses along the model converged.



Figure 81: Locations of the von Mises stress probes used in the calculation of the stresses.

The attached stress probes recorded the value of the stress calculated at the location of the node at which they were located. The stress values which were read were the equivalent or Von Mises stresses. While the Von Mises yield criteria does not work with orthotropic materials such as composites, the analysis was performed while the model had the isotropic materials applied to verify that the results for the

stresses converged. Figure 82 is a graph of the stress convergence analysis performed on the 19° handle, showing a comparison of the number of elements within the material to the Von Mises stresses in the locations of the probes.



**Figure 82: Stress convergence graph for isotropic behavior of 19° model. Plotted are the measured Von Mises stresses in the locations of the probes, and the number of elements present in the model at the evaluation.**

It can be seen in Figure 82 that as the number of elements within the handle increases, the values of the Von Mises stresses converge. The data in Figure 82 is taken from TABLE XXX and TABLE XXXI, which shows the element sizes used in the evaluation along with a detailed overview the changes in the mesh sizing resulted to in the results.

TABLE XXX:DATA FROM MESH CONVERGENCE PLOT PART 1

	Elements	Nodes	Max	1	2	3	4
Mesh Size [mm]			MPa	MPa	MPa	MPa	MPa
	2280	2292	225.57	221.42	225.57	103.32	71.84
0.005	4980	5000	227.42 0.82%	223.32 0.85%	227.42 0.82%	116.86 12.30%	75.67 5.20%
0.0025	18072	18108	248.95 9.04%	244.72 9.14%	248.95 9.04%	130.38 10.94%	76.30 0.83%
0.002	27588	27632	254.85 2.34%	250.55 2.35%	254.85 2.34%	133.32 2.23%	76.17 -0.18%
0.0015	49800	49860	262.64 3.01%	258.26 3.03%	262.64 3.01%	136.35 2.25%	75.98 -0.24%
0.00125	71928	72000	266.95 <b>1.63%</b>	262.53 <b>1.64%</b>	266.95 <b>1.63%</b>	138.00 <b>1.20%</b>	75.83 <b>-0.20%</b>

TABLE XXXI:DATA FROM MESH CONVERGENCE PLOT PART 2

	5	6	7	8	9	10
Mesh Size [mm]	MPa	MPa	MPa	MPa	MPa	MPa
	37.93	50.13	136.77	128.41	150.64	68.349
0.005	35.75 -5.90%	50.20 0.13%	151.71 10.36%	137.51 6.84%	168.35 11.10%	70.821 3.55%
0.0025	37.31 4.25%	54.18 7.64%	166.33 9.19%	141.14 2.61%	187.93 10.99%	71.332 0.72%
0.002	38.00 1.84%	55.33 2.10%	169.53 1.91%	141.35 0.15%	192.20 2.25%	71.258 -0.10%
0.0015	38.73 1.91%	56.63 2.31%	173.01 2.03%	141.41 0.04%	196.62 2.27%	71.137 -0.17%
0.00125	39.20 <b>1.21%</b>	57.40 <b>1.35%</b>	174.73 <b>0.99%</b>	141.29 <b>-0.08%</b>	199.09 <b>1.25%</b>	71.038 <b>-0.14%</b>

Through a comparison of both Figure 82, TABLE XXX, and TABLE XXXI it can be concluded that the results obtained from the FEA converge. This therefore validates the model and the applied meshing, along with validating further computations performed on the meshed model using FEA.

### **5.2.2 FINAL COMPOSITE LAYUP**

Using the newly created models, the design was run through ANSYS acp again to determine the required layup for the redesign. The process undertaken at this redesign step followed the same principles as the original lay-up evaluation. Based on the redesign, the lay-ups in TABLE XXXII,

TABLE XXXIII and TABLE XXXIV were computed to be suitable for the 19°, 38° and 51° variations respectively.

**TABLE XXXII: FINAL LAY-UP FOR 19° GRIP**

Lamina Orientation [°]			
Lamina	Section 1	Section 2	Section 3
1	0	0	0
2	0	0	0
3	0	0	0
4	90	90	0
5	90	0	0
6		0	0
7		0	0
8		0	0
9		45	90
10		-45	90
11		0	
12		0	
13		0	
14		90	
15		90	
16		90	

TABLE XXXIII: FINAL LAY-UP FOR 38° AND 51° GRIP

Lamina Orientation [°]			
Lamina	Section 1	Section 2	Section 3
1	0	0	0
2	0	0	0
3	0	0	0
4	90	90	0
5		0	0
6		0	0
7		0	90
8		0	90
9		45	90
10		-45	90
11		0	
12		0	
13		90	
14		90	

TABLE XXXIV: FINAL LAY-UP FOR 51° GRIP

Lamina Orientation [°]			
Lamina	Section 1	Section 2	Section 3
1	0	0	0
2	0	0	0
3	90	0	0
4	90	90	0
5		0	0
6		0	0
7		0	90
8		0	90
9		45	
10		-45	
11		0	
12		90	
13		90	

These new layups resulted in a decrease in the required amount of plies. As a result the 19° variation required a 5-16-10 lamina distribution over the sections of the design. The 38° variation required 4-14-10 lamina, and the 51° variation was found to only require 4-13-8 lamina

### 5.2.3 COMPOSITE FAILURE CRITERIA ANALYSIS

As discussed previously in section 4.6.1 one of the functions of ANSYS acp is to analyze the applied composite layup based on the user specified criteria. Using the same criteria listed in TABLE XXVI, the new layup was evaluated using ANSYS acp. TABLE XXXV through TABLE XXXVII contain the values for the IRF that each of the variations had per lamina.

TABLE XXXV: FAILURE CRITERIA ANALYSIS FOR 19° HANDLE

Lamina IRF			
Lamina	Section 1	Section 2	Section 3
1	0.48433	0.6206	0.98061
2	0.47182	0.5152	0.91065
3	0.45938	0.48805	0.84391
4	0.64389	0.45914	0.77665
5	0.67468	0.51753	0.70827
6		0.47669	0.65052
7		0.4364	0.6091
8		0.39623	0.57412
9		0.33334	0.51238
10		0.31868	0.51955
11		0.32474	
12		0.29383	
13		0.3215	
14		0.3508	
15		0.38257	
16		0.41535	



TABLE XXXVI: FAILURE CRITERIA ANALYSIS FOR 38° HANDLE

Lamina IRF			
Lamina	Section 1	Section 2	Section 3
1	0.41354	0.92233	0.94473
2	0.39899	0.84558	0.87583
3	0.38441	0.77177	0.80711
4	0.56671	0.78299	0.73742
5		0.6835	0.68213
6		0.61631	0.64431
7		0.55215	0.4997
8		0.48936	0.4997
9		0.40644	0.43835
10		0.36287	0.47559
11		0.31687	
12		0.31076	
13		0.45688	
14		0.59736	

TABLE XXXVII: FAILURE CRITERIA ANALYSIS FOR 51° HANDLE

Lamina IRF			
Lamina	Section 1	Section 2	Section 3
1	0.49587	0.98216	0.80491
2	0.47593	0.88811	0.73769
3	0.57348	0.79987	0.67055
4	0.57348	0.79636	0.60322
5		0.64924	0.56632
6		0.57225	0.5227
7		0.50108	0.46018
8		0.43753	0.46018
9		0.4524	
10		0.41279	
11		0.30704	
12		0.42054	
13		0.61865	

### 5.3 SUMMARY OF RESULTS

The decrease in the required lamina resulted in significant reductions in the mass of the redesigned broom. Based off of the final volume of each of the three angled designs, and the density of the selected carbon fibre, TABLE XXXVIII outlines the calculated mass of the new models.

TABLE XXXVIII: FINAL MODEL VOLUME AND MASS

Angle	Volume [m <sup>3</sup> ]	Mass [g]
19°	2.648 e-4	394.6
38°	2.4774 e-4	369.1
51°	2.4646 e-4	367.2

Comparing the masses calculated in TABLE XXXVIII, the masses determined for the original models listed in, TABLE XXIX outlines the decrease in the mass of the broom handle.

TABLE XXXIX: COMPARISON OF ORIGINAL MODEL TO FINAL MODEL MASS

Angle	Old Mass [g]	New Mass [g]	Difference [g]
19°	400	395	~5
38°	370	369	~1
51°	390	367	~23

As can be seen in TABLE XXXIX this results in up to a ~23 g decrease in the mass of the design. Along with the decrease in the mass, this also results in a decrease in the cost of the raw materials to produce the design.

## 6. MATERIAL AND MANUFACTURING

With the concept selected and the FEA results validated, the material and manufacturing process for the final design needed to be determined. To do so, multiple methods were utilized. Through analysis of the existing handle, the manufacturing method for the first generation handle was estimated. Then, the principal stresses that had been evaluated using the isotropic FEA were used to determine the required strength in the handle sections. Based on the required strength, various forms of carbon fibre were compared against each other to determine the form most suitable for the design. From the selected material, the material properties, required lay-up and manufacturing processes were determined.

### 6.1 FAILURE MODE EFFECTS ANALYSIS

A Failure Mode Effects Analysis (FMEA) is useful to identify ways that the product can fail, and to eliminate or reduce the risk of failure. For this design, the FMEA was used to analyze the likelihood and severity of failure for the components that make up the handle. The results were then used to determine the actions that should be taken to reduce the risk. The components that will be examined are the grip, the shaft and the adhesive.

The first component that was analyzed was the grip. The grip will fail if its strength is not enough to carry the load applied, resulting in fracture. If this occurs, the broom will most likely not be able to be repaired. Also, since curlers put a large amount of force into the sweeping motion, if the broom were to suddenly yield, it may cause the curler to fall and possibly be injured. Failure could be especially dangerous if the handle experiences brittle fracture resulting in sharp edges on the broken pieces. Since this type of failure results in destruction of the broom and possible injury to the user, the severity is very high. The grip is being designed to carry a conservative load of 150 lb with a safety factor of 2, making this type of failure unlikely. However, there are variations in quality of manufactured parts, as well as the strength of individual curlers, so the failure is not impossible. The

likelihood of detecting the failure before it occurs is quite low, since composite material failure is usually sudden, and curlers will most likely not be inspecting their brooms for cracks.

The second component of the handle analyzed was the shaft. The shaft will fail in a similar manner to the grip, if its ultimate strength is exceeded. Failure of the shaft will have a similar effect to the grip as well, resulting in the destruction of the broom and possible injury to the user. Unlike the grip, the shaft does not have complex geometry and is less prone to defects. Therefore, the frequency of shaft failure should be lower than that for grip failure. Similar to the grip, detection of potential shaft failure before it occurs will also be difficult, even more so since the user does not interact with the shaft as much as the grip.

The third component of the handle analyzed was an adhesive that joins the grip to the shaft. The adhesive will fail if the sections debond. The most likely cause for debonding is deterioration of the adhesive material over time. If adhesive failure occurs, the broom will not be usable, but there is a possibility of repairing the broom. In addition, there is a lower chance of injury due to adhesive failure compared to the grip or shaft and the user may detect the bond loosening before complete failure occurs, so the adhesive failure will have lower severity and detection scores than the other failure modes. However, adhesive failure is the most likely failure to occur as it has more potential for deterioration over a long period of time.

TABLE XL: FMEA

Component	Potential Failure Mode	Potential Effect	S E V	Potential Causes	F R E Q	Current Controls	D E T	R P N
Grip	Fracture	Broom damaged, possible injury	9	Insufficient strength or excessive load	2	Material, wall thickness	6	108
Shaft	Fracture	Broom damaged, possible injury	9	Insufficient strength or excessive load	1	Material, wall thickness	8	72
Adhesive	Debonding	Broom damaged, repair possible	7	Deterioration	3	Type of adhesive, bonding area	4	84

The risk priority number is highest for the grip fracture, and second highest for the adhesive debonding. Actions taken to mitigate the risk of fracture are selecting a strong material for the grip and increasing wall thickness. Also, debonding can be mitigated by selecting an adhesive that has high performance with the grip and shaft materials as well as having a large contact area between the grip and shaft for a strong bond.

## 6.2 EXISTING HANDLE MATERIAL AND MANUFACTURING

Understanding the materials and manufacturing processes used in the first generation Xtreme Force handle will help in the design of the second generation handle. Due to the lack of transparency of how the first generation handle was produced, the handle needed to be examined and tested to determine the materials and manufacturing method.

### 6.2.1 VISUAL INSPECTION

Initial inspection of the grip suggests a woven fabric with a black colour. The colour led us to suspect the reinforcement to be carbon fibre. The shaft appears to have the same texture as the grip, so the shaft was likely manufactured using the same

material. Also visible is a seam running down opposite sides of the grip, shown in Figure 83, which suggests that the grip consisted of two parts before curing together.



Figure 83: Seam along the middle of the grip.



Figure 84: Cross section of cut grip showing internal core.

Upon cutting apart the grip it was revealed to contain a foam core, as seen in Figure 84. This shows that the grip was produced by laying up or moulding the fabric or pre-preg around the core before curing. After extracting the core from the grip, the seam visible on the outside of the grip was found to continue into the inside, shown in Figure 85, further reinforcing the idea that two separate halves were cured together. The seam appears to exist in the resin as well as the reinforcement,

so the grip was most likely produced using two pieces of pre-preg material formed around the core rather than resin injection into two pieces of fabric.



Figure 85: Inside view of coreless piece C highlighting the seam.

Inspection of the interface between the grip and the shaft shows that the grip has a length of thinner cross section on each end that fits into the shaft, and an adhesive is used to bond this section of the grip to the inner surface of the shaft.

### 6.2.2 ANALYSIS OF TEST RESULTS

In section 2.1, the method and results of testing on the generation one handle were discussed. The results of the improved tensile tests are shown in TABLE XLI.

TABLE XLI: SUMMARY OF IMPROVED TENSILE TEST RESULTS

Specimen	Length (mm)	Cross-Sectional Area (mm <sup>2</sup> )	Peak Load (N)	Ultimate Tensile Stress (MPa)	Modulus of Elasticity (MPa)
1	50.8	10.4	1326	127	9611
2	50.8	8.2	1016	124	9353

The tensile strength determined for the grip samples in TABLE XLI confirms the grip material to be carbon fibre, as it is within 5% of the theoretical strength of 120 MPa. For the core material, after consulting with the client we came to the conclusion that

it was most likely polyurethane foam, and the measured density agrees as it is within the common range of densities for polyurethane. Due to the lack of a reliable stress measurement for the bond strength, we cannot determine what type of adhesive is used, but we can use the peak load measurements as a guideline for setting a target specification for the bond strength in the new design.

### **6.2.3 SUMMARY OF EXISTING HANDLE MATERIAL AND MANUFACTURING**

From the information found through inspection and testing, we have concluded that the first generation handle's grips were manufactured using woven carbon fibre pre-preg, cut into two pieces and shaped over a polyurethane foam core. The grip was cured in this shape, and then bonded to shaft sections using an adhesive. The shaft was most likely manufactured by roll wrapping the same pre-preg material to produce long tubes, which are later cut into the smaller shaft sections that make up the current handle.

## **6.3 MATERIAL ANALYSES**

The material and manufacturing process used for the first generation handle will be used as a basis for evaluating possible material and manufacturing processes for the second generation design.

### **6.3.1 CORE MATERIAL**

Cores are often used to produce complex geometry composite parts when more automated methods, such as filament winding, are less feasible. Cores can be advantageous or disadvantageous depending on their intended application. For example, a core may be essential to provide structural and/or geometrical integrity to a composite part, which can benefit the final product. However, the manufacturer of the part may desire a hollow cross section for the purposes of directing flow channels or reducing the mass of the final product. In these cases, the inclusion of a core would not be desirable.



Depending on how the part is manufactured around a core, seams in the laminate may result from the manufacturing process. These seams generally affect the composite's strength, so seamless composites are most desirable in high performance applications which demand high strength to weight ratios.


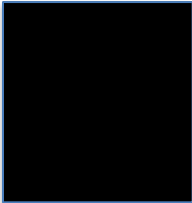
Depending on the complexity of the end-part, it may be possible to easily remove the core, provided that the geometry is relatively simple. If the part geometry is complex such that the core is trapped inside, special sometimes sacrificial tooling may be required to remove the core. Furthermore, the processes required to remove the core from a complex geometry part can be harsh, where there exists high risk for damaging the part [45].


In the context of the second generation handle design, the client has expressed a desire for a high strength to weight ratio design which is able to withstand the loading conditions outlined in section 3.2. Even though common core materials are relatively lightweight, a hollow design would yield a lighter final product. Although, if the relative rankings of the customer needs are considered (TABLE II in section 1.4.1), the strength of the final design is of greater importance than its mass. To ensure that this strength requirement is met, the team felt that it was necessary to consider both hollow and cored cross sections, even if it resulted in a heavier final design.

#### **6.3.1.1 CORED CROSS SECTION**

A composite featuring a cored cross section is generally known as having a sandwich structure. This name arises from the method in which these parts are generally manufactured: "sandwiching" a low density lightweight core material between thin face sheets [46]. The presence of the visible seam along the grip discussed in section 6.2.1 led the team to conclude that the first generation handle grips were manufactured using this method [7]. Different types of core materials used in sandwich structuring are given in TABLE XLII.

TABLE XLII: TYPES OF CORE MATERIALS USED IN SANDWICH STRUCTURING [46] [47]

Material type	Description
<p>Balsa Wood</p> 	<ul style="list-style-type: none"> <li>- Harvested from Balsa trees. Effectively a natural composite whose pattern of cellulosic fibers resemble a honeycomb at microscopic level.</li> <li>- Lumber is dried to reduce moisture as much as possible, then planed, cut, measured and weighed to determine density. Once cut, pieces are glued together, pressed into blocks and cut into sheets. Wood fibers are oriented perpendicular to the core sheet face (this orientation yields highest compression and shear properties).</li> <li>- Relatively low cost.</li> <li>- High compression and shear strength.</li> <li>- Excellent fatigue performance.</li> <li>- Available densities range from <math>72 \text{ kg m}^{-3}</math> to <math>256 \text{ kg m}^{-3}</math>.</li> </ul>
<p>Honeycomb</p> 	<ul style="list-style-type: none"> <li>- The tessellated geometry which is the foundation of a sheet is known as the cell. Cell geometry varies by manufacturer and desired application. Common geometries include hexagonal, triangular or tubular.</li> <li>- Cell structure is achieved by extruding the core through metal die which produces a sheet having a well-defined cell size. Extruded core sheets are stacked and fused to create large blocks, which are then sliced to a specified thickness (ranging from 4.7 mm to 450 mm).</li> <li>- Hollow cells permit excellent sound and vibration dampening capabilities. This characteristic can be desirable in applications involving motor vibrations/noise.</li> <li>- Hollow cell structure is tough and damage-tolerant, qualities which are advantageous in absorbing and dissipating impact</li> <li>- Shear and compression properties are lower than some densities and grades of foam or balsa cores.</li> <li>- Lowest relative density, so it is the lightest of the core types</li> <li>- Comparably strong to other core types, so it possesses the highest strength to weight ratio</li> <li>- Honeycomb edge treatments are comparatively difficult, since it does not machine as easily as foam or wood. Additionally, honeycomb cores have negligible screw retention, so special treatments are needed for to incorporate fasteners</li> <li>- Core sheets are plastic (commonly thermoplastic polypropylene (PP)) or metallic (commonly aluminum).</li> <li>- Available densities range from <math>28 \text{ kg m}^{-3}</math> to <math>80 \text{ kg m}^{-3}</math> which are dependent on both the manufacturer and cell geometry (hexagonal, triangular or tubular)</li> </ul>

Material type	Description
Foam 	<ul style="list-style-type: none"> <li>- Produced by mixing blowing agents and liquid polymers into metal molds, permitting a partial cure under high heat and pressure</li> <li>- A wide variety of both thermoplastics and thermoset polymers are used to produce these core, including polyvinyl chloride (PVC), polyurethane (PU), polystyrene (PS), styrene acrylonitrile (SAN), polyetherimide (PEI) and polymethacrylimide (PMI)</li> <li>- Thermoset foams such as polyurethane (PU) have fairly good mechanical properties and are relatively tough. They can be tailored to their application for better temperature resistance and greater compressive strength by varying the concentration of each component in the mixture.</li> <li>- Thermoset polymers it can be used in higher temperature applications than thermoplastic foams, but they tend to be less fatigue-resistant and more brittle in contrast to thermoplastic foams.</li> <li>- Polyurethane (PU) foams tend to be the most economical foam core since its manufacturing process yields are higher than for other foams like PVC. It is either made in batches ("bun casting") or a continuous foaming process.</li> <li>- Available densities range from 30 kg/m<sup>3</sup> to 800 kg/m<sup>3</sup>. Density is easily controllable by varying the ratio of the polymer ingredients to blowing agents and adjusting gas pressure.</li> </ul>

Each of the core types listed in TABLE XLII exhibit different advantages which are suitable to different applications. However, a common advantage with all cored structures is that they are a significantly inexpensive reinforcement option in contrast to composite reinforcement material. They are inexpensive because they require less supporting structure (i.e. a thinner skin) than solid laminate.

As the core typically takes the majority of a sandwich structure volume, the sandwich panel bending stiffness is mainly proportional to the core thickness. Cores also help distribute the stresses acting on the skins, which can ultimately extend the life of a working part. For example, a core's compression strength can help prevent wrinkling and/or buckling of thin skins, or its shear modulus will help resist independent sliding of skins when subject to different bending loads. It should be noted that the adhesive used to bond the core and skins must also be strong enough to withstand the constant stresses associated with dynamic loading.

It follows that the sandwich structure must be an entirely compatible system in order to ensure that the end product possess the intended properties. In some cases, cores can be cocured with their skins, however all sandwich structures must have compatible thermal expansion coefficients between the core, laminate and the adhesive such that thermal cycling will not cause debonding.

#### 6.3.1.2 HOLLOW CROSS SECTION

Female (or clamshell) molds are typically used to produce irregular hollow composite geometries. In these molds, the fabric is laid up into a shell, typically in two halves. Each half of the clamshell mold is then closed such that the two laid up halves are on top of one and other, at which point curing begins. There are many advantages associated with this manufacturing method, the majority of which relate to the ease of part repeatability. However, the final product of a clamshell mold is guaranteed to have a seam in the lamina, which presents a significant structural disadvantage.

Hollow complex seamless composites have historically been made possible through the use of sacrificial cores. However, traditional materials used as sacrificial cores are difficult to remove from their cured composite, as harsh tooling is necessary for removal. Relatively new developments in the composites manufacturing industry have been able to improve the quality of hollow complex seamless composites through the use of soluble cores. Essentially, this type of core is removed from its cured composite by submerging it into a detergent solution which acts as a solvent that decomposes the soluble core. The end product is a hollow, seamless composite with a smooth internal surface finish. This method of composite manufacturing has recently been gaining relevance in manufacturing high performance automotive applications [48]. Hollow composites manufactured using this method allow for the production of geometrically complex parts which exhibit favorable flow characteristics (from the smooth internal surface finish) while being aesthetically pleasing (from the seamless laminate).

Since the end part has no seams, the core is often manufactured as one piece. The additive manufacturing (AM) method of fusion deposition molding (FDM) is the most common method used to produce these soluble cores.

AM is general manufacturing process category which builds 3D objects by continually building up small layers of a material into a desired geometry. The geometry is defined through the use of CAD software [49].

FDM injects a molten thermoplastic through a fine nozzle in a computer-generated pattern which builds the desired geometry. Between the application of each successive layer, the thermoplastic is first given time to harden such that the next layer will be applied to a “solid” surface. These two steps are repeated until the full geometry has been constructed [49]. A schematic noting some of the main components used in FDM is given in Figure 86.



Figure 86: FDM process schematic [50].

Common thermoplastics which are currently used to produce these one piece core geometries through FDM are outlined in TABLE XLIII.

TABLE XLIII: COMMON THERMOPLASTICS USED IN FDM [51]

Material Name	Max Temperature [°F]	Max Pressure [psi]
SR-30	180	80
SR-100	250	80
S1	350 (out of autoclave) 300 (in autoclave)	100

In the context of the second generation broom handle, the client has specified a preference for a strong and lightweight final design. Given the potential increases in strength to weight ratio yielded by this manufacturing process, the team felt that it was reasonable to consider the possibility of manufacturing an entirely hollow unibody handle.

### **6.3.2 SHAFT AND GRIP MATERIAL**

For the redesign of the new handle, since the exact conditions of the material and manufacturing processes are unknown, along with the material properties, it was necessary to select a new material to use in manufacturing the new handle.

Following in a similar manner to the needs, metrics and concept generation, a material weighting matrix was first created. The purpose of the weighting matrix was to determine which aspects of a material were more crucial to the design and to determine which material was the most optimal for the design.

As a group, collectively 5 metrics were determined to be of critical importance while selecting a composite material for the design. The 5 criterias are ease of layup, wettability, part repeatability, appearance, and cost of material.

Ease of layup is the ability of the manufacturer to lay-up all lamina within the composite material. This shall affect the ability of the manufacturer to create the part for production.

Wettability is the ability of the selected composite material to become fully impregnated with resin. If a selected material doesn't become fully wetted during the curing cycle, this results in dry spots within the material. These dry spots are weak spots within the design.

Part repeatability is the ability of the manufacturer to create multiple copies of the redesigned handle, each being as near an exact replica as the original as possible. If the part is to be commercially sold, the ability to manufacture the part multiple times with the same consistency in standards is necessary.

Appearance relates how the selected material looks after curing has taken place. While this does not affect the performance of the created design, it will have an impact on the willingness of a customer to purchase the design.

Cost of the material is important, as it is often desired to minimize costs as much as possible to maximize the profits. If the concept is too expensive to manufacture, the customer is less likely to pursue the design.

With these selected metrics for determining an appropriate material for the design, TABLE XLIV, is a criteria weighting matrix comparing each of the criterion against each other to determine an importance.

**TABLE XLIV: MATERIAL CRITERIA WEIGHTING MATRIX**

Criteria		Ease of Layup	Wettability	Part Repeatability	Appearance	Cost of Material
Ease of Layup Wettability Part Repeatability Appearance Cost of Materials	ID	A	B	C	D	E
	A	-	B	C	A	A
	B	-	-	B	B	B
	C	-	-	-	C	C
	D	-	-	-	-	E
	E	-	-	-	-	-
Metric Occurrence Weight (%) Rank		A	B	C	D	E
		2	4	3	0	1
		20	40	30	0	10
		3	1	2	5	4

With the selected criteria now weighted based on their importance to the design, the next step was to evaluate different potential materials. Three composite material types were selected to be evaluated, carbon fibre prepreg, a woven fabric, and lastly a woven sleeve. Using weighting of the criteria determined in TABLE XLIV, TABLE XLV presents a material scoring matrix, which applies the weighted

scores of all needs to the selected materials and determines the optimal one to proceed with for the final design.

**TABLE XLV: MATERIAL SCORING MATRIX**

			Concept					
Metric	ID	Weight %	Prepreg		Fabric		Sleeve	
			Rating	Weight	Rating	Weight	Rating	Weight
Ease of layup	A	20	4	0.80	3	0.60	5	1.00
Wettability	B	40	5	2.00	3	1.20	3	1.20
Part Repeatability	C	30	3	0.90	3	0.90	5	1.50
Appearance	D	0	4	0.00	4	0.00	4	0.00
Cost of material	E	10	5	0.50	3	0.30	4	0.40
Total Weight			4.20		3		4.1	
Ranking			1		3		2	
Continue?			Yes		No		No	

From TABLE XLV, it is visible that the prepreg scores the highest in the material scoring matrix, and has therefore has to been selected to be proceeded with into the final design.

## 6.4 MANUFACTURING METHODS ANALYSIS

With prepreg chosen as the material, the next step is to select a compatible manufacturing method. Using prepreg limits us to manual layup, and only methods that do not require dry fibers. Of the manufacturing methods discussed in section 2.3.4, all methods except the vacuum bag method require the use of dry fibers. The considerations that need to be made in regards to the manufacturing process are whether the part is to be cured in an autoclave or a simple oven, and whether the handle will be produced as a single piece (unibody) or in components.

The advantage to using an autoclave is that it allows precise control over the pressure and temperature during curing, allowing for greater control over material properties as well as faster curing times. However, autoclaves are very expensive to purchase, and have higher energy costs than other methods. The design's



application as a handheld broom does not require the precision of autoclave curing, so the benefits of an autoclave do not justify its cost. Instead, the parts should be oven cured.

The advantages to unibody production of the handle include better properties and the elimination of the assembly process and use of adhesives. The improved properties arise from the removal of the joint sections where the grip and shaft are connected, where stresses will be concentrated. Elimination of the assembly process means there will be fewer materials to store and labor costs will be reduced. Also, misalignments in joining the grip and shaft will be avoided. The disadvantage to unibody production is that it complicates the earlier stages of production. In component-based production, grips can be manufactured in large quantities and shafts can be manufactured as long, straight tubes. The shafts can then be cut to any desired length and attached to the grip. To achieve this same effect in unibody production, the desired length must be specified before the process begins, and the mold used to shape the handle will need to have adjustable length. Additionally, the part will take up much more space and will likely require a larger oven for curing.

The team decided that the advantages of unibody production outweigh the added complexity in manufacturing, and will therefore proceed with the unibody design. Since roll wrapping can no longer be used to produce the hollow shaft sections, the team proposes using aluminum rods coated with a release film as a core for the shaft sections. During layup, these rods would be positioned with the grip's foam core between them, and will remain until curing is finished, at which point the rods can be removed. The result is that the shaft will be hollow to minimize weight, the foam core for the grips will not be more complex than the one used in the generation 1 broom, and the rods will be reusable. To allow the rods and foam core to be more easily lined up, the foam core should have an axial protrusion on either side that can fit into an equally sized hole drilled into the ends of each rod. The steps to producing an oven-cured unibody handle will be as follows:

1. **Produce foam core:** the core will be carved from polyurethane foam in the desired shape of the grip. Production of foam cores can be machine automated to ensure accurate and consistent cores.
2. **Prepreg Layup:** the aluminum rods and the foam core will be lined up to create the full core in the shape of the handle. The prepreg material will then be cut and molded by hand onto the core. The tackiness of the prepreg will help to hold the shape of the handle.
3. **Debulking:** debulking should be performed once every 3 plies during the layup process, and once again when layup is complete. The part is placed in a vacuum bag along with a breather material to allow air flow. A vacuum is then applied to compact the plies by extracting air and excess resin.
4. **Heating:** While maintaining vacuum pressure, the part will slowly be heated in an oven. A standard temperature ramp rate will usually be around 3 °C/min. As the temperature increases, the viscosity of the resin will decrease until the gel point is reached. The gel point occurs when the partial curing of the resin reaches a point where the composite solidifies and ceases to flow. The oven is often maintained at a "hold temperature" below the curing temperature for a period of time to allow additional consolidation of the part before the gel point.
5. **Curing:** After sufficient time at the hold temperature, the oven is ramped up to the cure temperature, which is maintained for long enough for the part to achieve full curing.
6. **Cooling:** Once the part is fully cured, the part will be slowly cooled back to room temperature. The cooling process must be gradual in order to prevent creating internal stresses within the part. The cooling rate is usually selected to be equal to the ramp rate used in the heating process.
7. **Finalize:** The finished composite can be removed from the vacuum bag, the aluminum rods removed, and treated with the surface finish. The plastic end cap and any decals will also be added at this stage. If desired, the shaft below the grip can be cut to modify the height of the grip above the ice during sweeping.

## **6.5 RECOMMENDATION FOR FINAL MATERIAL AND MANUFACTURING**

Analyses on suitable materials and manufacturing processes have revealed the appropriate choices for this design. Specific details regarding the final material selection, chosen layup, and manufacturing process are outlined in this section.

### **6.5.1 FINAL MATERIAL PROPERTIES**

With the final selected material being a carbon fibre prepreg, as there are numerous variations and different types of carbon fibre prepregs, the group had to select one that would meet the design requirements. Looking at the maximum stresses calculated in TABLE XXIII through TABLE XXV, these values were compared with common carbon fibre prepregs.

TABLE XLVI: PROPERTIES OF SELECTED UNIDIRECTIONAL CARBON FIBRE PREPREG

Property	Value	Unit
Density	1490	kg/m <sup>3</sup>
<b>Orthotropic Elasticity</b>		
Young's Modulus X Direction	1.21E05	MPa
Young's Modulus Y Direction	8600	MPa
Young's Modulus Z Direction	8600	MPa
Poisson's Ratio XY	0.27	-
Poisson's Ratio YZ	0.4	-
Poisson's Ratio XZ	0.27	-
Shear Modulus XY	4700	MPa
Shear Modulus YZ	3100	MPa
Shear Modulus XZ	4700	MPa
<b>Orthotropic Stress Limits</b>		
Tensile X Direction	2231	MPa
Tensile Y Direction	29	MPa
Tensile Z Direction	29	MPa
Compressive X Direction	-1082	MPa
Compressive Y Direction	-100	MPa
Compressive Z Direction	-100	MPa
Shear XY	60	MPa
Shear YZ	32	MPa
Shear XZ	60	MPa
<b>Orthotropic Strain Limits</b>		
Tensile X Direction	0.0167	
Tensile Y Direction	0.0032	
Tensile Z Direction	0.0032	
Compressive X Direction	-0.0108	
Compressive Y Direction	-0.0192	
Compressive Z Direction	-0.0192	
Shear XY	0.012	
Shear YZ	0.011	
Shear XZ	0.012	

It should be noted that the analyses which facilitated the selection of these material properties were performed on hollow broom handles. Since these hollow designs can currently withstand the client defined loading conditions, the incorporated core material will not serve any structural purposes. Ideally, a soluble core would have been preferred, as its decomposition could have been added into the manufacturing process to yield a fully hollow seamless design. However, production of the 51° grip core was quoted at \$620 [52], which is well beyond the acceptable budget.

Therefore, the most appropriate core material having the lowest density was the chosen core material to provide geometrical integrity for the grip formation during the layup process.

Referring to the cored cross section material types discussed in section 6.3.1.1, honeycomb was the core material available in the lowest density at  $28 \text{ kg/m}^3$  (TABLE XLII). While this would be the ideal choice in minimizing the mass of the final design, honeycomb available in this density is not rigid. Since the sole application of the core material in this design is to provide the grip with geometrical integrity, preference is given to rigid materials. Therefore, honeycomb was quickly dismissed due to its lack of rigidity.

Unlike honeycomb, the next lowest density core type (polyurethane foam) is rigid. Additionally, foam is easily machinable, so it can be formed into the desired grip geometry with relative ease. Therefore, low density polyurethane foam was chosen as the pursued core material help minimize the mass of the design.

Upon researching suppliers of low density polyurethane foam, the team discovered a manufacturer that sells the lowest density polyurethane foam on the market in the form of a liquid solution at  $32 \text{ kg m}^{-3}$ . This solution was regarded as the preferred choice as larger quantities of the foam may be stored in smaller spaces, the price per unit volume was cheaper than other available rigid form factors, and it presents an opportunity for custom casting, which presents the potential of reducing both material waste and labor time in future improvements to the manufacturing process. Additionally, the solution requires minimal labor to cast customizable pieces [53]. Therefore, this core material was pursued in the final design.

#### **6.5.2 FINAL MANUFACTURING RECOMMENDATION**

The tools required for the manufacture of the final handle design are as follows:

- Casting mold for the foam core, in the shape of the grip with 2 inch long protrusions for fitting into the removable cores.

- Two aluminum rods as reusable cores, with release film coating. The diameters of the rods should be equal to the inside diameters of the hollow shaft for the grip angle currently being manufactured. The rods should also have a 2 inch deep bore to fit the foam core's protrusion for alignment.
- Vacuum bag and vacuum pump, capable of 345kPa pressure.
- Oven with capacity for a 1231.9 mm long part, capable of 135°C.

The process for manufacturing the handle is as follows:

1. Mix 3.25mL of #24 and 3.25mL of #25 polyurethane mix and pour foam in the core casting mold. The foam will expand to 30 times the volume to fill the mold. After 220 seconds, the foam will be set [53]. Remove the core from the mold and remove excess foam.
2. Apply release film to the aluminum rods and place the foam core in line between the rods to form the full core.
3. Lay up the prepreg by hand onto the core. The number and directions of plies are specified in TABLE XXXII,

4. TABLE XXXIII or TABLE XXXIV depending on the grip angle of the part being manufactured.
5. After the first ply, and every subsequent 3 plies, perform debulking by placing the part in the vacuum bag and applying full vacuum for 20 minutes [54].
6. After the final ply has been applied, perform a final debulking step before placing the part in the oven.
7. Maintaining a pressure of 345kPa using the vacuum bag, heat the part in the oven with a temperature ramp rate of 1.7°C/min, up to 135°C [55]. Hold at cure temperature for 60 minutes, then cool to below 60°C.
8. Remove aluminum rods from the handle. Apply decals and coating to finish the handle.

## 6.6 COST ANALYSIS

Based on the optimized final design, TABLE XLVII provides a cost breakdown for the materials required to produce the design. It should be noted that the total cost does not include the manufacturing and labor costs associated with the production of the handle.

**TABLE XLVII: BILL OF MATERIALS FOR SECOND GENERATION XTREME FORCE BROOM HANDLE**

Product	Distributor	QTY	Unit Price	Total Price
Prepreg Carbon Fibre	Rock West Composites	100 lb	\$26.19/lb	\$2619 USD
Polyurethane Core	Fibre Glass	500 ft <sup>3</sup>	\$6.80/ft <sup>3</sup>	\$3400 USD

Based off of TABLE XLVII, the calculated cost of materials for the new Xtreme Force curling broom is \$6019 USD. Although this appears to be a relatively large capital expenditure for materials, it should be noted that this amount represents the purchase of bulk quantities. Purchasing the materials in bulk yields the lowest material cost per produced broom handle. Referring to the prepreg carbon fibre density and the required core volume given in TABLE XLVI and section 6.5.2 respectively, the values in TABLE XLVII may be used to derive the cost of material required per handle.

Sample calculations are provided for the material cost per 19° handle. For the cost of raw material per unit volume:

$$26.19 \frac{\$}{lb} \Big|_{prepreg} \times 1490 \frac{kg}{m^3} \times 2.2 \frac{lb}{kg} = 85\,850 \frac{\$}{m^3} \Big|_{prepreg}$$

$$6.80 \frac{\$}{ft^3} \Big|_{foam} \times 35.31 \frac{ft^3}{m^3} = 240 \frac{\$}{m^3} \Big|_{foam}$$

Using the volume of the hollow 19° model given in TABLE XXXVIII, the cost of prepreg needed to produce one handle is:



$$85\,850 \frac{\$}{m^3} \Big|_{prepreg} \times 2.648 \times 10^{-4} m^3 = \$22.73$$

The volume of the core required to provide the male mold needed to properly layup the grip was computed by treating the curved grip core profile as a cylinder. This geometrical assumption was made by using the grip profile length (found in ANSYS) and assuming a constant core diameter across the entire grip. Also considered in the foam cost calculation is the two inch core extensions required to allow a temporary fit for the removable aluminum rod core during the layup process.

$$240 \frac{\$}{m^3} \Big|_{foam} \times \frac{\pi}{4} (.01876\,m)^2 \times \left( .33221\,m + \left( 2 \times 2\,in \times .0254 \frac{mm}{in} \right) \right) = \$0.03$$

Similar computations were performed on both the 38° and 51° models. Each of the three material costs per unit production (in \$USD) are given in TABLE XLVIII

**TABLE XLVIII: COST OF MATERIAL PER UNIT FOR EACH HANDLE VARIATION**

Variation	Prepreg cost per unit	Core cost per unit	Grips cost per unit	Total cost per unit
19°	22.73	0.03	10.50	<b>22.76</b>
38°	21.27	0.04	11.05	<b>21.37</b>
51°	21.16	0.04	11.60	<b>21.20</b>

Although the final material cost per unit is of greatest interest to the client, the material cost per unit of specifically producing grips is also given in TABLE XLVIII. As discussed in section 1.4, the team was tasked with producing the grip within a \$5 - \$10 budget. As such, this cost was included in the analysis to confirm the degree to which the final manufacturing method utilizes materials in the neighborhood of this budget.

Although the grip material cost per unit given in TABLE XLVIII fall outside the required budget, the team felt that the advantages presented by this design outweigh this marginal cost overage.

## 7. RECOMMENDATIONS

At this point, the team has developed multiple iterations of an optimized final design that adhere to the constraints and limitations of the project. Prior to concluding the final design report, future recommendations for further modification of this design are given in this section.

Revisiting the project objectives and scope as defined in section 1.3, recommendations for refinements to the design are made using the out of scope tasks. To aid the reader's understanding of recommended refinements, the out of scope tasks relating to design refinement are restated in TABLE.

**TABLE XLIX: RECOMMENDATIONS BASED ON OUT OF SCOPE TASKS**

Out of scope task	Recommendation
Make the new handle adaptable to different users' handling styles	
Production of a physical prototype of the second generation broom handle	The need to produce a physical prototype is important in order to evaluate the ergonomics of the handle, which was not considered in this project due to time constraint. Producing a prototype also allows validation of the FEA results.
Preliminary FEA on both the first and second generation broom handles under dynamic loading	All preliminary FEA that was performed in this project assumes a static loading condition. In order to measure the actual performance of the handle under real life scenario, it is highly recommended that effort is put into analyzing the designs under dynamic loading.

In addition to the recommendations regarding the out of scope tasks given in TABLE XLIX, further recommendations were developed throughout the design process which do not relate to any tasks mentioned in section 1.3. The recommendations which are independent of any previously discussed scope tasks are given in TABLE L.

**TABLE L: RECOMMENDATIONS INDEPENDENT OF AFOREMENTIONED SCOPE TASKS**

<b>Out of scope task</b>	<b>Recommendation</b>
Reduce mass further by optimizing the ratio of core to ply volume to yield significant mass improvements without any strength changes	
Production of a physical prototype of the second generation broom handle	
Preliminary FEA on both the first and second generation broom handles under dynamic loading	

## CONCLUSION

Based on the user feedback and the reaction to the first generation of the Xtreme Force curling broom handle, the team was tasked with designing a second generation model. This new model was to incorporate user feedback into the new design by improving both the ergonomics and the geometry of the design.

The project has been done in three phases. The first, the project definition phase, defined and identified the needs of the customer, Gerry Sande. The second phase was the concept definition phase, which consisted of the team performing tests and analyses on the provided first generation Xtreme Force broom handle in order to determine the properties of each unique material along the shaft. Additionally, as a group 30 concepts were screened and scored to select the best overall concept. The third phase, which concludes with the submission of this report was the final design phase. This phase consisted of the development of the selected concept from the concept definition report, to create a product which best matched the customer's needs. This first phase of the project was completed on October 3, 2016. The second phase of the project was completed on October 28, 2016. Lastly, the third phase is the final design.

To better understand the customer needs, interviews were conducted with the customer to determine their desires for the new product. From the interviews, 14 discrete customer needs were identified to match what the customer envisioned. 16 metrics were determined as a measuring stick to determine the convergence with the needs. Using a criteria weighting matrix, the top ranked needs were, the handle material selection and manufacturing processes, the handle is to be strong, not to injure user's hands, and maintain the sweeping efficiency which the first generation was known for.

With the customer's needs and associated metrics developed, the next step was to develop the target specifications of the design. Using equipment provided by the University of Manitoba, the sample handle provided by Gerry Sande was tested. The

sample handle was cut up into different geometries to permit the testing of the handle. Tensile, compression, and three point bending tests were used to approximate values for the yield strengths of each material found along the handle to aid in material identification. Density was the other key property determined from the samples which aided in identifying each of the materials. In phase 3, this data was revisited to assist in the optimization and design of the selected conceptual design.

Research was conducted into aspects which ultimately affected the final design. The mechanics of sweeping were analyzed, as well as the ice surface characteristics, and the biomechanics involved in the sweeping motion. As a composite is comprised of both fibres and a matrix, research was done into both of these aspects. Carbon fibre, fibreglass, Kevlar, were all investigated and compared based on their physical properties. Matrices, or resin systems, were researched, including epoxy, polyester, and vinyl ester. A comparison of resin systems based on their physical properties was also performed. As a broom handle design with more than one piece was being considered, bonding agents, including curing, mechanical fasteners and adhesives were explored. As well, different manufacturing processes were investigated to determine which methods would be most appropriate for the design. The manufacturing processes explored were: Contact Moulding, autoclave, filament winding, resin transfer moulding, and pultrusion.

Through initial concept generation, 30 preliminary designs were created. During the first round of concept generation, the concepts were generated individually. This stage of the concept generation process resulted in very few concepts being rejected, to promote creativity. Using the first generation of the Xtreme Force handle as a reference, each of the 30 concepts were screened objectively compared to the existing product in an effort to start eliminating designs. The top 12 ranked designs proceeded through to the next round of objective evaluation. Based on the rejected concepts and the accepted concepts, concept features were combined together, resulting in a total of 10 unique concepts to further evaluate. These 10

concepts were scored based on their strength of their correlation to the needs criteria weighting. From this, concept BCFP was determined to be the optimal design to proceed forward with. This concept features only a single handle, with an adjusted grip angle and reduced lip size, as well as adjustments to the grip locations. To further confirm the result of BCFP being the optimal design, a sensitivity screening was performed.

Based on the assessment presented in this report, the team is confident that the final selected concept will result in the timely delivery of a quality finished product which meets the customer's needs and requirements.

## 8. REFERENCES

- [1 Composites Innovation Centre, *Logo*, Winnipeg, 2016.  
]
- [2 L. Schulz, *Self taken photos*, Winnipeg, 2016.  
]
- [3 R. Brower, "Brooms Continue to Evolve," 16 July 2016. [Online]. Available:  
] <http://vancurl.com/news-item/brooms-continue-evolve-richard-brower>.  
[Accessed 2 October 2016].
- [4 Sande Curling Innovation, "Sample Pressure Reading," Winnipeg, 2016.  
]
- [5 A. Komus, *Xtreme Force Curling Broom*, Winnipeg, 2016.  
]
- [6 B. Wilson, Interviewee, *Private Communication*. [Interview]. 23 September  
] 2016.
- [7 G. Sande and A. Komus, Interviewees, *Initial Meeting*. [Interview]. 20 September  
] 2016.
- [8 Wikipedia, "Tensile Testing," Wikipedia, 13 October 2016. [Online]. Available:  
] [https://en.wikipedia.org/wiki/Tensile\\_testing](https://en.wikipedia.org/wiki/Tensile_testing). [Accessed 27 October 2016].
- [9 Engineering Archives, "Engineering Archives," Engineering Archives, 2012.  
] [Online]. Available:  
[http://www.engineeringarchives.com/les\\_mom\\_offsetyieldmethod.html](http://www.engineeringarchives.com/les_mom_offsetyieldmethod.html).  
[Accessed 20 10 2016].
- [1 F. Campbell, "Fibers and Reinforcements,," in *Structural Composite Materials*,  
0] ASM International, 2010.
- [1 M. Sanjay, P. Arpitha, L. Laxmana Naik, K. Gopalakrishna and B. Yogesha,  
1] "Applications of Natural Fibers and Its Composites: An Overview," *Scientific  
Research Publishing*, no. 7, pp. 108-114, 2016.
- [1 How Products are Made, "Carbon Fiber," Advameg, Inc., 2016. [Online].  
2] Available: <http://www.madehow.com/Volume-4/Carbon-Fiber.html>. [Accessed  
24 October 2016].
- [1 NILANJAN, "Generation Fibre: Carbon fibre vs human hair," Blogger, 4 March  
3] 2011. [Online]. Available: [http://ndaschakladar.blogspot.ca/2011/03/carbon-](http://ndaschakladar.blogspot.ca/2011/03/carbon-fibre-vs-human-hair.html)  
[fibre-vs-human-hair.html](http://ndaschakladar.blogspot.ca/2011/03/carbon-fibre-vs-human-hair.html)[c] Carbon\_Fiber\_Fabric . [Accessed 24 October 2016].
- [1 Parallel Worlds, "Carbon Fiber Fabric - Parallel Worlds (Malaysia) Sdn Bhd,"  
4] EC21, 2016. [Online]. Available:  
[http://jay70s.en.ec21.com/Carbon\\_Fiber\\_Fabric--6543217.html](http://jay70s.en.ec21.com/Carbon_Fiber_Fabric--6543217.html). [Accessed 24  
October 2016].
- [1 Fibre Glast Developments Corporation, "Carbon Fibre Tape plain weave 5.7 oz  
5] .012 thk in stock," Fibre Glast Developments Corp., N.D.. [Online]. Available:  
[http://www.fibreglast.com/product/Carbon\\_Fiber\\_Tape\\_597/carbon-fiber-](http://www.fibreglast.com/product/Carbon_Fiber_Tape_597/carbon-fiber-tapes-tow-and-sleeves)  
[tapes-tow-and-sleeves](http://www.fibreglast.com/product/Carbon_Fiber_Tape_597/carbon-fiber-tapes-tow-and-sleeves). [Accessed 25 October 2016].

- [1] fibreglass shop, "Sleeve Carbon Braided - The Fibreglass Shop," The Fibreglass Shop, 2016. [Online]. Available: <https://www.fibreglassshop.co.nz/products/carbon-braided-sleeve?variant=852584961>. [Accessed 25 October 2016].
- [1] ZOLTEK, "Prepreg - ZOLTEK Carbon Fiber," ZOLTEK, 2016. [Online]. Available: <http://zoltek.com/products/panex-35/prepreg/>. [Accessed 25 October 2016].
- [1] DragonPlate, "What is Carbon Fiber? Carbon Fiber Technology," Allred & Associates, 2016. [Online]. Available: <https://dragonplate.com/sections/technology.asp>. [Accessed 24 October 2016].
- [1] C. Demerchant, "Carbon Fiber Properties," N.D.. [Online]. Available: <http://www.christinedemerchant.com/carboncharacteristics.html>. [Accessed 25 October 2016].
- [2] J. Young, "Carbon Fiber vs Fiberglass," Fibre Glast Blog, N.D.. [Online]. Available: <http://blog.fibreglast.com/fiberglass/carbon-fiber-vs-fiberglass/>. [Accessed 25 October 2016].
- [2] How Products are Made, "Fiberglass," Advameg, Inc., 2016. [Online]. Available: <http://www.madehow.com/Volume-2/Fiberglass.html>. [Accessed 24 October 2016].
- [2] G. Gardiner, "The making of glass fiber: CompositesWorld," Gardner Business Media, Inc, 25 March 2009. [Online]. Available: <http://www.compositesworld.com/articles/the-making-of-glass-fiber>. [Accessed 25 October 2016].
- [2] F. T. Wallenberger, J. C. Watson and H. Li, "Glass Fibers," *ASM Handbook*, vol. XXI, no. 1, pp. 27-34, 2001.
- [2] J. Hearle, "Aramids," in *High Performance Fibres*, Woodhead Publishing, 2001.
- [2] DuPont, "Technical Guide: Kevlar Aramid Fiber," N.D.. [Online]. Available: [http://www.dupont.com/content/dam/dupont/products-and-services/fabrics-fibers-and-nonwovens/fibers/documents/Kevlar\\_Technical\\_Guide.pdf](http://www.dupont.com/content/dam/dupont/products-and-services/fabrics-fibers-and-nonwovens/fibers/documents/Kevlar_Technical_Guide.pdf). [Accessed 25 October 2016].
- [2] J. Young, "KEVLAR®: Composite grade vs Ballistic Grade," Fibre Glast Blog, N.D.. [Online]. Available: <http://blog.fibreglast.com/fibre-glast-products/kevlar-composites-grade-vs-ballistics-grade/>. [Accessed 25 October 2016].
- [2] Fibre Glast Developments Corporation, "The Fundamentals of Fiberglass," Fibre Glast Development Corp., N.D.. [Online]. Available: [http://www.fibreglast.com/product/the-fundamentals-of-fiberglass/Learning\\_Center](http://www.fibreglast.com/product/the-fundamentals-of-fiberglass/Learning_Center). [Accessed 25 October 2016].
- [2] F. Campbell, "Matrix Resin Systems," in *Structural Composite Materials*, ASM International, 2010.
- [2] NetComposites, "Resin Systems," NetComposites Ltd, 2016. [Online]. Available: <http://netcomposites.com/guide-tools/guide/resin-systems/>. [Accessed 26 October 2016].



- [3 AZo Materials, "Resin Systems for Use in Fibre-Reinforced Composite  
0] Materials," AZoNetwork Ltd., 25 October 2001. [Online]. Available:  
<http://www.azom.com/article.aspx?ArticleID=986>. [Accessed 25 October  
2016].
- [3 Automated Dynamics, "Thermoset vs thermoplastic composites," Automated  
1] Dynamics Ltd, 2016. [Online]. Available:  
<http://www.automateddynamics.com/article/composite-basics/thermoset-vs-thermoplastic-composites>. [Accessed 26 October 2016].
- [3 J. Soller, "Choosing the Appropriate Resin: Epoxy vs. Vinylester vs. Polyester  
2] Resins," Soller Composites, 2004. [Online]. Available:  
<http://www.sollercomposites.com/epoxyresinchoice.html>. [Accessed 26  
October 2016].
- [3 Fibre Glast Developments Corporation, "About Resins," Fibre Glast  
3] Developments Corp., N.D.. [Online]. Available:  
[http://www.fibreglast.com/product/about-resins/Learning\\_Center](http://www.fibreglast.com/product/about-resins/Learning_Center). [Accessed  
25 October 2016].
- [3 T. Johnson, "Vinyl Ester vs Polyester Resins," About Inc., 2016. [Online].  
4] Available: <http://composite.about.com/od/Resins/a/Vinyl-Ester-Vs-Polyester-Resins.htm>. [Accessed 25 October 2016].
- [3 MachineDesign.com, "Joining Composites," 15 November 2002. [Online].  
5] Available: <http://machinedesign.com/basics-design/joining-composites>.  
[Accessed 25 October 2016].
- [3 National Composites Network, "Adhesive Bonding of Composites," UK.  
6]
- [3 K. Potter, An Introduction to Composite Products: Design, Development and  
7] Manufacture, London: Chapman & Hall, 1996.
- [3 Bahhamas Team, "Xtreme Force Analysis," Bahhamas Team, 2016.  
8]
- [3 V. Martinsson, "Xtreme Force Handle Review," 2016.  
9]
- [4 TheAverageBody.com, "The Average Body," 2015. [Online]. Available:  
0] [http://www.theaveragebody.com/average\\_hand\\_size.php](http://www.theaveragebody.com/average_hand_size.php). [Accessed 23  
October 2016].
- [4 W. Frei, "Meshing Considerations for Linear Static Problems," Comsol, 22  
1] October 2013. [Online]. Available: <https://www.comsol.com/blogs/meshing-considerations-linear-static-problems/>. [Accessed 28 November 2016].
- [4 Rock West Composites, "Rock West Composites," 2016. [Online]. Available:  
2] <https://www.rockwestcomposites.com/14060-d>. [Accessed 01 December  
2016].
- [4 ASHAM Curling Supplies, "Handles," Metric Marketing, N.D.. [Online]. Available:  
3] <https://www.asham.com/category/handles>. [Accessed 29 November 2016].

- [4] D. P. Labossiere, *Interview*, Winnipeg, 2016.  
4]
- [4] Tony, "Soluble Cores - 3D printing hollow composite parts," SCHIVO 3D, 25  
5] August 2015. [Online]. Available:  
<http://www.schivo3d.com/index.php/blog/soluble-cores-3d-printing-hollow-composite-parts/>. [Accessed 29 November 2016].
- [4] S. Black, "Getting To The Core Of Composite Laminates," *CompositesWorld*, 1  
6] October 2003. [Online]. Available:  
<http://www.compositesworld.com/articles/getting-to-the-core-of-composite-laminates>. [Accessed 29 November 2016].
- [4] Fibre Glaz Developments Corporation, "Composite Sandwich Core Materials,"  
7] Fibre Glaz Developments Corp., N.D.. [Online]. Available:  
[http://www.fibreglast.com/product/guidelines-for-sandwich-core-materials/Learning\\_Center](http://www.fibreglast.com/product/guidelines-for-sandwich-core-materials/Learning_Center). [Accessed 28 November 2016].
- [4] R. Winker, "Create Better Hollow Composites with FDM Soluble Cores,"  
8] stratasys, N.D.. [Online]. Available:  
[http://usglobalimages.stratasys.com/Main/Secure/Webinars/SolubleCores\\_FDM\\_Webinar.pdf?v=635787075666617027](http://usglobalimages.stratasys.com/Main/Secure/Webinars/SolubleCores_FDM_Webinar.pdf?v=635787075666617027). [Accessed 28 November 2016].
- [4] Amazing AM, "What is Additive Manufacturing?," Amazing AM, LLC., N.D..  
9] [Online]. Available: <http://additivemanufacturing.com/basics/>. [Accessed 28 November 2016].
- [5] 3D Print Today, "What is Fused Deposition Modeling (FDM)?," DISQUS, 1 March  
0] 2016. [Online]. Available: [http://www.3d-print.today/What\\_is\\_Fused\\_Deposition\\_Modeling](http://www.3d-print.today/What_is_Fused_Deposition_Modeling). [Accessed 29 November 2016].
- [5] GoEngineer, "3D Printing - Hollow Composites," YouTube, 15 May 2015.  
1] [Online]. Available: <https://www.youtube.com/watch?v=kIxfUERrwIs>. [Accessed 28 November 2016].
- [5] Cimatrix Solutions Inc., "Quote on Soluble Core," Oshawa, 2016.  
2]
- [5] Fibre Glaz Developments Corporation, "2 Lb. Polyurethane Mix and Pour Foam  
3] Product Data Sheet," Brookville, Ohio, 2016.
- [5] Azo Materials, "Debulking and Autoclave Processing for Tooling Materials,"  
4] 2013.
- [5] Mitsubishi Rayon Carbon Fiber and Composites, "NB301 250-300F Cure Epoxy  
5] Resin System," 2014.
- [5] Curling Canada, "curling.ca," February 2014. [Online]. Available:  
6] <http://www.curling.ca/2014scotties-en/files/2014/02/Flaxey-slide-resized.jpg>. [Accessed 2 October 2016].
- [5] P. Weicek, "winnipegfreepress.com," Winnipeg Free Press, 5 January 2012.  
7] [Online]. Available: <http://www.winnipegfreepress.com/sports/curling/junior-provincial-curling-championships-birchards--aiming-for-junior-sweep-136722223.html>. [Accessed 2 October 2016].

- [5] Curling Canada, "curling.ca," 15 November 2010. [Online]. Available:
- 8] <http://www.curling.ca/blog/2010/11/15/hey-coach-the-last-straw-sweeping-fabrics-and-how-they-can-improve-your-game/>. [Accessed 2 October 2016].
- [5] Asham, "XTEME FORCE Curling Broom," 2016. [Online]. Available:
- 9] <https://www.asham.com/product/xtreme-force-curling-broom>.
- [6] J. L. Bradley, "The Sport Science of Curling: A Practical Review," *Journal of Sports Science & Medicine*, vol. viii, no. 4, pp. 495-500, 2009.
- [6] M. Volz, "Anatomical Planes & Body Cavities Quiz," ProProfs Quiz Maker, N.D..
- 1] [Online]. Available: <http://www.proprofs.com/quiz-school/story.php?title=anatomical-planes-body-cavities-quiz>. [Accessed 23 October 2016].
- [6] Sports You Never Hear Of, "Curling - Part 3: Sports You've Never Heard Of,"
- 2] Spalk, 23 May 2016. [Online]. Available: <https://www.spalk.co/blog-post/curling-part-3-sports-you-ve-never-heard-of>. [Accessed 23 October 2016].
- [6] D. Karim, "Is pronation/supination a movement part of the wrist or the
- 3] forearm?," ResearchGate, 14 January 2014. [Online]. Available: [https://www.researchgate.net/post/Is\\_pronation\\_supination\\_a\\_movement\\_part\\_of\\_the\\_wrist\\_or\\_the\\_forearm](https://www.researchgate.net/post/Is_pronation_supination_a_movement_part_of_the_wrist_or_the_forearm). [Accessed 23 October 2016].
- [6] CurlTech, "Section 6 - Sweeping," The Curling School, 2007. [Online]. Available:
- 4] <http://curlingschool.com/manual2007/Section6.html>. [Accessed 23 October 2016].
- [6] H2O Performance Paddles, "Fast Ferrule," [Online]. Available:
- 5] <http://h2opaddles.com/Technology/FastFerrule>. [Accessed 27 10 2016].
- [6] Kodiak Curling, "Foldable Curling Broom," [Online]. Available:
- 6] <http://kodiakcurling.com/idea-lab/#/foldable-curling-broom/>. [Accessed 27 10 2016].
- [6] Comsol Inc., "Comsol," [Online]. Available:
- 7] <https://www.comsol.com/blogs/meshing-considerations-linear-static-problems/>. [Accessed November 2016].

# APPENDIX A: NEEDS AND METRICS

---

## APPENDIX B: PRELIMINARY CONCEPT EVALUATION

---

# APPENDIX C: SUPPLEMENTAL DATA

---